The Feasibility of Using Robotic Systems at the

International Space Station for Exterior Inspections

by

Lisa Kaplan, B.S.

Thesis

Presented to the Faculty of the Graduate School

of The University of Texas at Austin

in Partial Fulfillment

of the Requirements

for the Degree of

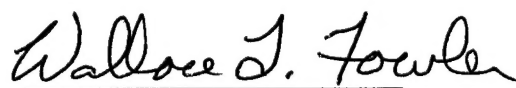Master of Science in Engineering

The University of Texas at Austin

December 1999

REPORT DOCUMENTATION PAGE

Form Approved
OMB No. 0704-0188

1. AGENCY USE ONLY *(Leave blank)*	2. REPORT DATE	3. REPORT TYPE AND DATES COVERED
	13.Jun.00	THESIS

4. TITLE AND SUBTITLE
THE FEASIBILITY OF USING ROBOTIC SYSTEMS AT THE INTERNATIONAL
SPACE STATION FOR EXTERIOR INSPECTIONS

5. FUNDING NUMBERS

6. AUTHOR(S)
2D LT KAPLAN LISA R

7. PERFORMING ORGANIZATION NAME(S) AND ADDRESS(ES)
UNIVERSITY OF TEXAS   AUSTIN

**8. PERFORMING ORGANIZATION
REPORT NUMBER**

9. SPONSORING/MONITORING AGENCY NAME(S) AND ADDRESS(ES)
THE DEPARTMENT OF THE AIR FORCE
AFIT/CIA, BLDG 125
2950 P STREET
WPAFB OH 45433

**10. SPONSORING/MONITORING
AGENCY REPORT NUMBER**

FY00-213

11. SUPPLEMENTARY NOTES

12a. DISTRIBUTION AVAILABILITY STATEMENT
Unlimited distribution
In Accordance With AFI 35-205/AFIT Sup 1

12b. DISTRIBUTION CODE

13. ABSTRACT *(Maximum 200 words)*

14. SUBJECT TERMS

15. NUMBER OF PAGES
156

16. PRICE CODE

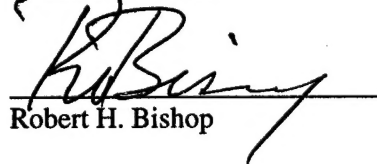| 17. SECURITY CLASSIFICATION OF REPORT	18. SECURITY CLASSIFICATION OF THIS PAGE	19. SECURITY CLASSIFICATION OF ABSTRACT	20. LIMITATION OF ABSTRACT

The Feasibility of Using Robotic Systems at the

International Space Station for Exterior Inspections

APPROVED BY

SUPERVISING COMMITTEE:

Wallace T. Fowler

Robert H. Bishop

Table of Contents

List of Tables

List of Figures

List of Acronyms

AERCam   Autonomous Extravehicular Activity Robotic Camera

C-W   Clohessy-Wiltshire

C&T   Communications and Tracking

CCTV   Closed Circuit Television

ERA   European Robotic Arm

ESA   European Space Agency

EVA   Extra Vehicular Activity

FGB   Functional Cargo Block

ISS   International Space Station

JEM   Japanese Experiment Module

JEMRMS   Japanese Experiment Module Remote Manipulator System

LEE   Latching End Effector

LVLH   Local Vertical Local Horizon

MBS   Mobile Remote Service Base System

MPLM   Mini-Pressurized Logistics Module

MRS   Mobile Remote Service

MSS   Mobile Servicing System

MT   Mobile Transporter

PDGF   Power and Data Grapple Fixture

PMA	Pressurized Mating Adaptor
PV	Photovoltaic
RMS	Remote Manipulator System
RWS	Robotic Work Station
SPDM	Special Purpose Dexterous Manipulator
SPP	Science Power Platform
SSRMS	Space Station Remote Manipulator System
SVS	Space Vision System

Chapter 1.0

Introduction

The ability to inspect or observe a structure from an external perspective is very important when that structure is an orbiting space station. In fact, whether or not the capability to do so exists at a space station could have a critical effect on the lives of the astronauts living and working on board. For example, in June of 1997, a Progress resupply vehicle struck the Space Station Mir during the testing of a manual redocking system. The collision caused the pressure in the damaged Spektr module to drop to vacuum.[6] Mir power and thermal control subsystems were also damaged in the collision. During a press briefing about the accident, Frank Culbertson, NASA Program Manager of the Shuttle-Mir Program, was asked what the plans were to recover from the accident and whether the astronauts on board could get up to Spektr to look around. His response included the following excerpt:

> [The Russians are] looking at several different ways they might repair a potential leak, but the problem is they don't know exactly what it looks like or where it's located. So until we know the exact character and location of the hole, it's difficult to build a specific repair procedure. So I believe that looking at the area, if they're going to do a repair, is critical. [5]

Repairs of the module could not even be planned because there was no immediate way to examine the exterior of the damaged station. Two whole months passed before two of the crewmembers spent six hours during an Extra Vehicular Activity (EVA) trying to look at the damage up close.[18] Even the Space Shuttle was used as an orbiting inspection device on occasion. Clearly, safer and more time efficient methods

of exterior inspection were required.

The need for observational tools is even greater now that a new space station is being constructed in orbit. The International Space Station (ISS) is the result of the first international effort to develop and build a laboratory in space. When completed, it will be the largest on-orbit facility ever created. While the large size and complex structure of the space station will allow for a variety of space-based experiments and research to be conducted in a habitable environment, they will also make external observation of the ISS even more difficult. For monitoring, visual support of EVA, and maintenance purposes, both preventative and reparative, ISS crewmembers will need to be able to observe the ISS from the outside. With a planned lifetime of at least ten years, there will be multiple instances during the ISS's operation when ISS or ground crewmembers will need to monitor some portion of the station's exterior from close range. Some examples of why such a need could arise are:

- "The lack of comprehensive end-to-end testing of the ISS components carries a great deal of potential for subsequent problems" with both mechanical and electrical systems, some external." [11]

- The suspicion of collision damage or puncture by space debris

- The development of a leak in one of the stations pressurized elements

- The need for a general inspection to determine the overall health/status of the station

The scheduled completion date for space station construction is in the year 2004. Until then, while engineers and astronauts complete construction and integration of the ISS, options can be explored which will aid in external observation, assisting or

2

preferably replacing an EVA. Unlike for Mir, there are options other than crewmembers on EVA or space shuttles available for use at the ISS for external visual inspections.

One partial solution to the problems surrounding external inspection is already built into the design of the station. There are three robotic arms on the ISS that operate in three different regions of the station. On each arm is a system of cameras, part of a Space Vision System (SVS) that can be used for inspection. Since the arms are mobile, so are the cameras. The arms can easily be maneuvered to allow the cameras to observe many areas of interest. Unfortunately, due to the complex geometry of the station, the combined visual range of the arms' cameras does not encompass the entire station. A description of the arms and the SVS along with a discussion of the operational limits of the arms will be discussed in more detail in Chapter 3.0.

The option always exists to send an ISS crewmember out on an EVA to perform an inspection of parts of the station hidden from view (as was done on Mir). EVAs are complex and are not desirable if other procedures are available. Any type of EVA is potentially hazardous to crewmembers since risk of injury increases any time they leave the relatively safe environment inside the station. It is best to minimize the number of EVAs required for routine operations.

Emergencies will occur which may require external observation. However, even in these situations, an EVA might not be the most ideal inspection alternative. Most EVAs must be planned at least a day in advance. The astronaut must have the opportunity to "camp out" overnight in the airlock. This "camp out" takes place in the equipment lock section of the Joint Airlock Module (see Appendix A) at a lowered pressure environment of

10.2 psi.[33] This procedure is necessary in order to purge the nitrogen from the astronaut's system and prevent the problem of decompression sickness, commonly known as the "bends." The "camp out" would not be possible before a last minute emergency EVA. For a last minute EVA, in order to leave the 14.7 psi pressure of the station to work safely in the 4.3 psi environment of the spacesuit outside the station, an astronaut following U.S. EVA procedures would have to spend a period of four hours breathing pure oxygen.[21] Thus, the remedy to any emergency requiring a crewmember's direct visual contact with the station's exterior would be, at a minimum, four hours in the making unless the astronaut makes use of a high pressure suit.

Fortunately, an alternative option is currently being considered which may potentially be used to inspect those parts of the station that are otherwise unobservable. It is a free floating robotic camera, called AERCam by its designers, which can be sent out by itself to view a target site up close. AERCam stands for Autonomous Extravehicular Activity Robotic Camera. One AERCam has already been tested successfully during STS-87 (see Section 4.1).

Though the idea of sending an autonomous camera out to perform inspections sounds promising, the feasibility and safety of using (flying) such an AERCam in close proximity to the station must first be determined. For the purposes of this study, successful use of an AERCam is defined as a situation in which the free-floater is released near the ISS, performs a single thrust to change its velocity relative to the station, flies along an obstacle-free trajectory to a target site, performs a "braking" thrust to bring its velocity relative to the station back to zero, maintains its position at the target site relative to the station, and returns safely to its docking station along an

4

obstacle-free path. A more thorough description of the AERCam option will be presented in Chapter 4.0, where the feasibility of using an AERCam at the ISS will be examined by analyzing an AERCam's motion relative to the station as it travels from specified "launch" points to selected targets.

The goal of the current study is to develop a set of guidelines that could be helpful in determining the manner in which any particular area of the ISS may best be inspected. To that end, this paper will first familiarize the reader with background information needed to better understand the topic area later discussions. This information includes a description of the ISS, an explanation of the coordinate system in which AERCam trajectories are described, a discussion of relative motion, and a description of the Clohessy-Wiltshire (C-W) equations used to model relative motion in this study. The thesis will then examine how and where the station's robotic arms may be used for external ISS inspection purposes. Ultimately, the concept of using an AERCam will be studied. First will be a familiarization with the AERCam itself and the software that will be used to generate its trajectories. Sample target locations will be selected and the trajectory generation process will be discussed. The motion of an AERCam relative to the station will then be analyzed to determine any rules which would be associated with AERCam use.

Chapter 2.0

Background Information

2.1 International Space Station

The International Space Station is an orbiting laboratory, the combined efforts of 16 nations including Belgium, Brazil, Canada, Denmark, France, Germany, Italy, Japan, the Netherlands, Norway, Russia, Spain, Sweden, Switzerland, the United Kingdom, and the United States.[17] It is a multi-functional research center designed to support on-orbit operations in areas ranging from microgravity sciences to commercial product development.[11] The station in which the astronauts will live and work is a complex facility comprised of over 100 components.[28] In addition to the pressurized elements of the station, there are an elaborate integrated truss structure, multiple solar panels and radiators, a "back porch" for experiments exposed to the space environment, and three remotely operated robotic arms. The facility is designed to support a crew of seven. The ISS is about 290 feet long and 356 feet wide when complete, with an approximate 43,000 cubic feet of internal volume.[8] Refer to Figures 1 and 2 for a rendering of the completed ISS and an exploded view of the NASA model which is the reference configuration for this study. Numerical labels correspond to the station components as listed in Table 1.
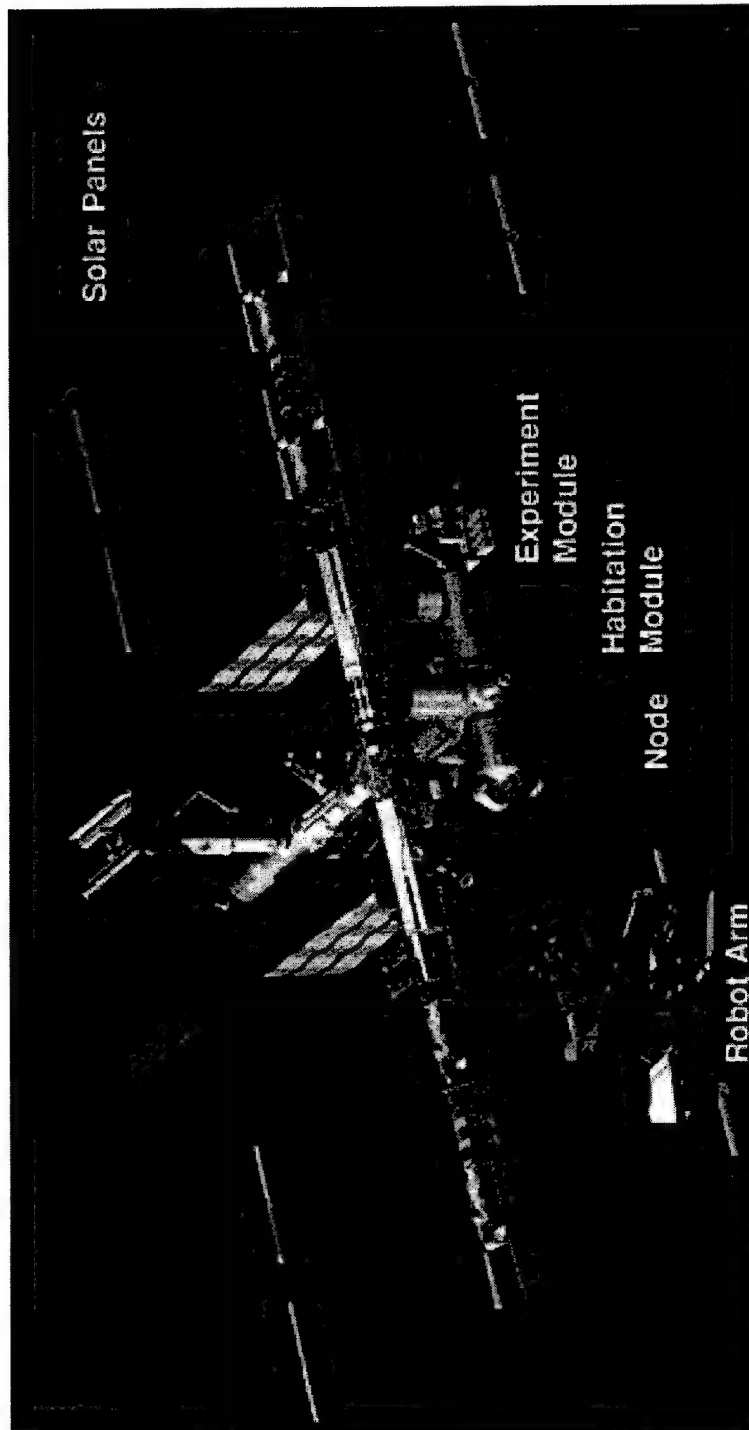
Figure 1. International Space Station [4]

7
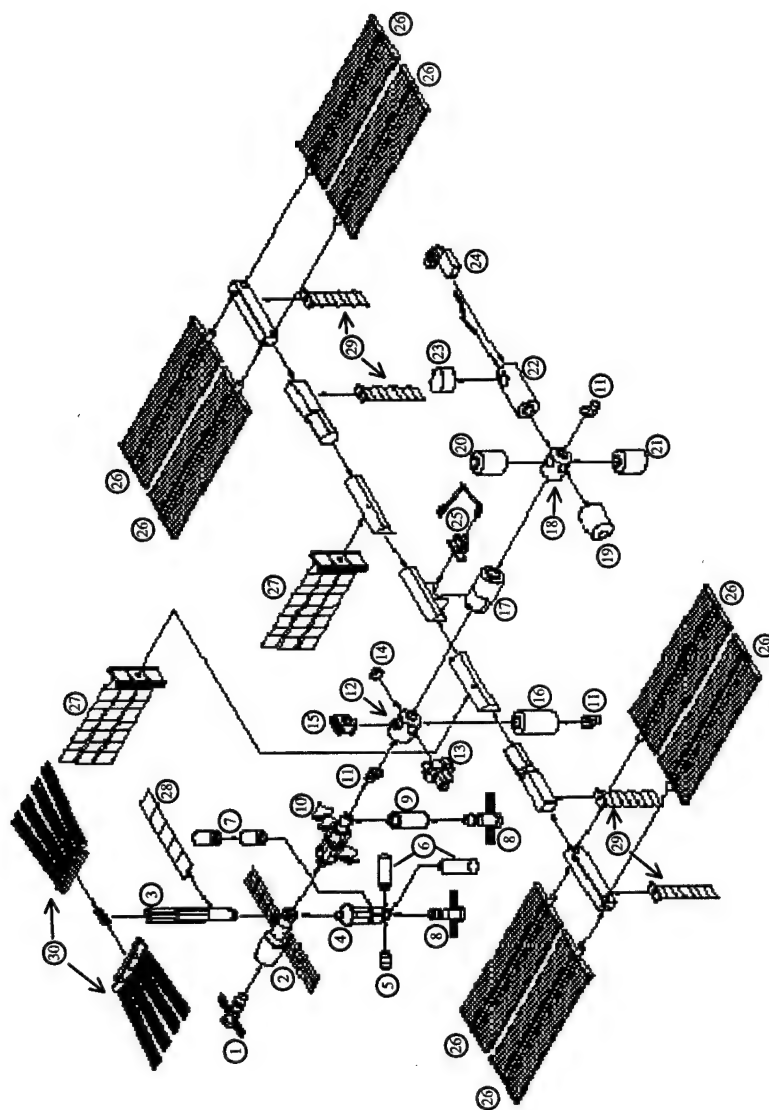
Figure 2. Exploded Model of the International Space Station [30]

8

Table 1. International Space Station's Principal Components [29]

	Component		Component
1	Progress	16	Habitat
2	Service Module	17	U.S. Laboratory
3	Science Power Platform (SPP)	18	Node 2
4	Universal Docking Module	19	Columbus Orbital Facility
5	Docking Compartment	20	Centrifuge Module
6	Research Module	21	Multi-Purpose Logistics Module
7	Life Support Module	22	Japanese Experiment Module (JEM)
8	Soyuz	23	JEM Experiment Logistics Module
9	Docking and Stowage Module	24	JEM Exposed Facility
10	Functional Cargo Module (Zarya)	25	Mobile Servicing System
11	Pressurized Mating Adapter (PMA)	26	Photovoltaic (PV) Array
12	Node 1	27	Thermal Control System Radiator
13	Joint Airlock	28	SPP Radiator
14	Cupola	29	Electrical Power System Radiator
15	Z1 Truss Segment	30	SPP PV Array

A summary description of some of these component as described by NASA is found in Appendix A.

The orbit of ISS about the Earth has the following characteristics:

Average altitude: 400 km [9] The orbit altitude is a compromise designed to allow space transportation systems to access the station while at the same time maintaining an altitude high enough to keep the station's orbit from deteriorating too quickly.

Inclination: 51.6° [26]

Eccentricity: 0.0008 [26]

2.2 Coordinate System

The reference frame in which the ISS is modeled is the Local Vertical Local Horizon (LVLH) coordinate system. This is a body-fixed coordinate system that rotates with the ISS. The positive X axis points in the direction of ISS motion. The Z axis points towards Earth's center, and the Y axis completes the system pointing opposite the angular momentum vector (see Figure 3).
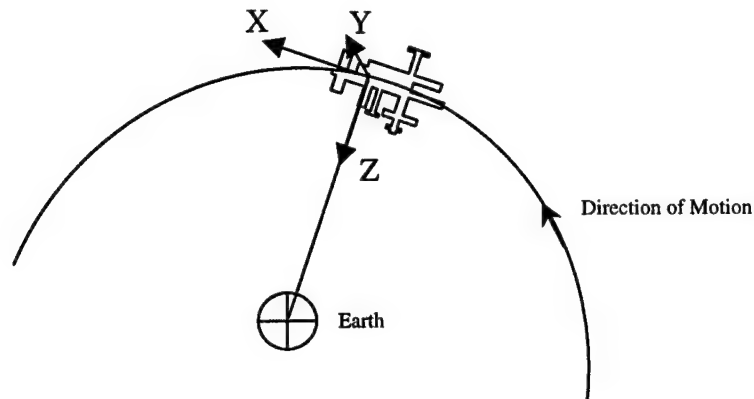
Figure 3. The Local Vertical Local Horizon Coordinate System at the ISS

An LVLH coordinate system is used often for rendezvous and relative motion studies when distances between the two objects are small. The center of the reference frame can be fixed to one object's (the ISS) center of mass. The acceleration of the other object (AERCam) with respect to the origin can then be determined directly instead of relating their motion to each other by referencing the motion of both objects separately to an Earth-centered frame. Since the relative motion discussions within this paper are based solely on an AERCam's motion with respect to the station and not the Earth, the LVLH reference frame is an ideal choice. An LVLH system is centered at the station's center of mass and the axes are oriented as described above. Figure 3 illustrates the orientation of the ISS within this coordinate system.

2.3 Relative Motion

Visualizing how one object will move relative to another in orbit is not an easy task. While a thrust in the forward direction by a trailing object would be expected to close the gap between the two objects on the Earth, in orbit it would have the exact opposite effect. Developing a feel for orbital relative motion is very important. It helps in the process of determining if employing an AERCam at the ISS is

10

advantageous. A basic description is now presented about how one orbiting object's position would change with respect to another's after the first accelerates.

Consider two satellites, A and B, one trailing the other in the same orbit, moving at the same speed. The velocity at which a satellite travels around the Earth is associated with its altitude. A change in altitude, no matter how slight, causes at least a small change in velocity. As it happens, the higher the orbit, the slower the velocity. So any thrust which serves to increase a satellite's altitude will slow the satellite down, and vice versa. For this study, only very small, impulsive maneuvers are considered. If satellite A changes its altitude while satellite B does not, their velocities will no longer be equal, and the distance between them will either increase or decrease according whether satellite A is now "above" or "below" satellite B. This is why when positioned on the positive Y axis, the only way in which an AERCam will appear to move from one point to another in the LVLH frame relative to the ISS is by travelling up and back or down and forward (up meaning away from the Earth). With a single impulsive thrust, there is no way for an AERCam to go above and forward with respect to the ISS because as soon as it went above, it would slow down and travel backwards relative to the station. Of course, an initial change in velocity directed forward and up will appear at first to move the satellite in that direction relative to B, but before long A's slower speed will "move" the satellite relatively backwards.

This description is only a 2-dimensional portrayal of relative motion in the orbit plane. As will be discussed in the next section, motion in and out of the plane is oscillatory in nature and is independent of the motion within the orbit plane.

2.4 Clohessy-Wiltshire (C-W) Equations (A Variation of Hill's Equations)

The C-W equations are a linearized version of the equations describing the motion of one body relative to another in a central gravitational force field. They are very convenient to use when trying to gain an understanding of relative spacecraft motion. The more accurate the equations of motion are, the more precise the results will be. However, the purpose of the relative motion portion of this study is to serve as an initial look at the operational feasibility of an AERCam in close proximity to the ISS. It is useful to examine how an AERCam will perform in the most basic of environments. A more in depth and time consuming evaluation is unnecessary if an AERCam cannot perform as desired under simple circumstances.

The C-W equations of motion for two objects in close proximity to each other are:

$$\ddot{x} - 2\omega\dot{z} = 0$$
$$\ddot{y} + \omega^2 y = 0 \qquad\qquad (1)$$
$$\ddot{z} + 2\omega\dot{x} - 3\omega^2 z = 0$$

where,

$$\omega = \sqrt{\frac{g_e r_e^2}{r_o^3}} = \text{constant} \qquad\qquad r_o - \text{orbital radius,}$$

x, y, and z are coordinates measured along the LVLH axes from the origin of the reference frame

Equations (1) may be solved to find the expressions for relative position and velocity:

$$x = -\left(\frac{2\dot{z}_o}{\omega}\right)\cos\omega t + \left(\frac{4\dot{x}_o}{\omega} - 6z_o\right)\sin\omega t + \left(6z_o - \frac{3\dot{x}_o}{\omega}\right)\omega t + \left(x_o + \frac{2\dot{z}}{\omega}\right)$$

$$y = (y_o)\cos\omega t + \left(\frac{\dot{y}_o}{\omega}\right)\sin\omega t \tag{2}$$

$$z = \left(\frac{2\dot{x}_o}{\omega} - 3z_o\right)\cos\omega t + \left(\frac{\dot{z}_o}{\omega}\right)\sin\omega t + \left(4z_o - \frac{2\dot{x}_o}{\omega}\right)$$

$$\dot{x} = \left(\frac{4\dot{x}_o}{\omega} - 6z_o\right)\omega\cos\omega t + 2\dot{z}_o\sin\omega t + \left(6z_o - \frac{3\dot{x}_o}{\omega}\right)\omega$$

$$\dot{y} = (-y_o\omega)\sin\omega t + \left(\dot{y}_o\right)\cos\omega t \tag{3}$$

$$\dot{z} = -\left(\frac{2\dot{x}_o}{\omega} - 3z_o\right)\omega\sin\omega t + \left(\dot{z}_o\right)\cos\omega t$$

See Appendix B for the summary of the derivation of the C-W equations.

The acceleration of an object in the Y direction is de-coupled from that in the X and Z directions, hence a satellite's out-of-plane motion is uncoupled from its in-plane motion. Also, the out-of-plane motion is oscillatory. A satellite will only travel a limited distance out of the orbit plane before changing direction and swinging back and through the orbit plane out in the opposite direction. The out-of-plane motion is described by the second expression in equation (2) and is dependent on the out-of-plane initial velocity component. Actually, the out-of-plane relative motion describes a situation in which two satellites are in two slightly different orbit planes. The LVLH reference system is centered within the original orbit plane (fixed to one satellite) and the second plane is defined by the other satellite's motion resulting from its out-of-plane initial velocity component. These planes

13

intersect along a line which passes through the center of the Earth. The oscillatory out-of-plane motion occurs as the satellites move around their respective orbital paths, crossing twice per orbit.

Chapter 3.0

Station Robotic Arms

There are three robotic arms designed for use on the ISS. These are the Space Station Remote Manipulator System (SSRMS), the European Robotic Arm (ERA), and the Japanese Experiment Module Remote Manipulator System (JEMRMS). These arms are designed to be available for the "inspection of the outer side of the space station via [their] cameras, in order to verify the integrity of the space station structure and the proper functioning of externally mounted systems and mechanisms."[20]

The cameras referred to are part of the Space Vision System (SVS) located on each of the three robotic arms. The SVS is a technological innovation originally used on the space shuttle's remote manipulator system (RMS). The system of cameras, lights, and video data transfer connections attached to the RMS itself gives the operator an independent view of arm operations when maintaining direct line of sight is not possible. The SVS is an indispensable resource. NASA writes:

> It allows the Shuttle arm to be operated with great precision even when visibility is obstructed, and the system was used operationally during the first assembly mission as astronaut Nancy Currie, with her view partially obstructed, attached the first station component, the Zarya control module, to the second component, the Unity connecting module. [34]

3.1 Space Station Remote Manipulator System (SSRMS)
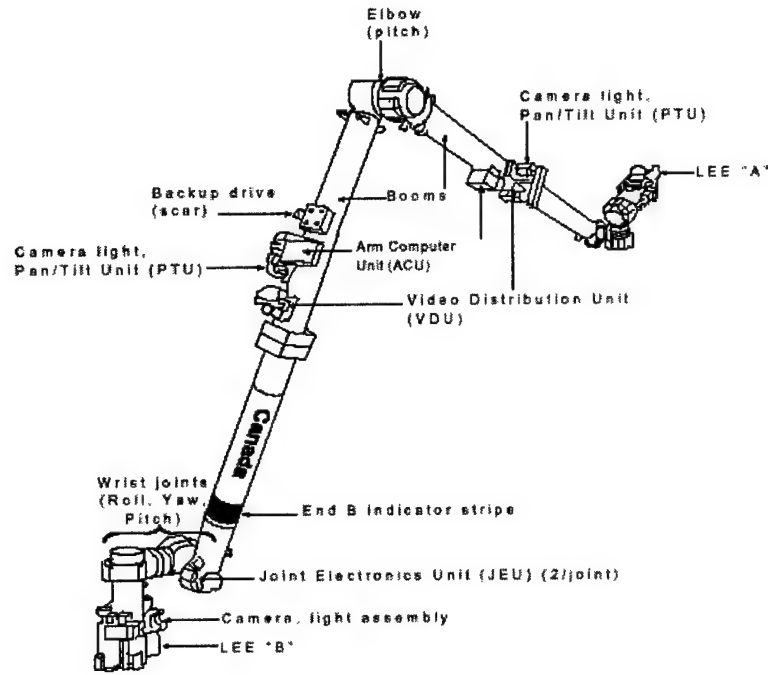
Figure 4. SSRMS [11]

Built by Spar under contract to the Canadian Space Agency, the SSRMS will be the largest, most versatile mechanical arm on the station. It will be used primarily for station assembly and maintenance. It is 17.6 meters in length and can move with seven degrees of freedom.[36] The SSRMS is symmetrical and at each end is a Latching End Effector (LEE), making it possible for the arm to move like an inchworm around the station. It does this by connecting its free end to one of the Power and Data Grapple Fixtures (PDGF) then disconnecting the other to pivot forward to another PDGF. The PDGF provide "power, data, and video connections to the arm. The PDGF is the only interface from which the arm can operate."[11] These fixtures are located in strategic positions "throughout the ISS (Lab, Mini-Pressurized Logistics Module (MPLM), JEM, Hab, Functional Cargo Block (FGB),

16

MBS, SPDM)..."[11] A total of seven cameras are mounted to the arm, comprising the visual components of the SVS.

The SSRMS is considered part of the station's Mobile Servicing System (MSS), the other components of which can serve to increase the versatility of the SSRMS. In addition to the SSRMS, the MSS includes the Mobile Remote Service (MRS) Base System (MBS), the Mobile Transporter (MT), and the Special Purpose Dexterous Manipulator (SPDM). (ref Appendix A)

The SSRMS gains the greatest mobility by connecting itself to one of the PDGF on the MBS. This platform will be able to move up and down the length of the station's integrated truss system on top of the MT, providing SSRMS access to much of the station. At its fastest velocity of one inch per second, it will take 50 minutes for the MT's translation from one end of the truss to the other [11].

Connectable to the end of the SSRMS is the Special Purpose Dexterous Manipulator (SPDM).
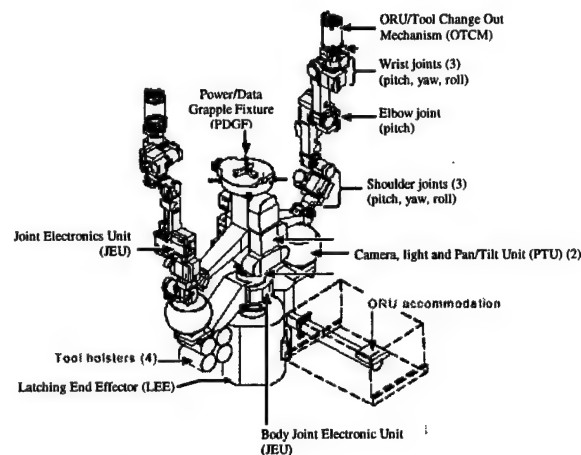
Figure 5. SPDM [11]

This "hand" is composed of two 3.5 meter, seven-joint arms. "It can provide lighting and Closed Circuit Television (CCTV) monitoring of work areas…"[11]. It can also be used for the capture of free-floating payloads. [36]

3.2 European Robotic Arm (ERA)
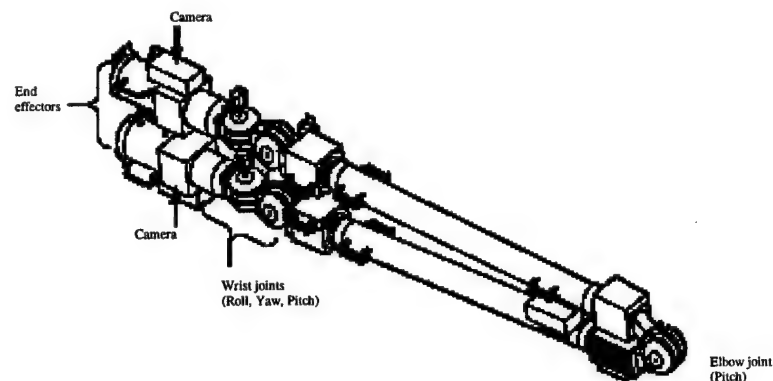
Figure 6. ERA [11]

The ERA is a smaller arm developed by Fokker Space under contract of the European Space Agency (ESA). It will be used primarily for assembly and maintenance of the Russian segment of the ISS. "The ERA has similarities to the SSRMS, including the power, data, and video transfer capability by the end effectors."[11] The arm is 11.3 meters long.[20] It can move in 7 degrees of freedom and is mobile, able to connect to various "grapple fixtures specifically designed for them"[11] on the Russian segment.[1] The ERA has only four cameras mounted to it, one on each limb and on the end effectors.

3.3 Japanese Experiment Module Remote Manipulator System (JEMRMS)
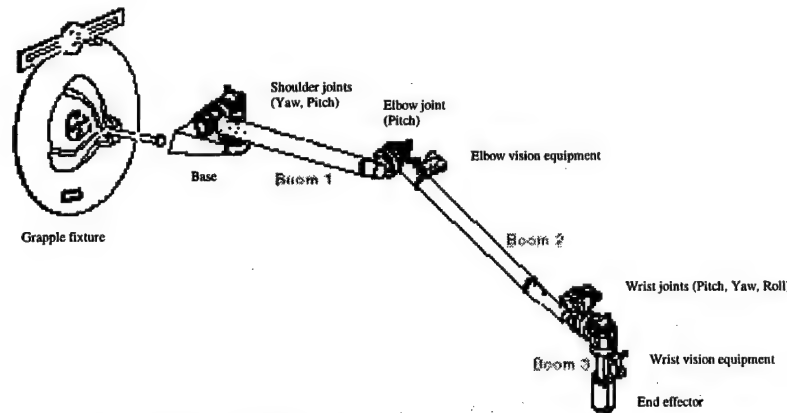
Figure 7. JEMRMS [11]

The JEMRMS is "a 32.5-ft . . . six-joint robotic arm with two main booms."[11] It is equipped with camera units like the other two robotic arm systems. Unlike the other systems, however, this arm is not mobile. Its base is fixed in place on the end of the JEM module. The JEMRMS is used primarily to support experiments on the "back porch" exposed facility, manipulating any devices or experimental components as required.

3.4 Robotic Arm Utilization

Each robotic arm has lights that may be used to illuminate the target site for the cameras, and the arms may be positioned so the cameras view the target site from the best angle and distance. Advantages to using the station's robotic arms for external observations are that no personnel would be placed in any additional risk, and the only additional resource that would be used is power, a resource that is easily allocated for arm use given the solar panels under normal circumstances. The robotic arms are easily controllable and predictable. If there does happen to be a disruption in the power supply to one of the arms, it would just stop. There will be no contact with any part of the station that is not intended. There is, however, one major problem with

19

depending on the robotic arms for external inspections: their limited coverage. As the reach of each arm is limited by its design, these cameras may view only a limited amount of the exterior surface area of the station. Taken from a NASA's ISS Familiarization Manual, Figure 8 highlights the regions of the station in which the three robotic arms operate.
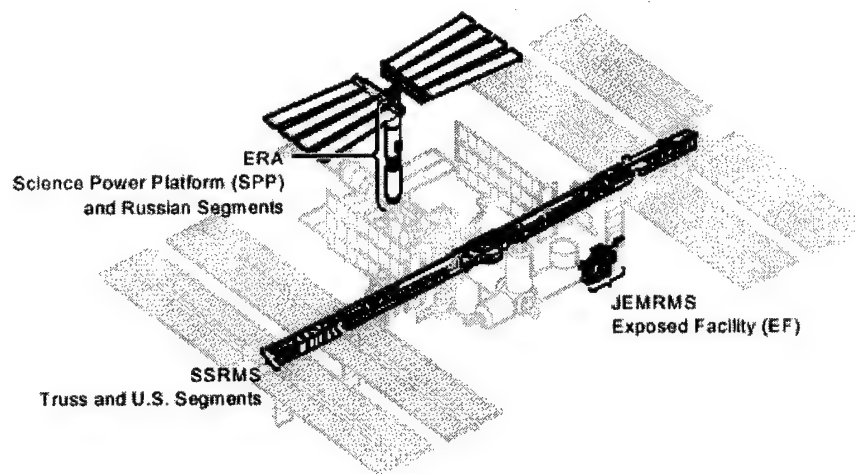
Figure 8. ISS Locations Where the Robotics Systems are Used

Given the information currently available regarding attachment points and arm dimensions, Figure 9 indicates in general the pressurized regions of the ISS where there are areas not completely visually accessible to the robotic arms' SVSs.
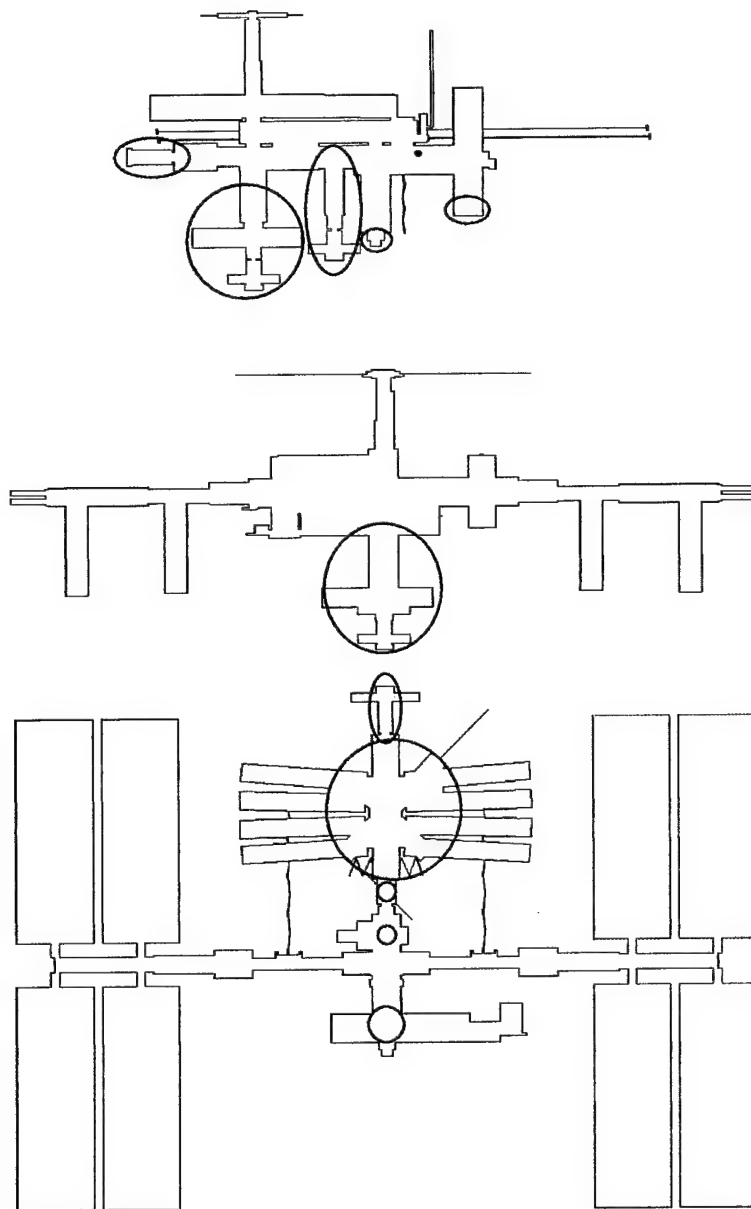
Figure 9. Portions of the ISS not Observable with a SVS

Ideally, if its usefulness and safety can be proven, the AERCam could assume the
responsibility of inspecting those exterior portions of the station indicated in Figure 9.

Chapter 4.0

Autonomous Extravehicular Activity Robotic Camera (AERCam)

4.1 AERCam

AERCams are free-floating cameras conceived to provide increased visual inspection capabilities to crewmembers within the Space Shuttle or the ISS. For the ISS, an AERCam's purpose would be to support an EVA or to preferably eliminate the need for one. Regarding EVA support, an AERCam could be sent out prior to the scheduled operation to inspect and identify the site of interest. This capability would have been of great benefit on Mir. An AERCam could also provide an independent view and another perspective of any EVA to crewmembers within the ISS. Using an AERCam in lieu of an EVA would of course be preferred whenever observation alone is the purpose of the mission. Such a camera could provide coverage of ISS locations not visible to SVS cameras, of those portions of the station which otherwise would be hidden from view.

There has already been one such AERCam designed and operationally tested in space. It is called the Sprint AERCam. Sprint is 14 inches in diameter. It incorporates a series of lights and painted stripes on its surface to allow the operator to visually monitor its orientation. "The AERCam's thrusters, basic avionics, solid-state rate sensors, attitude hold electronics, nitrogen tank and hand controller are identical to those used on the SAFER," the Simplified Aid for EVA Rescue backpack worn by astronauts during EVA in case of accidental un-tethering.[31] Using small nitrogen thrusters, AERCam is designed to provide
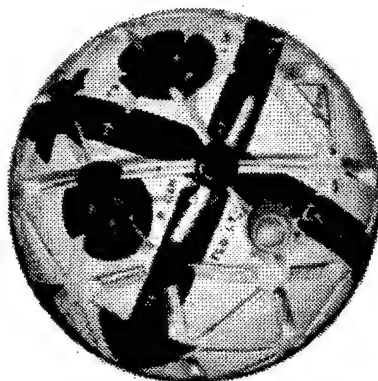
Figure 10. The Sprint AERCam [3]

22

only one-tenth of the thrust of the SAFER thrusters and travels at less than 0.25 ft/s (7.62 cm/s). This AERCam is able to move in six degrees of freedom and "its electrical supply and nitrogen supply are designed to last at least seven hours, the maximum length of a normal spacewalk."[31] Two cameras are built into Sprint, "one with a six millimeter lens and another with a twelve millimeter lens," along with a floodlight exactly like the ones on spacesuit helmets.[3] The exterior of Sprint is covered with a thinly padded material to protect it and any object with which it may inadvertently come into contact. Sprint was flown in the cargo bay of the space shuttle during STS-87 in 1997. It was controlled remotely by Pilot Steve Lindsey from inside the shuttle and flight-testing was declared a success.[31,13] Sprint is the only AERCam operationally tested in space, so for the purposes of this study, its characteristics will be used for reference.

4.2 AERCam Relative Motion Study

The primary reason for using free-floating camera instead of an astronaut is to minimize the astronaut's exposure to the hazards of space. Thus, for all of those parts of the station not visible to the SVS cameras, the preference should be to use an autonomous AERCam instead of an astronaut. Whether using AERCam around the ISS is practical or not will be examined by attempting to generate clear trajectories which allow the camera to move from a starting point to various target locations about the ISS.

Related research was completed by Paul Lockhart in his thesis entitled "Unassisted Rendezvous Techniques for the Manned Maneuvering Unit."[38] Lockhart's study focused primarily on creating a set of trajectory charts an astronaut could easily reference and follow for return to the Shuttle cargo bay from a free-floating position some distance away. When choosing which of the trajectories should be implemented in a given situation,

Lockhart considered the astronauts' visual perception as the only method of attitude determination and had them referencing the pre-formed set of charts in order to determine the magnitude and direction of the burn required to return them to the shuttle bay. The relative motion trajectories were limited to the orbit plane only and the astronaut's paths began at distances between 50 and 1500 ft (15.24 and 457.2 m) from the target. In most cases, given the distances the astronaut traveled to get back to the shuttle, the majority of flight time was spent in obstacle-free space. However, Lockhart's research showed that even with the shuttle's relatively simple geometry and the mostly clear path the astronaut could follow, there were problems with the astronaut bumping into parts of the shuttle in some situations when approaching the final target location.

The problem of determining relative motion trajectories needed to travel from one point on the ISS to another is much more complex. Motion both in and out of the orbit plane must be considered given the ISS geometry and the fact that the precise distances to be traveled are limited to the added dimensions of the ISS elements. In Lockhart's paper, he says that for travel over distances of less than 100 ft, "line of sight maneuvering" worked best. In other words, instead of determining the direction required for a single burn return to target, the astronaut induces a series of small thruster maneuvers as needed to make any course changes required to reach the target. The AERCam study does focus on very close proximity travel over distances of typically less than 100 ft. However, line of sight maneuvering is not possible since the current level of AERCam programming is not "smart" enough to allow the AERCam to evaluate its surroundings and perform maneuvering thrusts as required. AERCam should be as autonomous as possible, but line of sight maneuvering would require either a level of autonomous "thinking" not yet available for an AERCam or

it would require constant control by an ISS crewmember. That in turn would also require the crewmember to maintain a constant visual fix on the AERCam. This is not always possible due to the limited number of windows on the station. So for this study, the goal is to have the AERCam perform a single thrust maneuver that results in its safe arrival at its target. An AERCam, unlike the astronaut in Lockhart's study, will have the advantage of accurate attitude determination capabilities as well as more precise control over velocity changes. Whereas Lockhart's astronauts had to determine their own attitudes and relative distance, the use of AERCam will be much more regulated and controlled. In this study, its determined trajectory will be pre-generated by a computer for each specific set of initial and target locations. The program operator will enter the parameters of the AERCam's specified flight (initial and target locations and probable travel times) into a computer program (discussed later) and will determine the exact velocity thrust needed in what direction to allow the AERCam to travel along an obstacle-free path to the target, if one exists.

The most significant impediment to generating problem-free trajectories from launch point to target at the ISS is the station's complex geometry. In order to determine if a derived trajectory around the ISS will make contact with any part of the station, a detailed station model of appropriate shape and size must be assumed. To this end, for the purposes of this study a geometric representation of the ISS was developed using a 3D Studio Max Graphics Program. The diagrams in Appendix C were chosen to be the basis for the station characteristics and dimensions used in the geometric representation. A more basic geometric shape represents each module and component. For example, if a module is generally cylindrical in shape, it will be modeled by a cylinder with diameter and length

wide and long enough to encompass the entire module. The geometric representation

developed is illustrated in Figure 11.
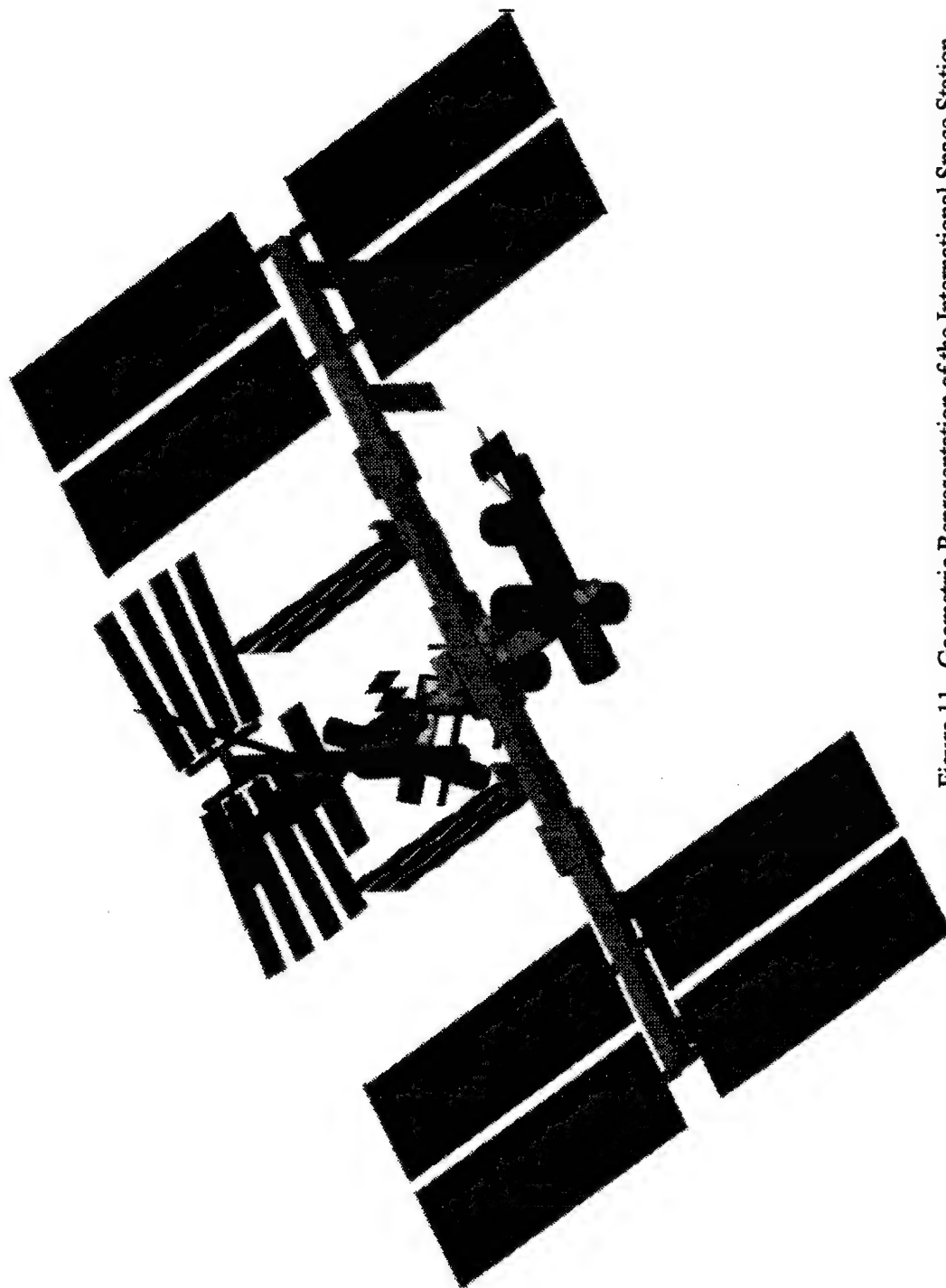
Figure 11. Geometric Representation of the International Space Station

The idea is that if a trajectory can be found which allows an AERCam to travel safely around and through the shapes which encompass the size of the station elements, then the AERCam will be able to maneuver around the station itself.

Assumptions made for the purposes of this study are :

-Circular ISS orbit

-The thrusts that will be required by the AERCam in all directions occur at the same time and instantaneously

-Two-body orbital motion

-C-W equations are adequate representations of the relative equations of motion (i.e., other than those accounted for by the C-W equations, no perturbing forces affect motion)

As mentioned before, the origin of the coordinate system used for this study is located at the station's center of mass. That center of mass is assumed to be fixed within the U.S. Laboratory, centered from front to back and side to side, at a point ¾ of the way up from bottom to top as shown in Figure 12.
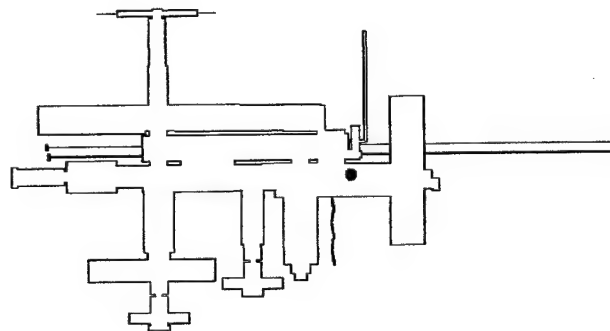
Figure 12. Location of Approximate ISS Center of Mass

Some components of the ISS are pressurized and some are not, some are sturdy and

some are delicate, and they extend from the ISS's central axes in all directions. If an AERCam is to work virtually autonomously in close proximity to the station, ISS crewmembers or computers must be capable of generating point to point trajectories which avoid numerous obstacles. The AERCam must not collide with delicate solar panels or bounce off the station walls. To test the feasibility of using AERCam successfully, a sampling of target sites were selected in those regions of the ISS's pressurized elements not easily accessed by the station's robotic arms (refer to Figure 9). Relative trajectories from likely starting points to the target locations are generated using the C-W equations. If paths can be found to allow the AERCam to safely (without collision or near-miss) arrive at various targets, the trajectory is examined more closely.

Good paths that the AERCam may follow from one point on the station to another should meet the following criteria in order for the operational concept to be deemed feasible:

-AERCam should not collide with any part of the ISS in route to its target.

-AERCam should not collide with any part of the ISS if it continues upon its trajectory past the target location for a specified period of time (if it overshoots due to propulsion system malfunction at target).

-The fuel and power requirements to follow the specified path in the given time, perform any required minor station keeping maneuvers, and return for capture cannot exceed AERCam limits. Sprint is designed to operate in space for a period of seven hours. The longer it takes the AERCam to reach the target, the less time remains for it to stay at the target to inspect.

-The specified travel time cannot be excessive; time spent monitoring an AERCam's

29

status should be minimized.

-AERCam should never move at high relative velocities.

With these conditions in mind, the following constraints were developed and considered in the process of generating potentially useful trajectories.

-At no point along its path should the AERCam come within one foot of any part of the station

-The AERCam will be targeted to a point in space three feet out from the actual target site

-Duration of travel to the target must be less than two hours

-The magnitudes of initial and final velocity change thrusts should not exceed 0.25 ft/sec (7.62 cm/s)

-AERCam's extended path must be clear for at least ten minutes after passing the intended target location along its specified trajectory

The intent is to examine the in-plane and out-of-plane charts illustrating the path the AERCam follows with respect to station for the different initial and target points at a variety of travel times. If any specific trajectories exist which meet all the stated constraints, their characteristics will be compared to those of the unsuccessful trajectories. A thorough understanding of where trajectories of any particular shape take an AERCam with respect to the various station elements is important. This understanding will aid users in later determining the types of trajectories needed to reach any other targets at the ISS.

4.2.1 Trajectory Generation Process

The close proximity trajectories of an AERCam from a "launch" position to the target coordinates were generated using a TK Solver program. The program and a description of

how it may be used is located in Appendix D. In short, the user inputs the initial and final coordinates and the desired time of travel from point to point. A list of the values determined from Equations (2) and (3) for position and velocity relative to the station's center of mass are generated at designated time intervals until the specified time of travel has been reached (until the AERCam reaches the target). These values of state can also be generated for an arbitrary period of time after the travel time specified (after the AERCam reaches its target) to represent the extended path along that trajectory. Graphs illustrating how position in one direction changes with respect to another direction over the duration of travel are plotted to show in-plane and out-of plane motion.

To determine if a trajectory can be found that meets all the specified constraints, the following process is followed for each target site. The initial and final coordinates are entered into the program. Beginning with a specified travel time of 5 minutes, the data specifying the path from initial to target coordinates is generated. The number of points for which position and velocity data is generated along the path depends upon the number of steps into which the travel time has been divided. "Steps" is a variable within the program which the user may set as desired. Each set of position coordinates for every time step along the path is compared to the dimensions of the ISS indicated in each of the Figures 13, 14, 15, and 16. When required for specific applications, the coordinates of any part of the station not indicated in Figures 13-16 were determined from the diagrams in Appendix C.

Figure 13. Coordinate Breakdown of the ISS (XZ)

32
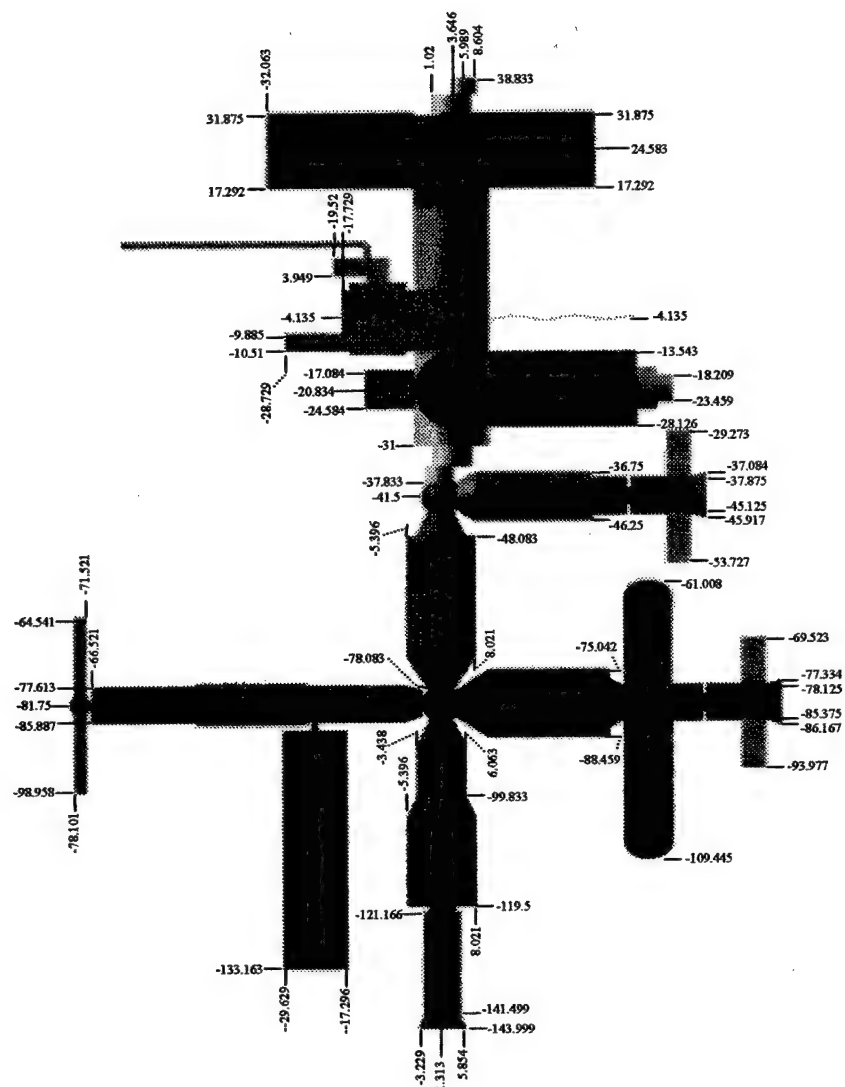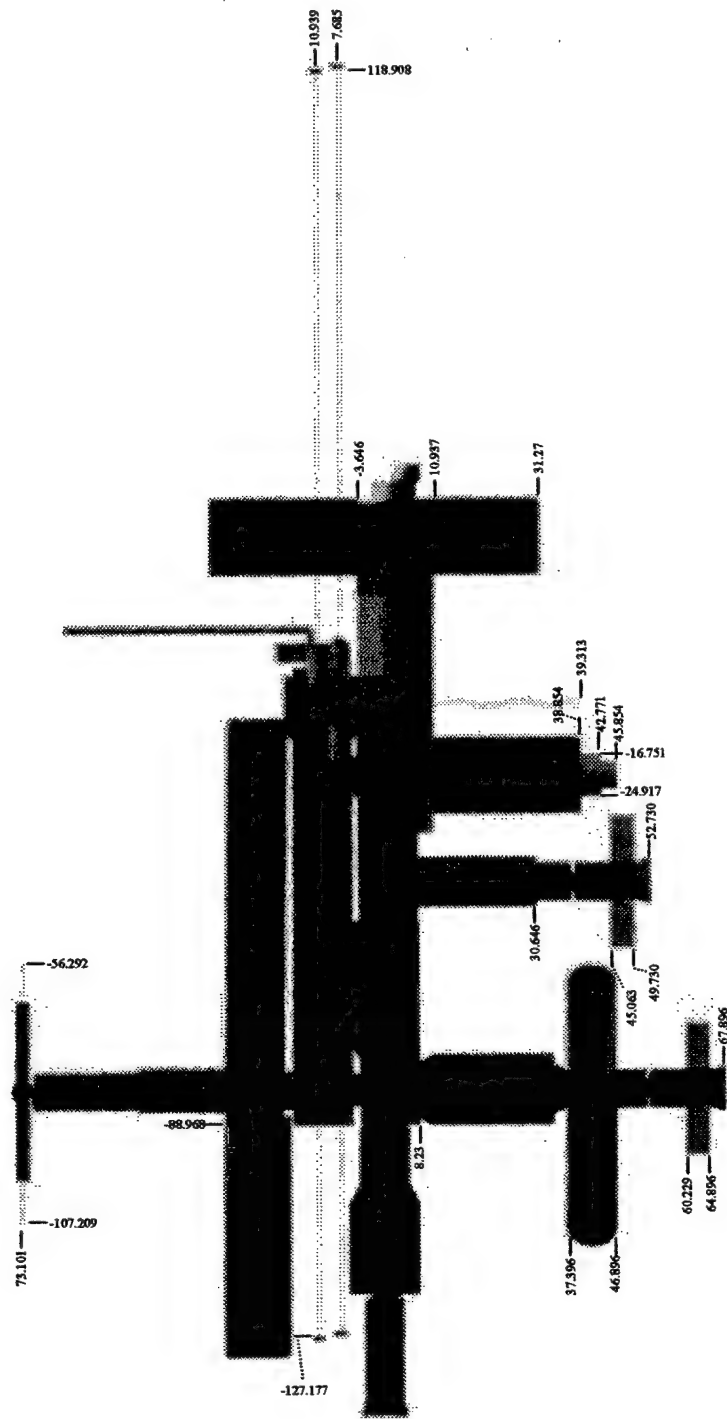
Figure 14. Coordinate Breakdown of the ISS (XZ)

33

Figure 15. Coordinate Breakdown of the ISS (XY)
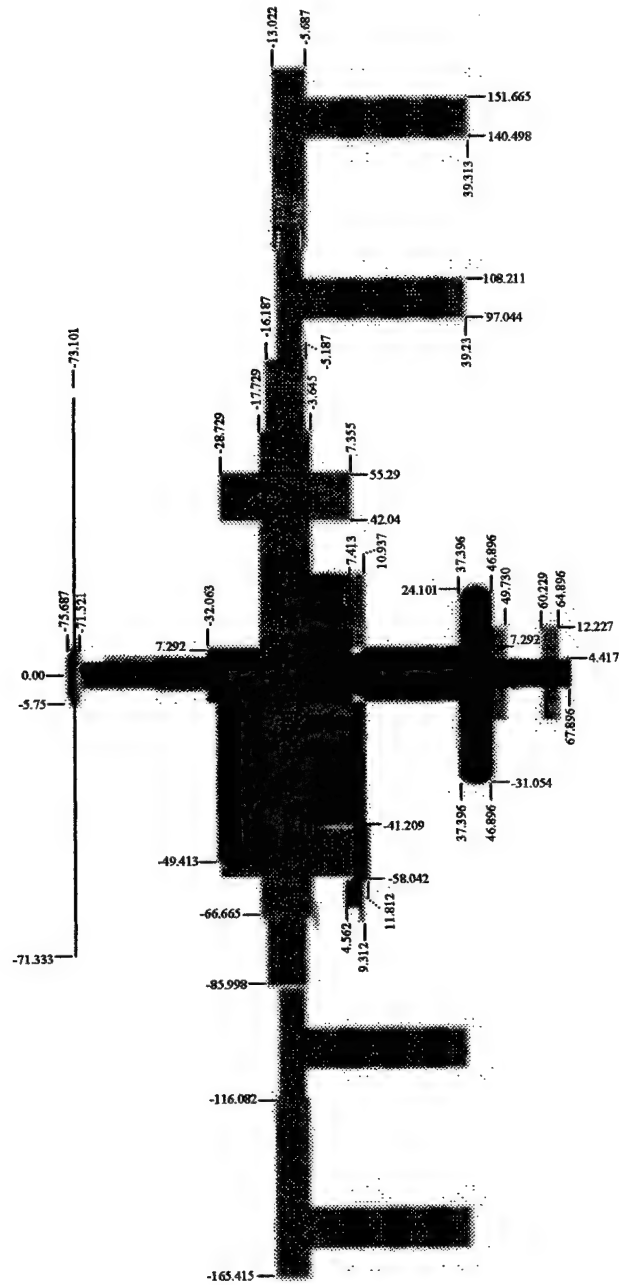
Figure 16. Coordinate Breakdown of the ISS (YZ)

If the trajectory passes within one foot of the station, it is rejected. However, care must be taken when determining whether a trajectory is acceptable. Too few points along the trajectory (too large a time interval) may lead to the assumption that an unacceptable path is acceptable. Thus the individual points alone are not enough to determine whether a path is acceptable. As the points are examined, the user must use all three perspectives of the station and its dimensions at the same time to visualize the motion of the AERCam with respect to individual station elements.

If a candidate trajectory is rejected, the travel time from the initial point to the target is increased by five minutes and a new trajectory is generated. Each new trajectory is checked to see if it meets the constraints until an acceptable trajectory is found, or until the time of travel reaches the two hour limit. If two five minute interval checks indicate that a time of travel somewhere in between them might work, the intermediate trajectory is evaluated.

Since the initial and target coordinates are fixed, the only independent variable affecting the trajectory defined is time of travel. That time determines the initial AERCam velocity, which in turn dictates the AERCam's subsequent motion relative to the station.

4.2.2 Trajectory Analysis and Results

At the ISS, there are two main locations from which objects or people might ordinarily be released into space: the Joint Airlock Module and the JEM scientific/experiment airlock (see Appendix A). The JEM airlock is large enough for an AERCam to pass through. There are, of course, other alternatives which could possibly be used in unusual circumstances, such as the Transfer Compartment of the Russian Service Module.[11,10] The Transfer Compartment is the generally spherically shaped portion of the Service Module. It will be used as an airlock for Russian EVAs (those using Russian spacesuits)

36

during station construction before use of the Joint Airlock is possible.[10] This study, however, is concerned with standard operations and will focus on release of the AERCam directly out of either the Joint or JEM airlock. At the Joint Airlock, once the interior to the station is isolated from exposure to the space environment, the outer door may be opened. A crewmember may then ensure the AERCam is guided out to its initial, or launch, position where autonomous operations of the AERCam will take over.

The initial position coordinates within the LVLH coordinate system for "launch" of the AERCam along its path were set at a distance of one foot out from either airlock. The coordinates used are:

Joint Airlock: (-20.834, 25.458, 3.646)   (ft)

JEM airlock: (22.250, -43.709, 3.646)   (ft)

Figure 17 indicates the location of the two airlocks on the station. Note that both airlocks open in the direction of the station's Y axis.
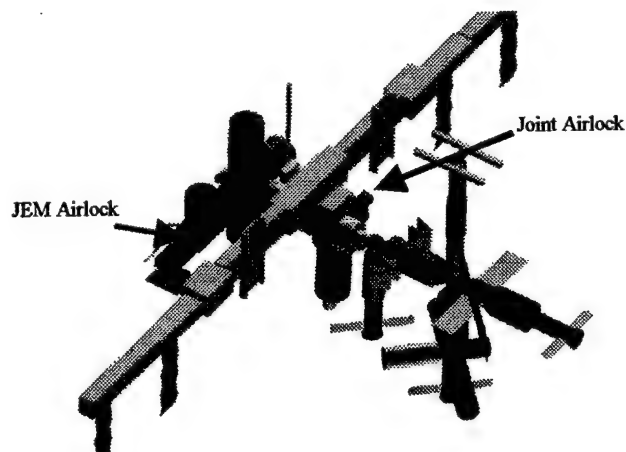
Figure 17. Joint and JEM Airlock Locations on the ISS

To get a good idea of how easy or difficult it would be for an AERCam to reach any target successfully and what sort of problems or obstacles it may possibly encounter, a

sampling of targets within those regions circled back in Figure 9 were selected for analysis. All possible target sites within the viewing range of the SVS cameras were eliminated from the list of candidate test targets for this AERCam study. The target sites listed in Table 2 were therefore selected to be examined.

Table 2. Target Sites Used in AERCam Trajectory Analysis

Target #	Description of Target Location
1	Immediately behind the station; behind the Progress module
2	Right under the Pressurized Mating Adapter connected to the Habitat module
3	X – side of the top part ("spherical") of the Soyuz closest to the truss system
4	Right underneath the Columbus Orbital Facility, next to the Mini Pressurized Logistics Module
5	X + side of the top part ("spherical") of the Soyuz closest to the truss system
6	Y – side of the top part ("spherical") of the Soyuz farthest from the truss system
7	Y – side of the "spherically" shaped part of the Service Module
8	Y – side of the ISS where Progress connects to the Service Module
9	X + side of the "spherically" shaped part of the UDM, between the research and storage modules
10	Y – side of the "spherically" shaped part of the UDM, between the research/storage module and the life support module
11	X – side of the "spherically" shaped part of the UDM, between the life support module and the docking compartment
12	Y + side of the "spherically" shaped part of the UDM, between the docking compartment and the research/storage module
13	Y – side of the top part ("spherical") of the Soyuz closest to the truss system

Once the coordinates for the target site are determined from Figures 13-16 and the drawings in Appendix C, three feet is added to the appropriate vector component in order to bring the AERCam target coordinates to a distance of three feet out away from the station. Refer to Figure 18 to get a better idea of where these targets are on the station.
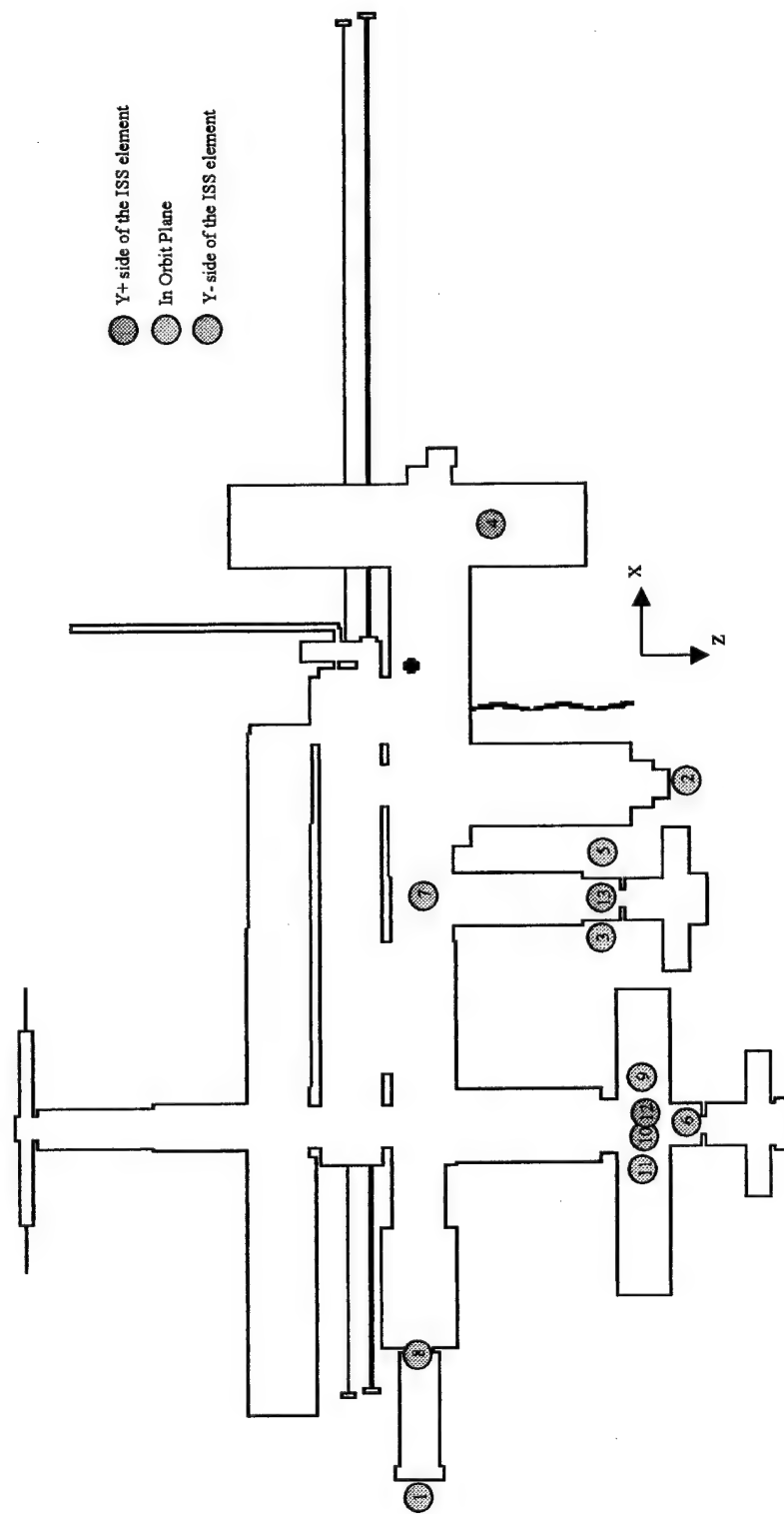
Figure 18. Location of Target Sites at the ISS

39

Analysis of paths from the Joint Airlock Module to the various targets was completed

first. Precise trajectories meeting all the stated constraints were eventually found for seven

of the 13 target sites examined. The data characterizing these trajectories are found in

Table 3. Graphs depicting the in-plane and out-of-plane motion of the AERCam with

respect to the station's center of mass for these trajectories and any others discussed in this

paper may be found in Appendix E. A sample of a data list with the points used to generate

such graphs are also found there. Two sample trajectory plots for the trip to target #1 are

shown in Figure 19. For display purposes, the "display" Z axis, Zout, on the plots points

away from the Earth. This is not consistent with the defined LVLH reference directions,

but it reduces confusion when examining the plots since it is difficult to reconcile going

"up" the Z axis with going toward the Earth.

Joint Airlock to Target #1   Time of Flight - 26 minutes
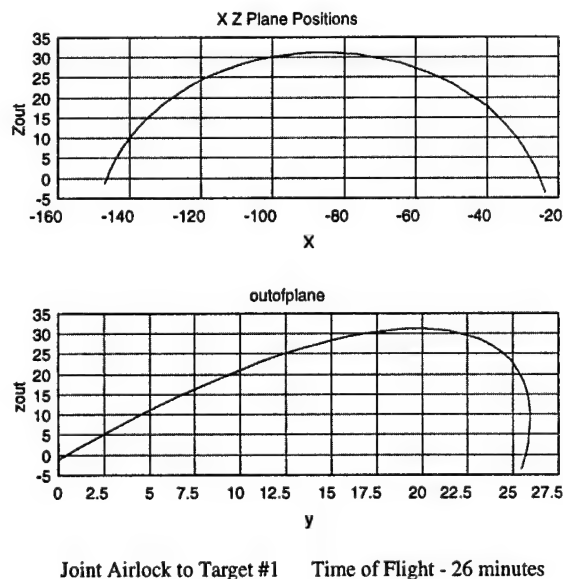
Figure 19. Sample Trajectory Plots

Table 3. Trajectory Characterization Data for Paths Originating at the Joint Airlock

Target (Travel time in min)	Initial Position (ft) (X, Y, Z)	Target Position (ft) (X, Y, Z)	Initial Velocity (ft/s) (X, Y, Z)	Velocity at Target (ft/s) (X, Y, Z)
1 (26)	(-20.834, 25.458, 3.646)	(-146.999, 0, 1.313)	(-0.027001, 0.005654, -0.083488) .087928	(-0.032283, -0.029147, 0.081318) .092219
2 (5)	(-20.834, 25.458, 3.646)	(-20.834, 0, 48.854)	(-0.049509, -0.081572, 0.1345290) 0.164934	(0.052847, -0.086513, 0.163955) 0.192766
3 (10)	(-20.834, 25.458, 3.646)	(-49.25, 0, 35)	(-0.071723, -0.035695, 0.001447) 0.080128	(-0.000734, -0.045877, 0.099017) 0.109131
4 (3.5)	(-20.834, 25.458, 3.646)	(24.583, 10.292, 13.937)	(0.203110, -0.068528, 0.086891) 0.2313	(0.221882, -0.0733339, -0.008301) 0.233834
5 (12)	(-20.834, 25.458, 3.646)	(-33.75, 0, 35)	(-0.043702, -0.026945, 0.005692) 0.051656	(0.027286, -0.039289, 0.076527) 0.090247
9 (5)	(-23.834, 25.458, 3.646)	(-72, 0, 42)	(-0.196510, -0.081572, 0.060828) 0.221292	(-0.109673, -0.086513, 0.192403) 0.237764
12 (7)	(-23.834, 25.458, 3.646)	(-81.75, 10, 42)	(-0.168669, -0.031246, 0.010111) 0.171837	(-0.081832, -0.040972, 0.004296) 0.091617

The path to target #1 goes up above the ISS pressurized components, back and down to the target site in a simple arc, remaining at all times on the same side of the station as the Joint Airlock and below the SPP PV array (refer to Figure 2 for component locations). To arrive at target #2, which is almost directly below the airlock, the AERCam travels quickly downward, arcing slightly back in the negative X direction along the way. The path to target #3 is a downward slope back and in toward the target, arcing around the Y+ side of the front Soyuz to arrive at the target site on the X – side of that Soyuz. The path to target

41

#4 is a simple forward path to the target, going slightly down and in along the Y axis to arrive under the Columbus Orbital Facility. Path #5 is also uncomplicated, swinging back, down and in to the target on the X + side of the front Soyuz. The path to target #9 is almost linear in shape for both in- and out-of-plane motion. It arcs just slightly as it goes directly back, down under the Functional Cargo Module panels, and in to arrive from above at the target site between the two Research modules. The path to target #12 is almost the same as that to #9, going just a little farther back and not as far in along the Y axis. An AERCam would float down to target #12 from above, in between the Docking Compartment and the starboard side Research Module.

Note that the initial position value along the X axis for the first five target sites is different than for subsequent targets. The trajectories were originally generated starting at the center of the airlock. After examining those trajectories to a few of the target sites, it was clear that the AERCam would have problems in some later cases at the start of its journey with bumping into the edge of the airlock itself. Changing the starting position just slightly so the AERCam began its journey aligned with the back edge of the airlock made it easier to generate clear-path trajectories. Such a change makes no significant difference in the operational procedure for AERCam release since the crewmember can just guide the AERCam farther back before releasing control.

For four of the remaining targets, no trajectory could be found which would allow the AERCam to arrive at the target safely while conforming to all the specified constraints. However, paths could be determined for which the AERCam met all of the constraints except the free path overshoot requirement. The relevant data for these paths are in Table 4 including the velocities at which the AERCam would bump into the station and where after

42

passing the target (refer back to Figure 2 and Table 1 for location references).

Table 4. Trajectory Characterization Data for Paths Originating at the Joint Airlock

Target (Travel time in min)	Initial Position (ft) (X, Y, Z)	Target Position (ft) (X, Y, Z)	Initial Velocity (ft/s) (X, Y, Z)	Velocity Magnitude at Bump (ft/s; cm/s) (description of bump location)
6 (65)	(-23.834, 25.458, 3.646)	(-81.75, -7.4, 50)	(0.004154, -7.E-05, -0.049373) 0.049547	0.11397; 3.4738 (hits the bottom of the Soyuz closest to the truss system)
8 (65)	(-23.834, 25.458, 3.646)	(-121, -6.584, 1.313)	(0.012195, -0.001037, -0.013476) 0.018205	0.03252; 0.99121 (bumps into the back edge of the Service Module)
11 (70)	(-23.834, 25.458, 3.646)	(-91.5, 0, 42)	(0.007230, 0.001218, -0.045450) 0.046038	0.09839; 2.9989 (will hit the UDM, right at target site)
13 (65)	(-23.834, 25.458, 3.646)	(-41.5, -7.4, 34)	(-7.E-05, -0.030813, 0.073021) 0.079256	0.07903; 2.4088 (bumps into the bottom of the Habitat)

Hence, safe travel from the Joint Airlock to these targets along the determined paths is possible, but if something goes wrong with the propulsion systems when the AERCam reaches the target, a collision would occur. The velocities at which the AERCam would hit the station after passing by the target are rather low, and the parts of the ISS with which the AERCam will come into contact are sturdy. If a malfunction did occur and the collision resulted, minimal damage would be sustained by either the ISS or the padded AERCam. The only major problem would be in then retrieving the rebounding AERCam.

No trajectory at all could be found for targets #7 and #10 (the Y – side of the Service Module's front section and the Y – side of the bottom of the UDM) that the AERCam could follow to get to the target coordinates without running into some part of the station. Their initial and final coordinates are

43

7: r_o = (-23.834, 25.458, 3.646) r_{tgt} = (-41.5, -7.667, 1.313)

10: r_o = (-23.834, 25.458, 3.646) r_{tgt} = (-81.75, -10, 42)

The accuracy with which the initial velocities are recorded in Tables 3 and 4 may seem excessive. However, very precise velocities are typically required for an AERCam to successfully reach the target site in every case.

An extremely small deviation in the magnitude of thrust could cause the AERCam to bump into the station. While in many cases this would not cause significant damage to the station or the AERCam, there is a chance that the camera could float into one of the more delicate solar panels or radiators. To illustrate this sensitivity to initial velocity, the initial thrust magnitudes for the trajectories of two sample targets were altered just slightly. The differences in velocity magnitudes for each target are shown in Table 5.

Table 5. Examples of Initial Velocity Deviations which Significantly Alter a Trajectory

Target	Original Initial Velocity (ft/s)	Altered Initial Velocity (ft/s)	Approximate Change in Initial Velocity (ft/s)
5	(-0.043702, -0.026945, 0.005692) 0.051656	(-0.0367, -0.0177, -0.00624) 0.04125	0.007 0.009 -0.0006 -0.01
6	(0.004154, -7.E-05, -0.049373) 0.049547	(0.00260, -0.00849, -0.04917) 0.04997	-0.002 -0.008 0.0002 0.0004

The resulting trajectories in these cases were not acceptable. For a complex path like that from the Joint Airlock to target #6 (requiring passage close by many station components to the other side of the station), the extremely small deviation introduced causes the AERCam to glide into the SPP instead of arriving at the target. The same type of sensitivity, though not as extreme, is also present even for a more straightforward path. When the velocity change thrust required to send the AERCam from the Joint Airlock to

target #5 was decreased by about only 1/100 ft/s, the AERCam would end up floating right into the Docking and Stowage Module. An AERCam designed for use at the ISS would have to have atypically precise thrust control and very accurate relative position and velocity determination capabilities. The calculation of the initial thrust velocities would also have to be meticulous.

The data in Tables 3 and 4 and the associated relative motion plots for each trajectory (Appendix E) lend themselves to the development of certain guidelines from which a target may be characterized as being easier or more difficult to reach. These preliminary guidelines do not always hold true for every case, but in general a trajectory with the following characteristics is less likely to be problematic:

-It minimizes close range fly-bys

-It allows the AERCam to arrive at the target from above (if the target has obstacles on either side of it the camera can just float down in from above instead of over, around, under, and up; consider that the airlocks are about level with or above all the sampled targets)

-Out-of-plane motion is minimized

-There is no particular obstacle consistent within every path (like the truss system)

-It requires less than a 30 minute travel time

-The target is located on the same side of the station as the airlock

At this point the sample targets can be divided into two types: those which could possibly be more easily reached by starting the AERCam at the JEM airlock and those which would be more difficult to reach. Any target site located on the Y+ side of the station will be relatively easy to reach from the Joint Airlock since the initial position is farther out

45

the Y axis than any sampled target. An AERCam just swings back and in along the line of the axis. Targets on the X+ side of a station element seem to be more easily attainable from the Joint Airlock due to its position with in the ISS configuration. The AERCam can just float out and into position easily without having to pass by the integrated truss system.

The trajectories to targets #1 - #5, #9, and #12 from the Joint Airlock are relatively simple. Travel out-of-plane is kept to a minimum (none crossing over to the Y- side of the station) and passage very close to any of the station elements did not occur until just approaching the target site. After having gained a more thorough understanding of how the AERCam tended to move relative to the station, it is clear that these targets would definitely not be easier to reach from the JEM airlock. Trajectories to those targets originating at the JEM airlock would be more risky and time consuming given the airlock's and the targets' locations relative to the truss system. No attempt to calculate these trajectories was made.

The targets that could potentially be more easily reached by starting the AERCam at the JEM airlock include targets #6, #7, #8, #10, #11 and #13. Thus the procedure with the TK Solver program and trajectory generation was repeated for an AERCam originating at the JEM airlock for those six targets listed above only. Any clear-path trajectory data found for each of the targets is in Table 6.

Table 6. Trajectory characterization Data for Paths Originating at the JEM Airlock

Target (Travel time in min)	Initial Position (ft) (X, Y, Z)	Target Position (ft) (X, Y, Z)	Initial Velocity (ft/s) (X, Y, Z)	Velocity at Target (ft/s) (X, Y, Z)
6 (40)	(22.250, -43.709 3.646)	(-81.75, -7.4, 50)	(-0.01527, -0.126, -0.07171) 0.145781	(0.089684, 0.134499, 0.08302) 0.181729
7	(22.250, -43.709 3.646)	(-41.5, -7.667, 1.313)		
8	(22.250, -43.709 3.646)	(-121, -6.584, 1.313)		
10 (10)	(22.250, -43.709 3.646)	(-81.75, -13, 42)	(-0.18731, 0.037858, -0.06761) 0.202701	(-0.10047, 0.060539, 0.190503) 0.223719
11	(22.250, -43.709 3.646)	(-91.5, 0, 42)		
13	(22.250, -43.709 3.646)	(-41.5, -7.4, 34)		

Table 6 shows that precise trajectories meeting all the stated constraints were found for only two of the seven target sites examined, #6 and #10. For targets #7, #8, #11, and #13 no trajectories could be found to meet the constraints. A path that was at least clear to the target was found to get the AERCam to target #13, but the velocity required exceeded the 0.25 ft/s constraint.

Evaluating the paths to these six targets listed above indicated that the integrated truss system would be a significant obstacle when launching an AERCam from the JEM airlock. All of the targets an AERCam would be sent to examine (those that cannot easily be inspected with a SVS) are on the other side of the truss system from the JEM. One way or another, the AERCam would have to either pass over or under it safely. Unfortunately, this

is not an easy task. There are only specific paths which will meet the constraints of the study and adhere to the equations of motion. The AERCam cannot "duck under" the trusses then bob back up to continue undeterred on those paths to a target. However, certain patterns were revealed among the trajectories that were generated for the six sample targets as travel time was increased. These helped to determine whether or not a good trajectory was even a possibility.

No matter what the target, only travel times less than approximately 10 minutes gave trajectories on which the AERCam could travel under the truss system towards the back of the station. Such short times are associated with the most direct routes and require higher velocities. Also, the trajectories generated were straighter than most and tended to pass right through any station components situated between the JEM airlock and the target (instead of out and around them). Figure 20 shows the shape of such a trajectory.

JEM Airlock to Target #10   Time of Flight - 10 minutes
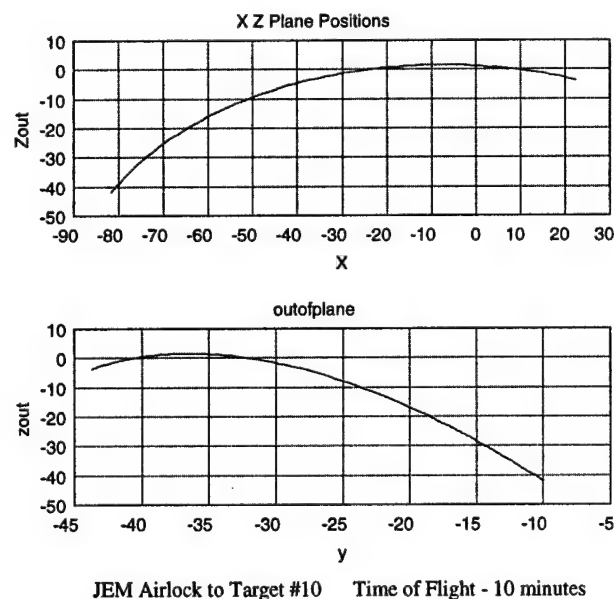
Figure 20. Example of a "Straight"-Line Trajectory

For travel times between approximately 10 and 25 minutes, the arc of the trajectory

48

moved "higher" in the negative Z direction and was almost be guaranteed to fly the AERCam into the truss system. When the trajectory was finally high enough for the AERCam to cleanly clear the top of the truss and potentially reach the target safely, the time of travel was approaching 50 minutes.

A sudden change in the direction of travel occurred when the duration of flight exceeded roughly 50 minutes. The out-of-plane component of the trajectory abruptly changes to send the AERCam out in the Y+ instead of the Y- direction. For travel times between 50 minutes and 60-70 minutes, this caused the AERCam to float right back into the JEM module.

In the instances when travel times over 70 minutes were checked, the increase in distance traveled due to the increased travel time typically caused the AERCam to encounter an obstacle. It seems that the longer the AERCam is in motion, the greater the risk of contact with the ISS. Occasionally, an obstacle appeared at the start of the journey, when the AERCam's trajectory would initially direct it down and through the JEM exposed facility before continuing on to travel up and over in the Y+ direction.

Figures 21 thru 24, plots of trajectories to target #13, illustrate the preceding descriptions.

In-Plane Trajectories from JEM Airlock to Target #13
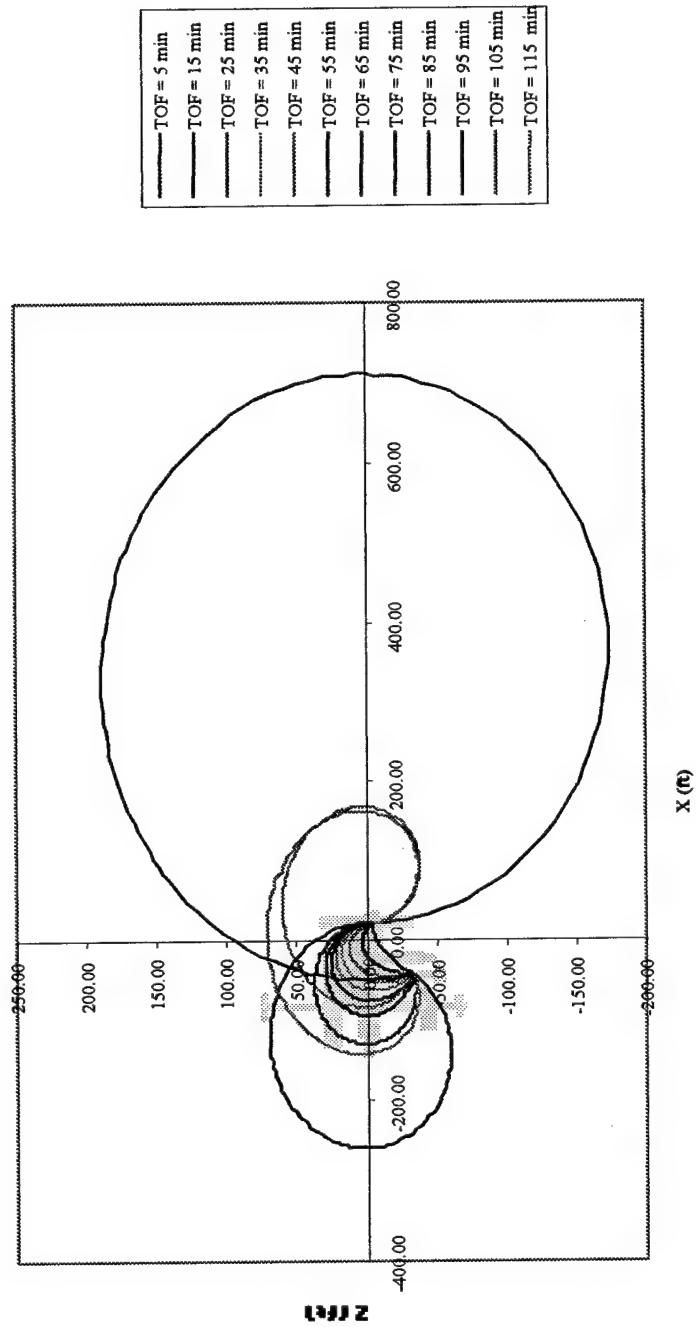
Figure 21.
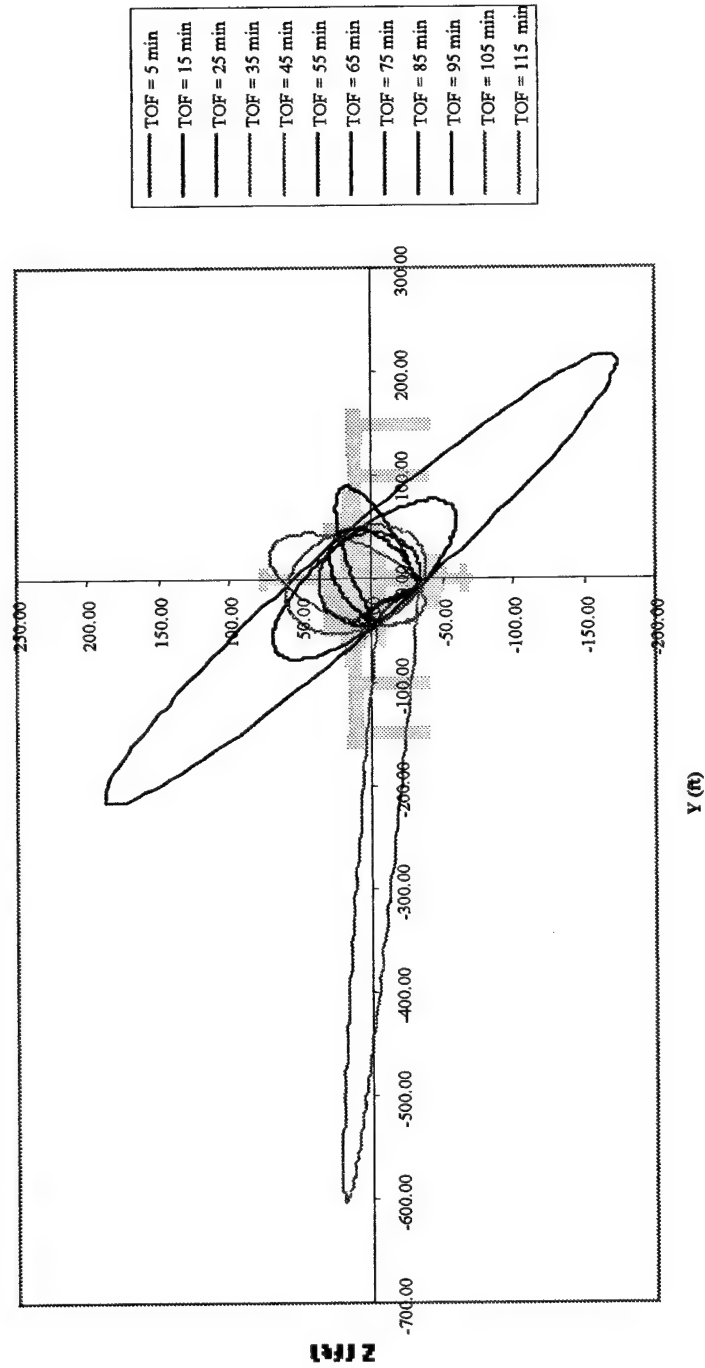
50

Out-of-Plane Trajectories from JEM Airlock to Target #13

TOF = 5 min
TOF = 15 min
TOF = 25 min
TOF = 35 min
TOF = 45 min
TOF = 55 min
TOF = 65 min
TOF = 75 min
TOF = 85 min
TOF = 95 min
TOF = 105 min
TOF = 115 min

Figure 22.

51

In-Plane Trajectories from JEM Airlock to Target #13
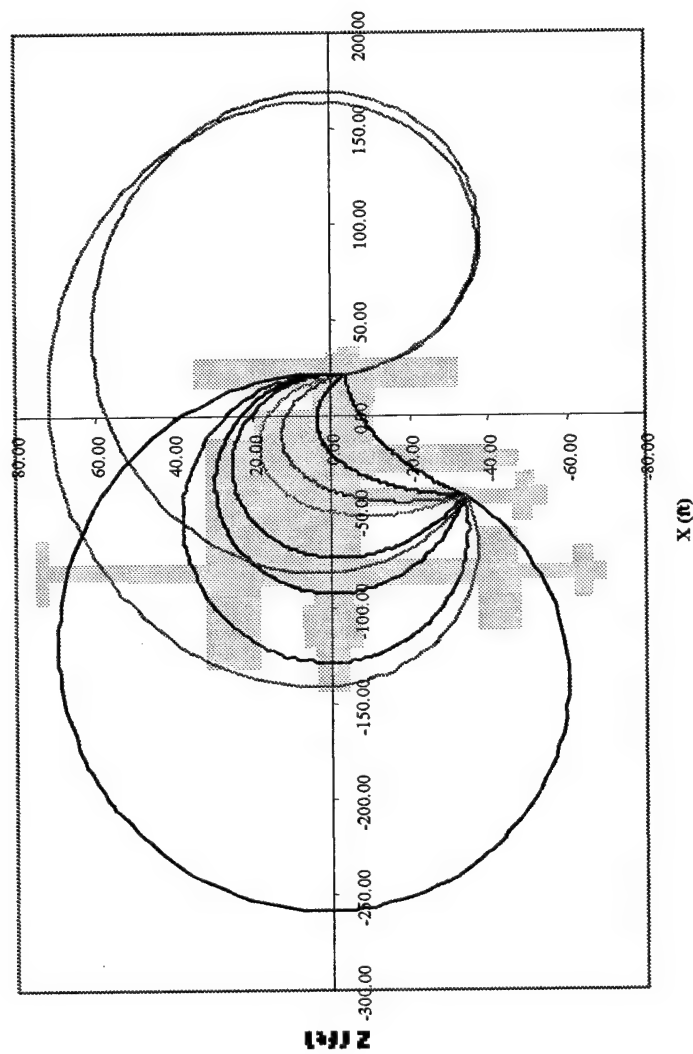
TOF = 5 min
TOF = 15 min
TOF = 25 min
TOF = 35 min
TOF = 55 min
TOF = 65 min
TOF = 75 min
TOF = 85 min
TOF = 105 min
TOF = 115 min

X (ft)

Z (ft)

Figure 23.

52

Out-of-Plane Trajectories from JEM Airlock to Target #13

Figure 24.

53
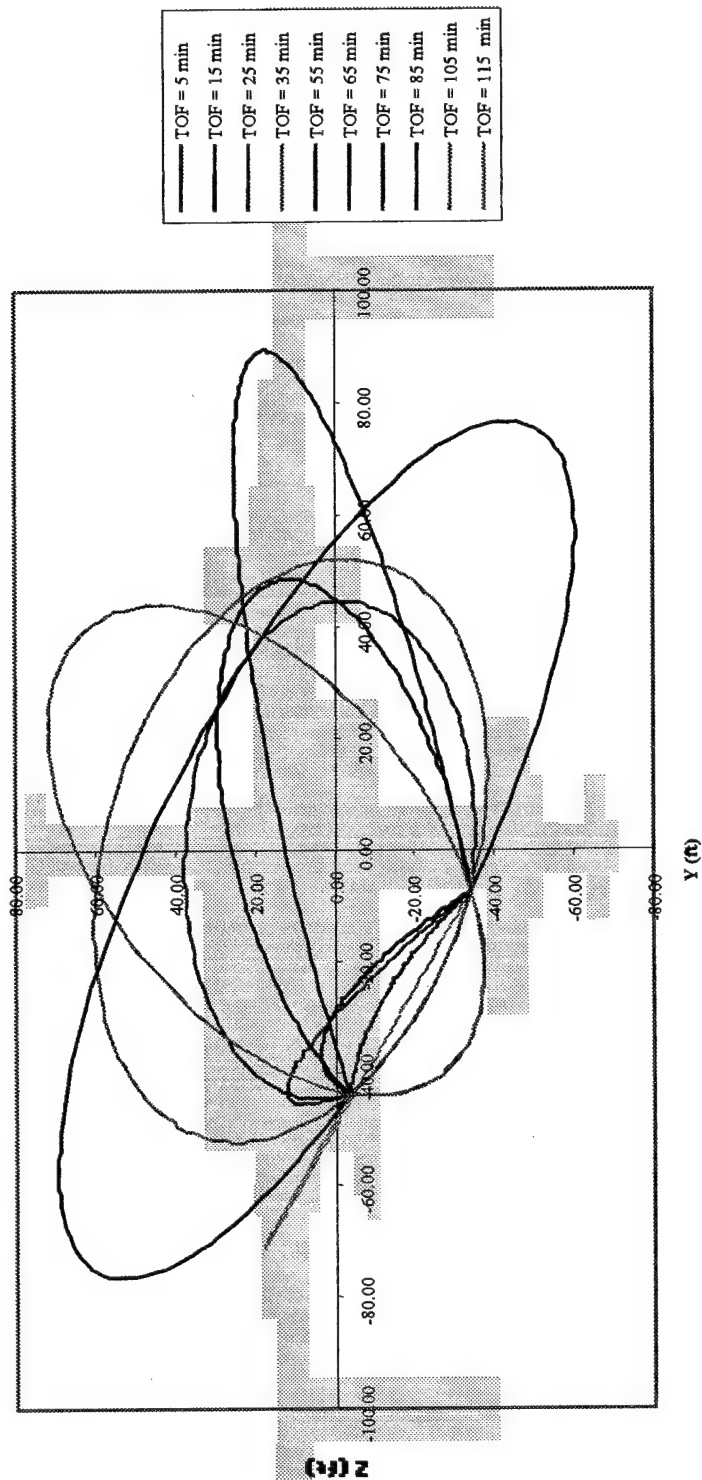
Regarding the change in travel in the Y direction for times over about 50 minutes, the same pattern was apparent in the trajectories generated from the Joint Airlock. However, the out-of-plane motion began in the Y+ direction and then switched over to the Y- direction for travel times over 50 minutes. This phenomenon is a consequence of the solutions of the C-W equations. Recognizing such trends in the flight paths resulting for various travel times was very useful in aiding the trajectory generation process, once the relative motion became intuitive to the user.

For both sets of initial coordinates, there were clear patterns to how the shape of the trajectory changed as flight duration was increased. As more targets were tested and the paths for those intermediate times leading up to the one that "worked" were examined, it became easier to predict what the approximate travel time range would be for various targets. A clearer intuitive understanding about the motion of the AERCam with respect to the station components was developed. It became easier to arrive at a working trajectory or to conclude that there would not be a path which met the constraints. For instance, clearly there were problems reaching target #7. The plots in Figures 25 and 26 illustrate the trend the shape of the trajectory follows as travel time is increased. The paths in Figure 25a,b originate from the Joint AIRLOCK, in Figure 26a,b from the JEM airlock.
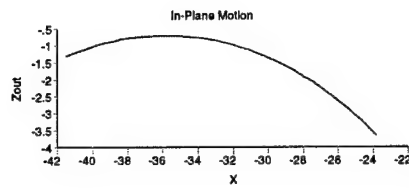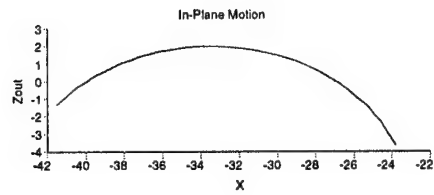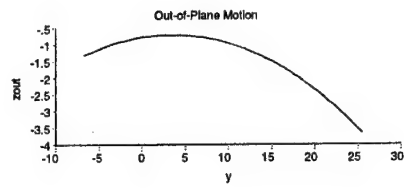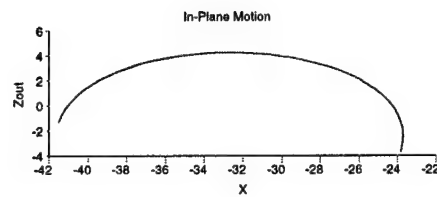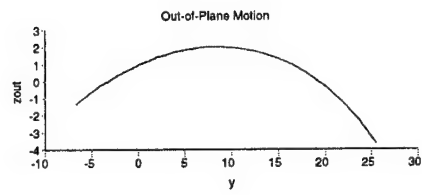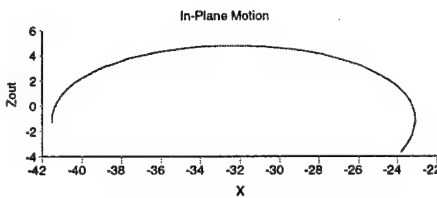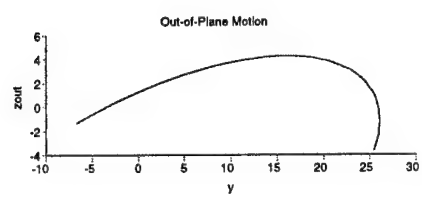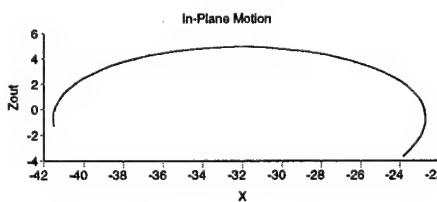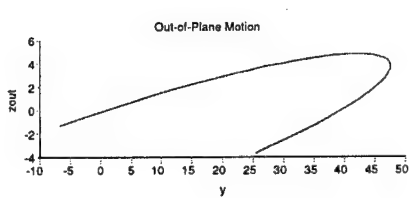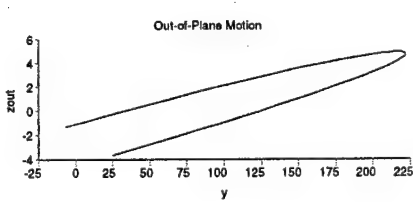
IN-PLANE   OUT-OF-PLANE

Figure 25a. Illustration of How In and Out of Plane Motion Changes as Time of Travel Increases-
Motion is from the Joint Airlock to Target #7

IN-PLANE   OUT-OF-PLANE
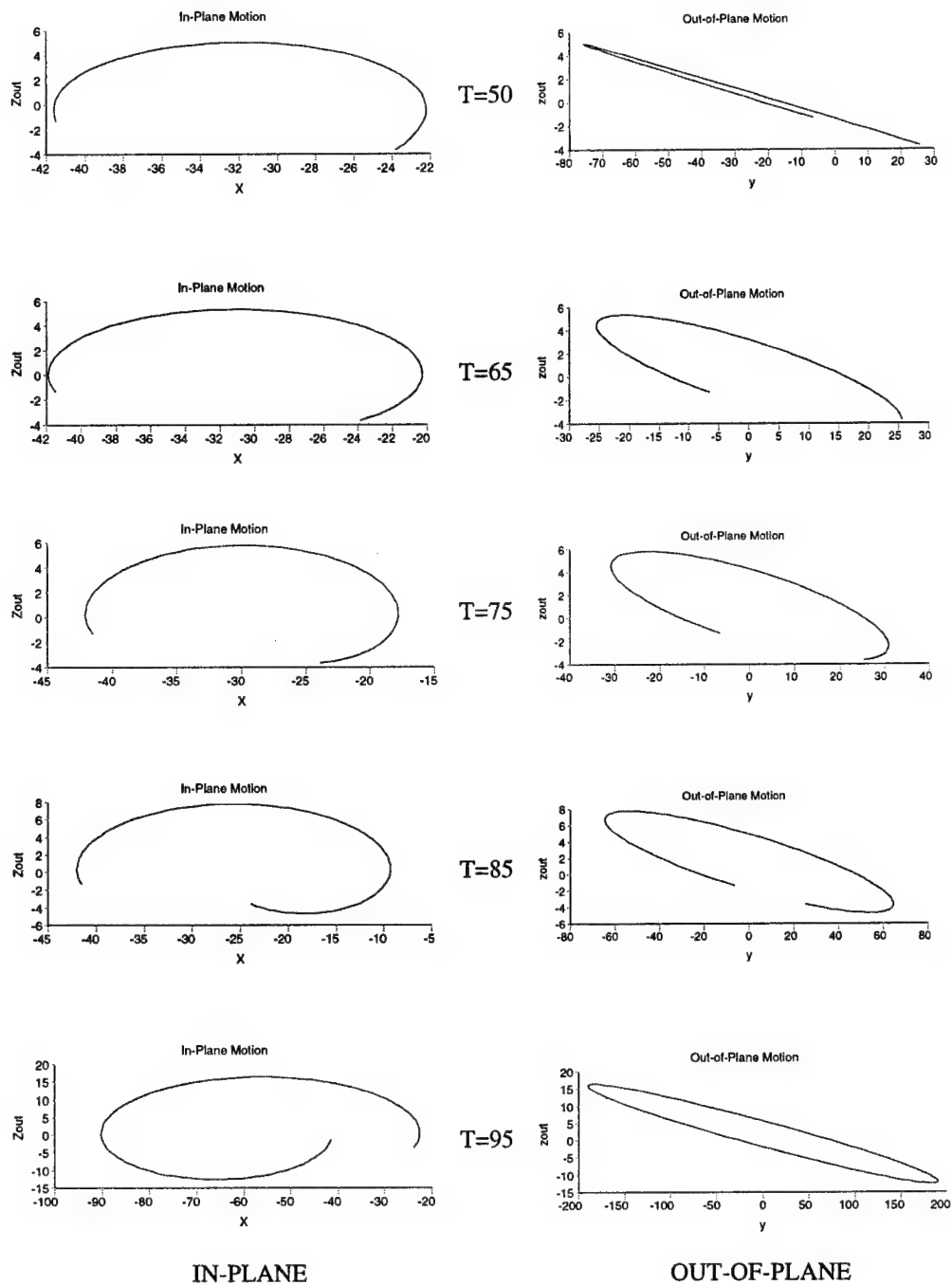
Figure 25b. Illustration of How In and Out of Plane Motion Changes as Time of Travel Increases-
Motion is from the Joint Airlock to Target #7

56
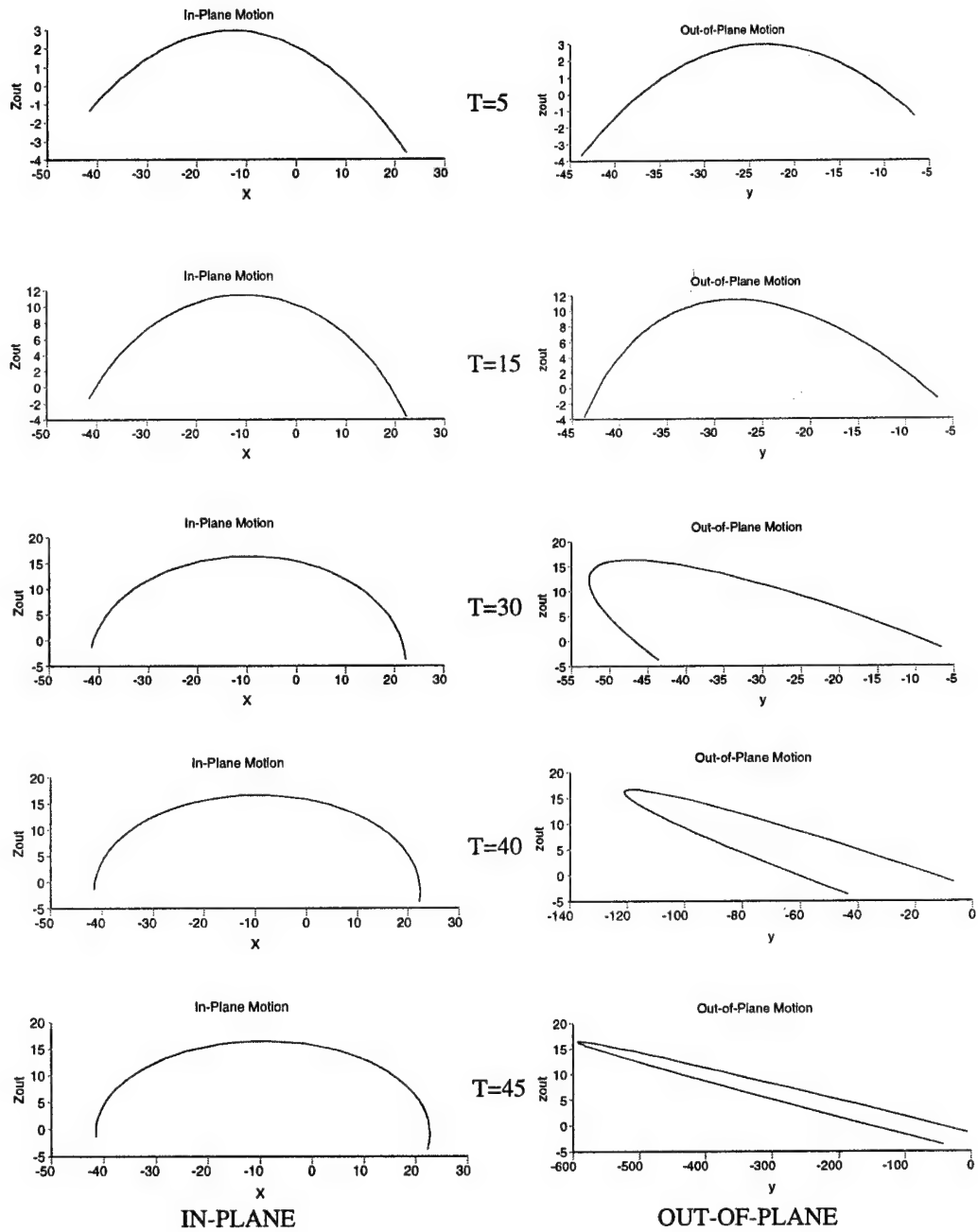
Figure 26a. Illustration of How In and Out of Plane Motion Changes as Time of Travel Increases-
Motion is from the JEM Airlock to Target #7
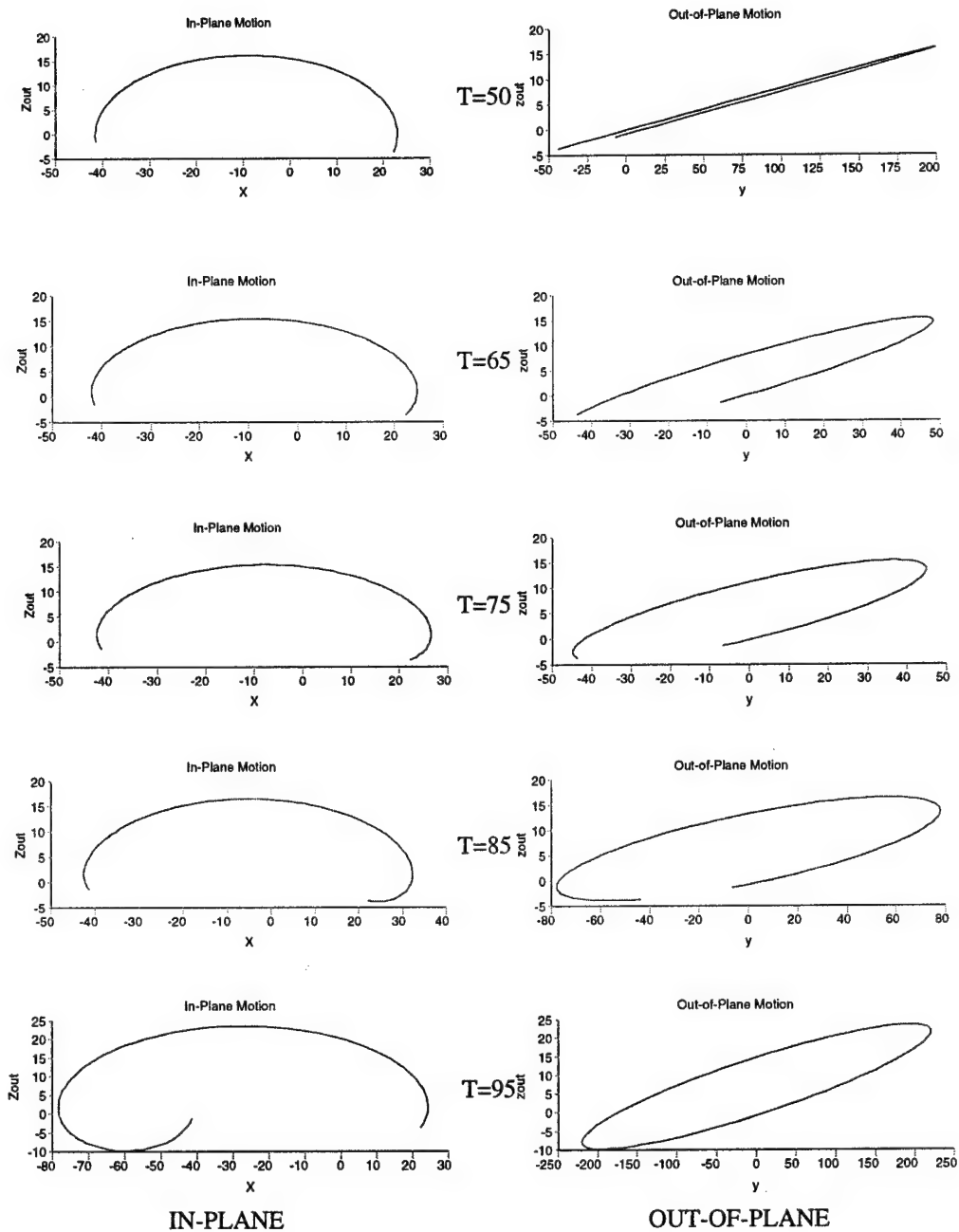
Figure 26b. Illustration of How In and Out of Plane Motion Changes as Time of Travel Increases-
Motion is from the JEM Airlock to Target #7

The figures show a distinct similarity in the plots when comparing the Joint Airlock and the JEM airlock regarding the manner in which the shapes of the trajectories change as travel time increases. The plots also show in general how the trajectories to all the targets tend to change as travel time was increased. Note the increase in out-of-plane motion as time approaches 50 minutes, and then the abrupt change in direction of travel (this could be predicted by the equations of motion in Section 2.4). As flight duration continues to increase, the periodic nature of the out-of-plane motions begins to appear.

After examining these trajectories for target #7 and recalling those from all the other targets already examined, certain conclusions can be drawn relating to how difficult it would be to send an AERCam to inspect certain portions of the ISS. For instance, the author hypothesized that it would be very difficult to arrive at another target on the Y – side of the station approximately the same distance back along the negative X axis as target #7. Target #13 was actually added to the target list to test this idea. The results showed that no path from either airlock met all of the constraints, supporting the author's hypothesis.

As the data in Table 4 showed, a trajectory from the Joint Airlock to target #13 met all but the overshoot constraint. The location of the target coordinates down the Z axis made that possible (the AERCam had to go around to the other side of the station, traveling under the Functional Cargo Module which was right in the path of any trajectory to target #7). From the JEM airlock, only one trajectory allowed the AERCam to arrive at target #13 without bumping anything along the way, but it required a thrust at the airlock and a "braking" thrust at the target with magnitudes of about 0.68 ft/s. That trajectory was for a flight duration of 45 minutes. Even if such a thrust magnitude were to be permitted, there is no free path beyond the target on that trajectory. If anything went wrong, an AERCam

59

would hit the station at a much higher speed than that associated with any of the other bump scenarios previously discussed. Obviously there are some problems inspecting certain target locations with either the robotic arms or an AERCam originating at one of the airlocks.

4.2.3 Alternatives Strategies for AERCam Use

There are strategies outside the focus of this study that might allow otherwise unreachable regions of the station to be inspected. Consider again the task of getting an AERCam to targets #7 and #13. The experience gained in this study leads to the following generalizations. The first is that the AERCam could be launched from either airlock to easily obtainable target coordinates on the Y- side of the station in the vicinity of #7 or #13 and brought to zero relative velocity there. Those positions should be within the viewing range of a crewmember within the cupola. The crewmember could then manually guide the AERCam in slowly toward the target site in the same manner that Astronaut Lindsey operated Sprint when it was tested in the shuttle bay. This is, of course, a very region-specific strategy. This procedure cannot be used for any targets except those in the immediate vicinity of the cupola.

A second alternate strategy would be more universal. It would require using the SSRMS in combination with an AERCam. When the SPDM is connected to it, the SSRMS is able to "pick up" the AERCam at an airlock and move along the truss while connected to the MBS. When it reaches the place along the Y axis coincident with the desired initial coordinates, it would position itself in the orbit plane to release the AERCam where preferred. There would be a virtually infinite number of initial positions for an AERCam released from the SPDM since the SSRMS can be positioned anywhere along the length of

60

the truss and the arm can be moved and rotated as desired. Release coordinates in the X and Z directions would be limited to the reach of the arm when connected to the MBS. No other PDGF would allow such mobility because with an AERCam at one end, the SSRMS must remain fixed to a single PDGF. Moving like an inch worm around the station requires two free ends. The facts that the MT's track runs along the X+ side of the truss system, that the JEM airlock is on that side of the trusses, and that the JEM airlock is a scientific/equipment airlock, make it clear that the AERCam "pick up" point should be the JEM airlock.

The final alternate strategy improves upon the second. The placement of the AERCam with respect to the station by the SSRMS is limited to the reach of the arm from the truss. However, with certain design modifications, it would be possible for the SSRMS to pick up the AERCam and maneuver it to virtually any point around the station, not just those within the arm's reach of the truss system. Mounting fixtures would have to be placed at various locations around the ISS in a manner similar to how the PDGFs are spread out. These fixtures could act as temporary holding stations for an AERCam. The SSRMS would pick up the AERCam, stretch to the fixture farthest from it in the direction of the target, and lock the AERCam down into the fixture. The SSRMS can then inch worm its way forward towards the target. It would then reach back to reacquire the AERCam from its locking fixture, move it forward to the next fixture, lock it in, etc., until the SSRMS can position the AERCam at the desired initial coordinates. The experience gained from studying relative motion trajectories around various components of the ISS leads to the conclusion that any target site on the ISS would be AERCam accessible if it is moved and released in this manner. This procedure puts virtually all of the station's pressurized elements within a short, easy flight from an AERCam's release point.

Note that the problem of returning an AERCam to its release coordinates is essentially the same one as getting to the target in the first place. It is important to remember, however, that the two paths will be completely independent of one another (they will not be the same path or even mirror image paths). The equations of relative motion do not permit the AERCam to retrace its original path back to where it started without an enormous expenditure of fuel, and this study is focused on only permitting a single, small, instantaneous thrust to get the AERCam from point to point. Just as the SSRMS-SPDM combination could potentially help in getting the AERCam to the target, it could also be used to make its recovery easier. The SSRMS could be positioned in any location convenient to the task and the SPDM could be used to capture the AERCam and return it to the JEM airlock.

4.2.4 Relative Drift Analysis

Once an AERCam successfully arrives at the target location and performs its thrusting maneuver to bring its velocity relative to the station back to zero, the remote camera will be in position to fulfill its inspection mission. However, the C-W equations reveal that over time, the AERCam will not remain at zero velocity relative to the station (unless it is located directly in front of or behind the ISS in its orbit at a Y=0 and Z=0 position; such a position can be referred to as a "stable V-bar" position).[38] It is useful to determine what acceleration the AERCam would undergo to see what part of the station the AERCam might drift into if its propulsion systems were not active. The magnitude of the acceleration would also indicate just what sort of thrusting maneuvers would be required to maintain a position relative to the target area. The latter would most likely determine the period of time that the AERCam could stay at the target site while still keeping enough fuel

in reserve to return to its point of origin or point of capture.

This study will now examine the acceleration an AERCam might undergo and have to correct for to remain at zero relative velocity when inspecting a target site for any period of time. Lists of coordinates for points three feet from and surrounding an outline of the ISS in three perspectives (from the positive Y axis, negative X axis and negative Z axis) were recorded (found in Appendix F). With the velocity relative to the ISS set at zero, the acceleration that would be experienced by an AERCam at each of the positions was calculated. These results are summed up in Figures 27, 28, and 29. The direction in which the arrows point indicated the approximate direction in which an AERCam would drift over time, and the arrow color represents the magnitude of that acceleration as indicated in the legend. The exact acceleration magnitude and directions are also listed in Appendix F.
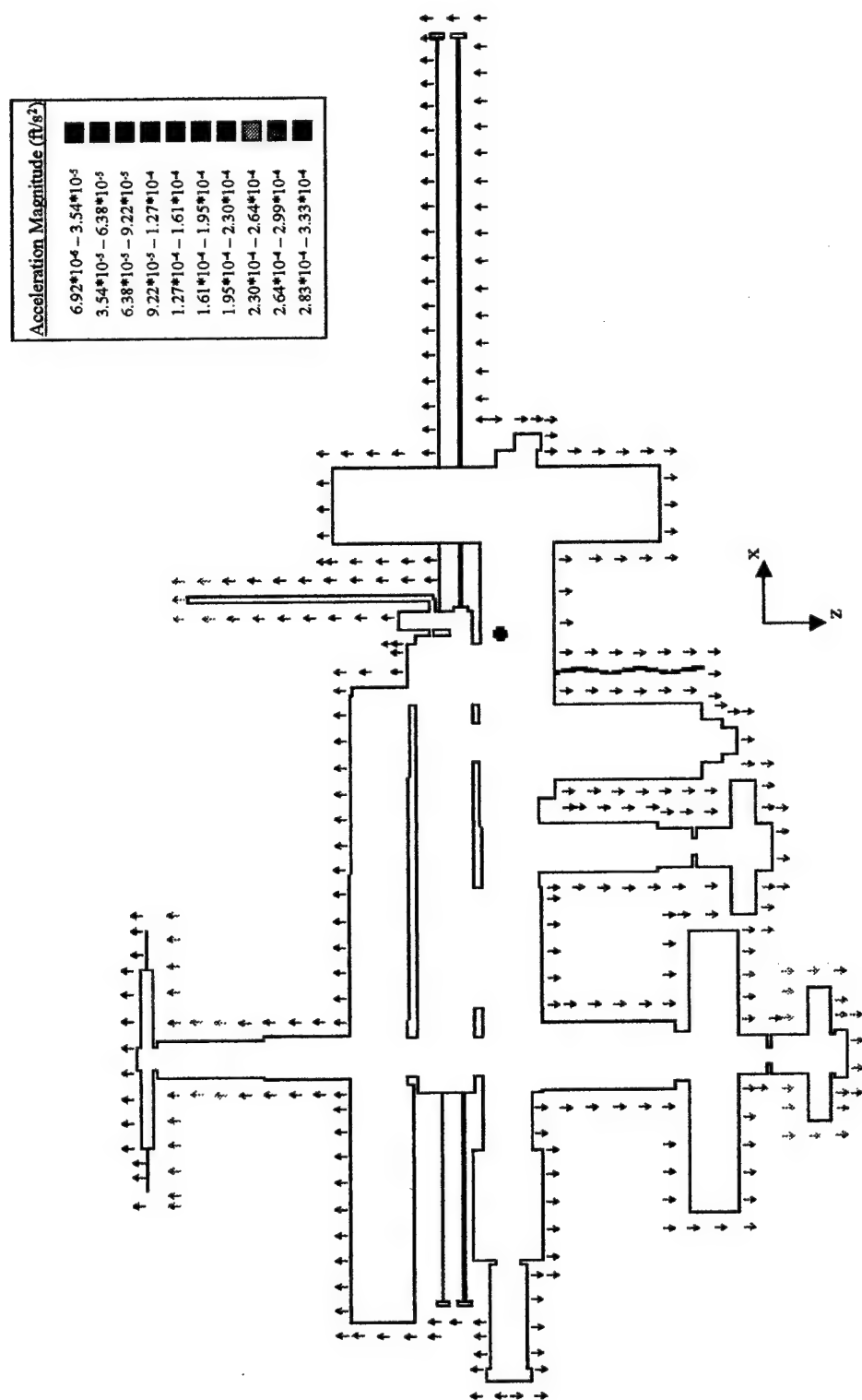
Figure 27. Direction of Acceleration Experienced by AERCam at Various Positions Around the ISS
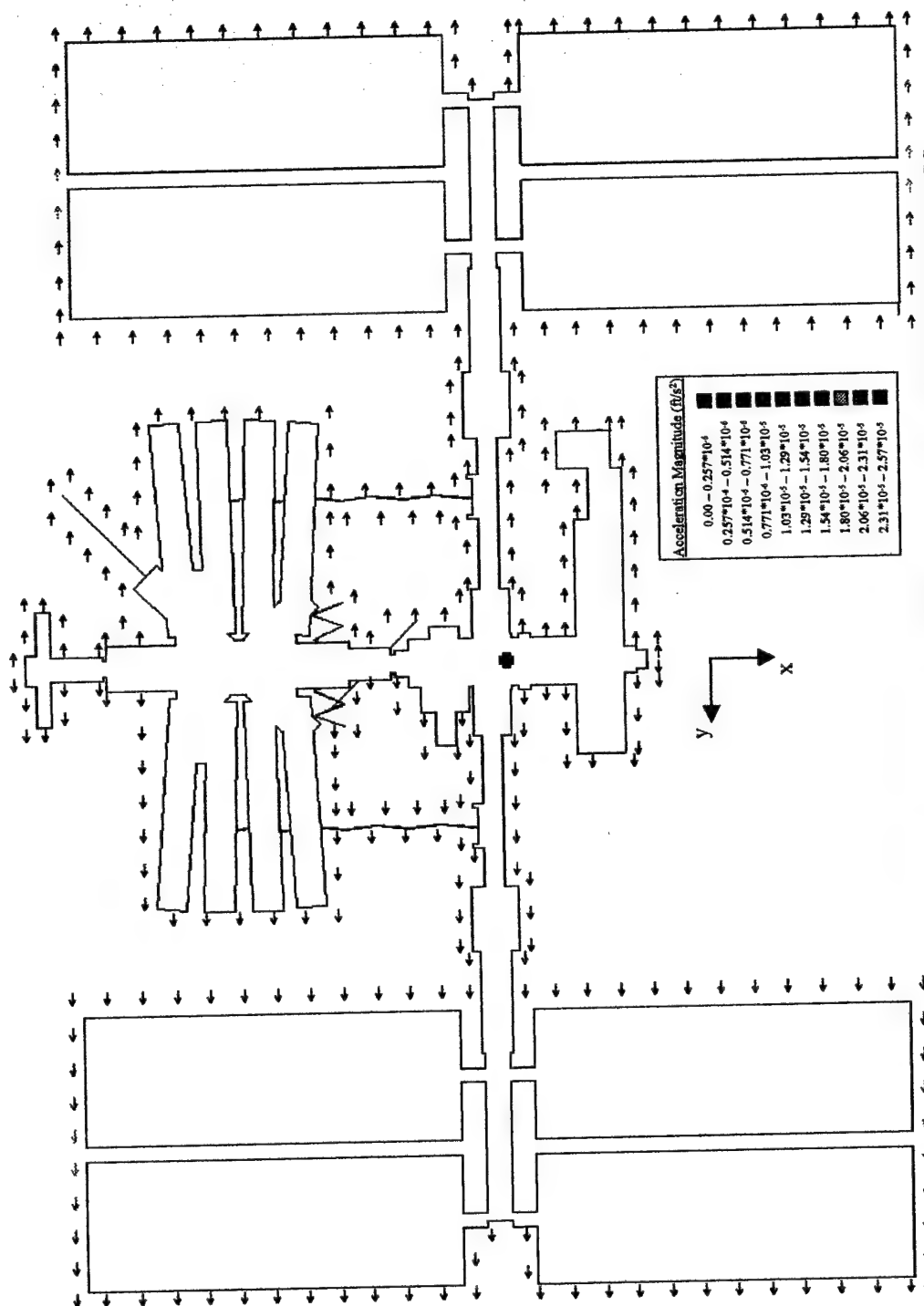
Figure 28. Direction of Acceleration Experienced by AERCam at Various Positions Around the ISS
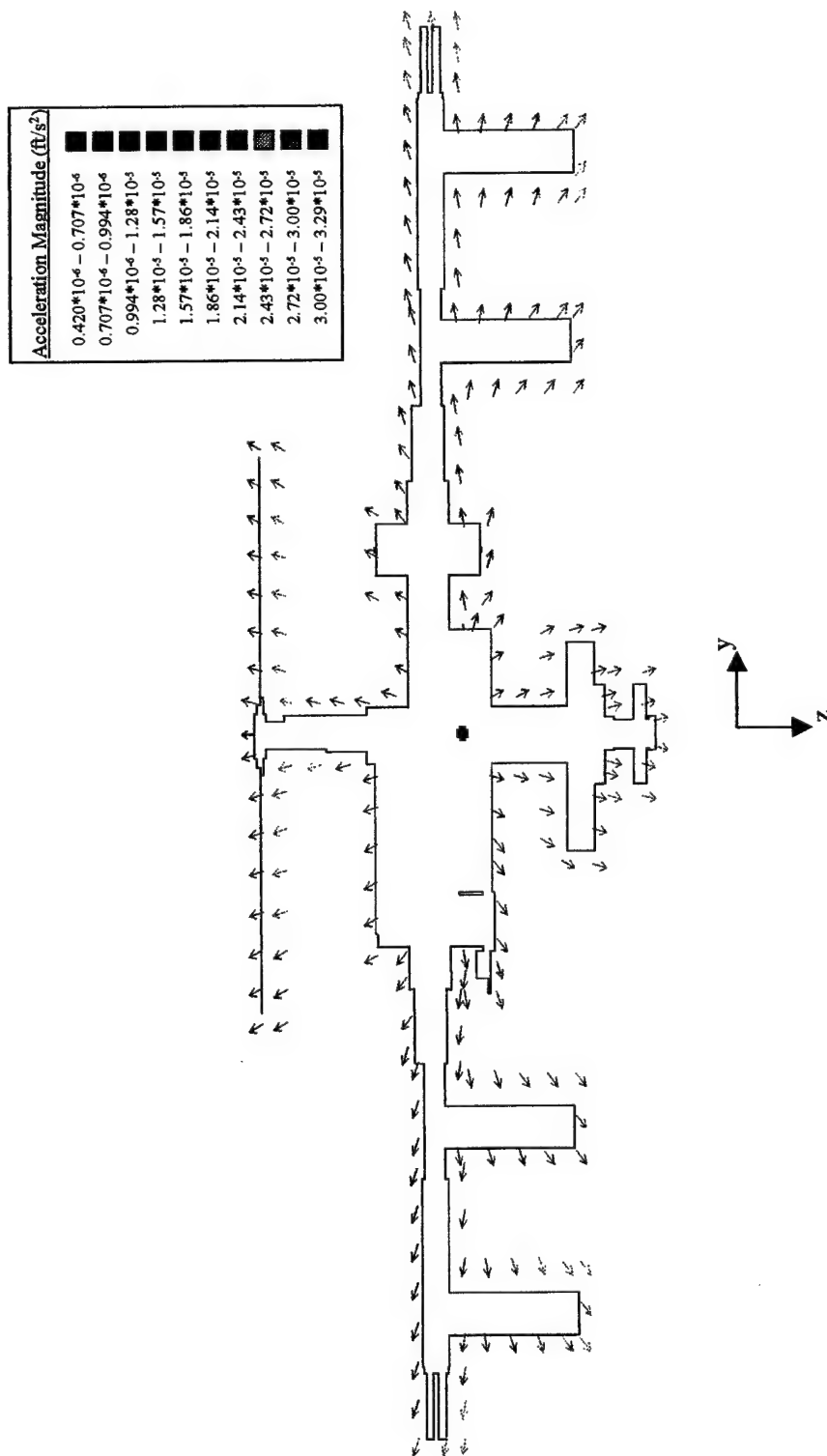
Figure 29. Direction of Acceleration Experienced by AERCam at Various Positions Around the ISS

In Figures 27-29, the tips of the arrows indicate the relative positions for which the accelerations were determined. They show that an AERCam will tend to drift away from the space station's center of mass. If an AERCam does not perform any station-keeping thrusts to keep its position relative to the station the same, it will drift to some position even farther away from the station's center of mass.

The acceleration an AERCam will experience varies from 0.420×10^{-6} ft/s^2 to 3.29×10^{-5} ft/s^2. These values are not large, but over time and combined with any other perturbative forces an AERCam would experience, they would be enough to alter the AERCam's relative position, possibly causing it to drift into some part of the station. The magnitude of the acceleration in a particular direction increases as the Y and/or Z distance from the ISS center of mass increases. It is very important to notice, however, that despite the differences in magnitude at different positions around the station along all axes, no acceleration is directed in either direction along the X axis. Referring to the C-W Equations (1) in Section 2.4 for acceleration in the X direction shows that the acceleration depends only on the velocity of the AERCam in the Z direction. This relative velocity will have been reduced to zero when the AERCam arrived to inspect the target site. Thus there will be no drift forward or backward within the orbit plane. There is only out-of-plane motion, and recall that out-of-plane motion is periodic. This means that even if the AERCam did manage to drift out without colliding into the ISS, it would change direction and begin to return in the direction of the station about ¼ of an orbit period later. Just how far out an AERCam would go depends on its initial distance from the ISS orbit plane. The time it takes for the AERCam to travel out, swing back across the orbit plane, and return to its original position along the Y axis (the period of its oscillation) is equal to the AERCam's

orbital period.

An analysis of all the data gathered in this study of AERCam does reveal some interesting points. The first is a consequence of the ISS design. Early on, it was anticipated that the targets on one side of the station (the sides being divided by the orbit plane) would always be more easily reached by originating an AERCam at the airlock on the same side of the station. Recalling that out-of-plane motion is de-coupled from in-plane motion anyway, it could be assumed that any path that did not have to cross through or over all the station components to the other side would reach the target more easily. This did not always prove to be true due to the complex geometry of the ISS. Neglecting the clear overshoot path requirement to focus just on getting an AERCam to the target site, consider the data for target #13, the target on the Y – side of the front Soyuz. Though the flight from the Joint Airlock did take 65 minutes, the trajectory was clear and not too complicated, while no trajectory could even be found from the JEM airlock that did not direct the AERCam into the ISS. The same type of argument holds true for targets #8 and #11 as Tables 4 and 6 indicate. This point actually leads to the second.

Every target case must be treated as completely unique. Whereas Lockhart's work created and was in fact based on a preformed set of trajectories [38], no generic set of trajectories can work for an AERCam at the ISS. In the same way that the smallest change in initial velocity significantly affected whether the resulting path would lead the AERCam to hit the ISS, so will a change in a target's coordinates. Changing the target site just slightly could require a change in the direction and magnitude of the initial velocity. Any small change could mean the difference between a clear path and one which impacts the

68

ISS.

Another reason each inspection situation must be considered unique from any other is that in reality, the ISS configuration is not fixed as it was for the purposes of this study. The radiators and solar panels rotate, and a small change in station configuration will create new clear paths and blockages. For example, consider an AERCam travelling out on a clear trajectory five to ten feet over the solar panels when they are oriented as they are in this study's configuration. With the panels rotated 80° (though station operations may keep them from doing so, the panels have the capability of rotating through 360° of motion [11]), the AERCam path would fly right into them. AERCam operations will require a detailed knowledge regarding the positioning of all the ISS components if an AERCam is to be used with any success.

Chapter 5.0

Conclusions

This study supports the conclusion that whenever possible, it is best to use the ISS's space vision systems on the space station arms (SSRMS, JEMRMS, or ERA) to inspect the exterior of the space station. This plan of action minimizes risk to both station personnel and resources. However, there are locations on the station which cannot be viewed by an SVS. Clearly if there were grappling fixtures (PDGF) placed on all portions of the station, the SSRMS could walk itself easily to wherever an inspection was required. The demand necessitating supplemental inspection technologies like an AERCam could be met without AERCam.

Since there are not PDGFs at a sufficient set of points to allow complete station coverage in the current design of the ISS, the station's robotic arms cannot be used as the only tool for inspection of the ISS. As a supplement, an AERCam is a logical choice over an astronaut for safety reasons. The relative motion study showed that for most targets sampled, the AERCam cameras could acquire the target with a minimal fuel requirement in under an hour's time. Release of the AERCam from the Joint Airlock appeared to offer more versatility in the number of ISS components that could be targeted due to the location of the JEM airlock with respect to the truss system. However, there were some regions of the ISS where an AERCam released from either one of the airlocks could not easily reach the target site.

An AERCam designed for use at the ISS would need atypically precise thrust control, and the determination of initial velocities would have to be very accurate. The slightest miscalculation or misfiring could have unfortunate results. Given these sensitivities, using

an AERCam at the ISS in the manner described within this study does not appear to be a very practical choice. The problems associated with its use probably overshadow any potential benefits.

If an AERCam is to be used, future research should be conducted to study using the SSRMS in combination with the AERCam. The combination offers the advantage of being able to release the AERCam from numerous locations relative to the station. Also, work should be continued in developing an advanced AERCam. If a new AERCam were available that could "see" for itself, determine its position relative to station components at any given time, actively avoid obstacles, and guide itself back on course to the target, this would be the preferred inspection device.

This AERCam relative motion study has served another purpose as well. Whether an evaluation of the data lists revealed a trajectory did or did not meet the constraints, for each travel time assessed, the examination of the plots representing in-plane and out-of-plane motion was very educational. It gave the author a feel for how the AERCam's motion relative to the station changed depending on the initial and target coordinates and travel time. Such knowledge is useful when evaluating the trajectories generated for subsequent targets. It allowed the omission of certain candidate travel times when attempting to determine a successful trajectory. In these cases, trajectories on which collisions could be predicted were omitted from consideration.

A similar learning process would be beneficial to the ISS crewmembers. Crewmembers should develop an intuitive feel for close proximity relative motion around the ISS. The crewmembers need to be familiar enough with station geometry and dimensions to know whether an SVS could be used. Assuming that some time in the near

71

future the "smarter" AERCam will be developed, the crewmembers would "know" which airlock would be the better release point. They could also recognize the situations where neither airlock would work for a direct release, those for which the SSRMS was required for a "pick up."

Another key fact learned in this study is that it would not be practical for a predetermined set of trajectories to be used for an AERCam-like inspection solution. There are an infinite number of potential target site coordinates around the station, and there is no easy way to foresee the exact configuration the station will be in when the time comes to use an AERCam (solar panel orientation, whether a shuttle is docked there, etc).

In conclusion, the best way to inspect the outside of the ISS depends on the coordinates of the target site. Every portion of the ISS should be categorized as either SVS accessible or not in the onboard database. When an inspection is required, this database should be consulted. If the target site is within a region of the ISS where using a robotic arm is possible, the arm should be positioned appropriately and the inspection made.

If the target site happens to be unobservable with a SVS, it should be evaluated in terms of EVA or AERCam accessibility with or without the help of the SSRMS. However, unless the design modifications mentioned above for both the station and the AERCam are made, the only option certain to succeed is to have the astronauts prepare for an inspection EVA.

APPENDIX A

Descriptions of ISS Elements

Centrifuge Accommodations Module[11]

The Centrifuge Accommodation Module (CAM) is a U.S. element that provides centrifuge facilities for science and research. It also houses additional payload racks.

Columbus Orbital Facility, Also Known as the Attached Pressurized Module[11]

The Columbus Orbital Facility (COF) is an European Space Agency (ESA) element that provides facilities for the ESA experiments and research. It is analogous to the U.S. Lab.

Cupola[11]

The Cupola is a U.S. element that provides direct viewing for robotic operations and Shuttle payload bay viewing.

Docking Compartment[11]

There are two Russian element Docking Compartments (DCs) used during the assembly sequence to provide egress/ingress capability for Russian-based EVAs and additional docking ports.

Docking and Stowage Module[11]

The Docking and Stowage Module (DSM) is a Russian element that provides facilities for stowage and additional docking ports.

Habitation Module[11]

The Hab is a U.S. element that provides six-person habitation facilities, such as personal hygiene (better waste management, full body shower), crew health care, and galley facilities (wardroom with eating facilities, oven, drink dispenser, freezer/refrigerator).

Japanese Experiment Module[11]

The Japanese Experiment Module (JEM) is a Japanese element that provides laboratory facilities for Japanese material processing and life science research. It also contains an external platform, airlock, and robotic manipulator for in-space ("exposed") experiments and a separate logistics module to transport JEM experiments.

Joint Airlock Module

The Joint Airlock is a U.S. element that provides Station-based Extravehicular Activity (EVA) capability using either a U.S. Extravehicular Mobility Unit (EMU) or Russian Orlon EVA suits.[11]

The Joint Airlock Module, which has the capability to be used by both Russian and U.S. spacesuit designs, consists of two sections, a "crew lock" that is used to exit the station and begin a spacewalk and an "equipment lock" used for storing gear. The equipment lock also will be used for overnight "campouts" by the crew, during which the pressure in the Joint Airlock Module is lowered to 10.2 pounds per square inch (psi), while the rest of the station remains at the normal sea level atmospheric pressure of 14.7 psi. The night spent at 10.2 psi in the Airlock purges nitrogen from the spacewalkers' bodies and prevents and prevents decompression sickness, commonly called "the bends," when they go to the 4.3 psi pure oxygen atmosphere of a spacesuit. Station crew members could perform a spacewalk

directly from the 14.7 psi cabin atmosphere, but they would have to go through a several hours-long prebreathe of pure oxygen first.[33]

Leonardo-Multipurpose Logistics Module (MPLM) [27]

The Italian Space Agency (ASI)-built Leonardo Multipurpose Logistics Module is the first of three such pressurized modules that will serve as the International Space Station's "moving vans," carrying laboratory racks filled with equipment, experiments and supplies to and from the station aboard the Space Shuttle.

The unpiloted, reusable logistics modules function as both a cargo carrier and a space station module when they are flown. Mounted in the Space Shuttle's cargo bay for launch and landing, they are berthed to the station using the Shuttle's robotic arm after the Shuttle has docked. While berthed to the station, racks of equipment are unloaded from the module and then old racks and equipment may be reloaded to be taken back to Earth. The logistics module is then detached from the station and positioned back into the Shuttle's cargo bay for the trip home. When in the cargo bay, the cargo module is independent of the Shuttle cabin, and there is no passageway for Shuttle crewmembers to travel from the Shuttle cabin to the module.

In order to function as an attached station module as well as a cargo transport, the logistics modules also include components that provide some life support, fire detection and suppression, electrical distribution and computer functions. Eventually, the modules also will carry refrigerator freezers for transporting experiment samples and food to and from the station. Although built in Italy, the logistics modules, technically known as Multipurpose Logistics Modules (MPLMs), are owned by the U.S. and provided in exchange for Italian access to U.S. research time on the station.

Mobile Servicing System (MSS)

Canada is contributing an essential component of the International Space Station, the Mobile Servicing System, or MSS. This robotic system will play a key role in Space Station assembly and maintenance, moving equipment and supplies around the Station, releasing and capturing satellites, supporting astronauts working in space, and servicing instruments and other payloads attached to the Space Station. Astronauts will receive robotics training to enable them to perform these functions with the arm.
The Mobile Servicing System comprises three parts:
Space Station Remote Manipulator System (SSRMS)

The next generation Canadarm is a bigger, better, smarter version of the space shuttle's robotic arm. It is 17 meters long when fully extended and has seven motorized joints. This arm is capable of handling large payloads and assisting with docking the space shuttle. The SSRMS is self-relocatable with a Latching End Effector, so it can be attached to complementary ports spread throughout the Station's exterior surfaces.
Mobile Base System (MBS)

A work platform that moves along rails covering the length of the Space Station, the MBS will provide lateral mobility for the Canadarm as it traverses the main trusses.
Special Purpose Dexterous Manipulator (SPDM)

The SPDM, or Canada Hand, is a smaller two-armed robot capable of handling the delicate assembly tasks currently handled by astronauts during spacewalks.[27]

The main functions of the MSS include assembly of ISS elements, large payload and ORU handling, maintenance, EVA support, and transportation. The MSS is controlled using the RWS [Robotic Work Station] from either the Lab or the Cupola. Until the Cupola arrives, there is no direct viewing; therefore, the MSS Video System and the Space Vision System (SVS) provide the main visual inputs. The Video System, combined with ISS Communication and Tracking (C&T) systems, provides video generation, control, distribution, and localized lighting throughout MSS elements. The SVS provides synthetic views of operations using cameras, targets, and graphical/digital real-time position and rate data.[11]

Research Module[11]

The Research Module (RM) is a Russian element that provides facilities for the Russian experiments and research. It is analogous to the U.S. Lab. There are two RMs.

Science Power Platform[11]

The Science Power Platform (SPP) is a Russian element that is brought up by the Shuttle to provide additional power and roll axis attitude control capability.

Service Module

The Service Module will be the first fully Russian contribution to the International Space Station and will serve as the early cornerstone for the first human habitation of the station.

The module will provide the early station living quarters; life support system; electrical power distribution; data processing system; flight control system; and propulsion system. It also will provide a communications system that includes remote command capabilities from ground flight controllers. Although many of these systems will be supplemented or replaced by later U.S. station components, the Service Module will always remain the structural and functional center of the Russian segment of the International Space Station. [27]

The Service Module (SM), similar in layout to the core module of Russia's Mir space station, provides the early Station living quarters, life support system, communication system, electrical power distribution, data processing system, flight control system, and propulsion system. Although many of these systems will be supplemented or replaced by later U.S. Station components, the SM always remains the structural and functional center of the ROS. Living accommodations on the Service Module include personal sleeping quarters for the crew; a toilet and hygiene facilities; a galley with a refrigerator/freezer; and a table for securing meals while eating. Spacewalks using Russian Orlan-M spacesuits can be performed from the SM by using the Transfer Compartment as an airlock.[11]

Soyuz [11]

Besides being an Earth-to-Orbit Vehicle (ETOV) used for crew rotations, Soyuz is the Russian element that provides the crew emergency return ("lifeboat") capability, at least through Assembly Complete. As such, there is always a Soyuz docked to the Station whenever the Station crew is onboard. Therefore, launch of the Soyuz marks the beginning of permanent human presence of a three-person crew. At least every 6 months, the docked

Soyuz is replaced with a "fresh" Soyuz. After Assembly Complete, the Soyuz may be replaced by the Crew Rescue Vehicle (CRV).

Truss[11]

Built over numerous flights, the truss is a U.S. element that provides the ISS "backbone" and attachment points for modules, payloads, and systems equipment. It also houses umbilicals, radiators, external payloads, and batteries. The truss is based on the Freedom pre-integrated truss design. The truss segments are labeled by whether they are on the starboard (right) or port (left side of the Station and its location. An example is the P6 truss is located on the outermost port side. Two exceptions to this labeling scheme are truss S0, which is actually the center truss segment, and during early assembly, the P6 truss segment, with its PVA, is actually mounted on the Z1 truss on the Lab. The Z1 truss itself is an anomaly in that it is not part of the main truss but a truss segment needed under the ISS design until the main truss is built.

Unity Node

Unity Node is a connecting passageway to living and work areas of the International Space Station. It is the first major U.S.-built component of the station, joining Zarya (FGB). Unity Node was delivered by the space shuttle with Pressurized Mating Adapter 1 prefitted to its aft port. The shuttle crew conducted three spacewalks to attach PMA 1 to Zarya.

In addition to its connection to Zarya, the node will serve as a passageway to the U.S. laboratory module, U.S. habitation module and an airlock. It has six hatches that serve as docking ports for the other modules. . . . Contains more than 50,000 mechanical items, 216 lines to carry fluids and gases, and 121 internal and external electrical cables using six miles of wire.[27]

The Node is a U.S. element that provides six docking ports (four radial and two axial) for the attachment of other modules. It also provides external attachment points for the truss. Finally, the Node provides internal storage and pressurized access between modules. There are three Nodes.[11]

Universal Docking Module[11]

The Universal Docking Module (UDM) is a Russian element that provides a five-port docking node for additional Russian modules and vehicles. It performs the same function as the U.S. Nodes.

US Laboratory [27]

The laboratory module is the centerpiece of the International Space Station, where unprecedented science experiments will be performed in the near zero gravity of space. The aluminum module is 28 feet long and 14 feet in diameter. The lab consists of three cylindrical sections and two endcones with hatches that will be mated to other station components. A 20-inch diameter window is located on one side of the center module segment. This pressurized module is designed to accommodate pressurized payloads. It has a capacity of 24 rack locations. Payload racks will occupy 13 locations especially designed to support experiments.

<u>Zarya Control Module [27]</u>

The Zarya control module, also known by the technical term Functional Cargo Block and the Russian acronym FGB, was the first component launched for the International Space Station. This module was designed to provide the station's initial propulsion and power. The 42,600-pound pressurized module was launched on a Russian Proton rocket in November 1998.

The U.S.-funded and Russian-built Zarya, which means Sunrise when translated to English, is a U.S. component of the station although it was built and launched by Russia. The module was built by the Khrunichev State Research and Production Space Center (KhSC) in Moscow under a subcontract to The Boeing Company for NASA. Only weeks after the Zarya reached orbit, the Space Shuttle Endeavour made a rendezvous and attached a U.S.-built connecting module called Node 1. The Zarya module will provide orientation control, communications and electrical power attached to the passive Node 1 for several months while the station awaits launch of the third component, a Russian-provided crew living quarters and early station core known as the Service Module. The Service Module will enhance or replace many functions of the Zarya. Later in the station's assembly sequence, the Zarya module will be used primarily for its storage capacity and external fuel tanks.

The Zarya module is 41.2 feet long and 13.5 feet wide at its widest point. It has an operational lifetime of at least 15 years. Its solar arrays and six nickel-cadmium batteries can provide an average of 3 kilowatts of electrical power. Using the Russian Kurs system, the Zarya will perform an automated and remotely piloted rendezvous and docking with the Service Module in orbit. Its side docking ports will accommodate Russian Soyuz piloted spacecraft and unpiloted Progress resupply spacecraft. Each of the two solar arrays is 35 feet long and 11 feet wide. The module's 16 fuel tanks combined can hold more than 6 tons of propellant. The attitude control system for the module includes 24 large steering jets and 12 small steering jets. Two large engines are available for reboosting the spacecraft and making major orbital changes.

APPENDIX B

Derivation of Clohessy-Wiltshire Equations

DEVELOPMENT OF THE C-W EQUATIONS

In order to develop the equations of motion for one spacecraft moving with respect to another, we will employ the Lagrangian approach.

Consider a spacecraft centered set of LVLH coordiantes. In contrast to the KAPLAN text, NASA sets the LVLH coordinates up with x forward (along $\bar{v}$ in a circular orbit) z radially downward, and y in a direction opposite to the orbital angular momentum vector.

The xyz LVLH coordinate system rotates with respect to inertial coordinates, and the origin moves in a two-body orbit about the center of the earth.

$$\bar{r} = \bar{r}_0 + \bar{\rho}$$
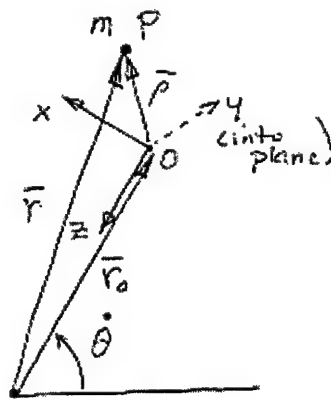
$$\bar{\rho} = x\bar{i} + y\bar{j} + z\bar{k}$$

Coordinate Rate:

$$\bar{\Omega} = - \dot{\theta}\bar{j}$$

$$\bar{r} = x\bar{i} + y\bar{j} + (z - r_0)\bar{k}$$

The Lagrangian for the particle P is

$$L = \frac{1}{2}m \, \bar{v}_p \cdot \bar{v}_p - m\mu/r$$

The velocity of P can be written as

$$\bar{v}_p = \bar{v}_{prel} + \bar{\Omega} \times \bar{r}$$

where

$$\bar{v}_{prel} = \dot{x}\bar{i} + \dot{y}\bar{j} + (\dot{z} - \dot{r}_0)\bar{k}$$

and

$$\bar{\Omega} \times \bar{r} = -\dot{\theta}\bar{j} \times (x\bar{i} + y\bar{j} + (z - r_0)\bar{k})$$

$$\bar{\Omega} \times \bar{r} = -\dot{\theta}(z - r_0)\bar{i} + \dot{\theta}x\,\bar{k}$$

If $\bar{v}_p$ is written as

$$\bar{v}_p = \bar{v}_{prel} + \bar{\Omega} \times \bar{r}$$

then

$$\bar{v}_p \cdot \bar{v}_p = \bar{v}_{prel} \cdot \bar{v}_{prel} + 2\bar{v}_{prel} \cdot (\bar{\Omega} \times \bar{r}) + (\bar{\Omega} \times \bar{r}) \cdot (\bar{\Omega} \times \bar{r})$$

Forming this in parts to avoid errors,

$$\bar{v}_{prel} \cdot \bar{v}_{prel} = \dot{x}^2 + \dot{y}^2 + (\dot{z} - \dot{r}_0)^2$$

$$2\bar{v}_{prel} \cdot (\bar{\Omega} \times \bar{r}) = -2\dot{x}\,\dot{\theta}(z - r_0) + 2\dot{\theta}\,x(\dot{z} - \dot{r}_0)$$

$$(\bar{\Omega} \times \bar{r}) \cdot (\bar{\Omega} \times \bar{r}) = \dot{\theta}^2(z - r_0)^2 + \dot{\theta}^2\,x^2$$

Thus,

$$\boxed{\begin{aligned}
T &= \tfrac{1}{2}m\left[\dot{x}^2 + \dot{y}^2 + (\dot{z} - \dot{r}_0)^2\right] \\
&\quad + m\left[-\dot{x}\dot{\theta}(z - r_0) + \dot{\theta}x(\dot{z} - \dot{r}_0)\right] \\
&\quad + \tfrac{1}{2}m\left[\dot{\theta}^2(z - r_0)^2 + \dot{\theta}^2 x^2\right]
\end{aligned}}$$

The potential energy, V, is given by

$$V = -m\mu/r = -\frac{mg_e r_e^2}{r}$$

81

$$V = -\frac{mg_e r_e^2}{[x^2 + y^2 + (z - r_0)^2]^{\frac{1}{2}}}$$

The Lagrangian is given by $L = T - V$

$$L = \frac{m\dot{x}^2}{2} + \frac{m\dot{y}^2}{2} + \frac{m(\dot{z}^2 - 2\dot{r}_0\dot{z} + \dot{r}_0^2)}{2}$$

$$- m\dot{x}\dot{\theta}(z - r_0) + m\dot{\theta}x(\dot{z} - \dot{r}_0)$$

$$+ \frac{m\dot{\theta}^2(z - r_0)^2}{2} + \frac{m\dot{\theta}^2 x^2}{2}$$

$$+ \frac{mg_e r_e^2}{[x^2 + y^2 + (z - r_0)^2]^{\frac{1}{2}}}$$

82

$$\underline{X - \text{EQUATION}} \qquad \frac{d}{dt}\left(\frac{\partial L}{\partial \dot{x}}\right) - \frac{\partial L}{\partial x} = 0$$

$$\frac{\partial L}{\partial \dot{x}} = m\dot{x} - m\dot{\theta}(z - r_0)$$

$$\frac{d}{dt}\left(\frac{\partial L}{\partial \dot{x}}\right) = m\ddot{x} - m\ddot{\theta}(z - r_0) - m\dot{\theta}(\dot{z} - \dot{r}_0)$$

$$\frac{\partial L}{\partial x} = m\dot{\theta}(\dot{z} - \dot{r}_0) + mx\dot{\theta}^2$$

$$+ \frac{mg_e r_e^2 (-\frac{1}{2})(2x)}{\left[x^2 + y^2 + (z - r_0)^2\right]^{3/2}} = 0$$

$$\boxed{\begin{array}{l} \ddot{x} - \ddot{\theta}(z - r_0) - 2\dot{\theta}((\dot{z} - \dot{r}_0) - x\dot{\theta}^2 \\[2mm] + \dfrac{g_e r_e^2 x}{\left[x^2 + y^2 + (z - r_0)^2\right]^{3/2}} \end{array}}$$

$$\underline{Y - \text{EQUATION}}$$

$$\frac{\partial L}{\partial \dot{y}} = m\dot{y}$$

$$\frac{d}{dt}\left(\frac{\partial L}{\partial \dot{y}}\right) = m\ddot{y}$$

$$\frac{\partial L}{\partial y} = - \frac{mg_e r_e^2 y}{\left[x^2 + y^2 + (z - r_0)^2\right]^{3/2}}$$

$$\boxed{\ddot{y} + \frac{g_e r_e^2 y}{\left[x^2 + y^2 + (z - r_0)^2\right]^{3/2}} = 0}$$

83

Z - EQUATION

$$\frac{\partial L}{\partial \dot{z}} = m(\dot{z} - \dot{r}_0) + mx\,\dot{\theta}$$

$$\frac{d}{dt}\left(\frac{\partial L}{\partial \dot{z}}\right) = m\ddot{z} - \ddot{r}_0 + + m\dot{x}\dot{\theta} + mx\ddot{\theta}$$

$$\frac{\partial L}{\partial z} = - m\dot{x}\,\dot{\theta} + m\dot{\theta}^2(z - r_0) - \frac{mg_e r_e^2 z}{[x^2 + y^2 + (z - r_0)^2]^{3/2}}$$

$$\ddot{z} - \ddot{r}_0 + \dot{x}\dot{\theta} + x\ddot{\theta} + \dot{x}\dot{\theta} - (z - r_0)\dot{\theta}^2 + \frac{g_e r_e^2 z}{[x^2 + y^2 + (z - r_0)^2]^{3/2}} = 0$$

$$\boxed{\ddot{z} - \ddot{r}_0 + 2\dot{x}\dot{\theta} + x\ddot{\theta} - \dot{\theta}^2(z - r_0) + \frac{g_e r_e^2 z}{[x^2 + y^2 + (z - r_0)^2]^{3/2}} = 0}$$

84

EQUATIONS SUMMARY

$$\ddot{x} - \ddot{\theta}(z - r_0) - 2\dot{\theta}(\dot{z} - \dot{r}_0) - x\dot{\theta}^2 + \frac{g_e r_e^2 x}{[x^2 + y^2 + (z - r_0)^2]^{3/2}} = 0$$

$$\ddot{y} + \frac{g_e r_e^2 y}{[x^2 + y^2 + (z - r_0)^2]^{3/2}} = 0$$

$$\ddot{z} - \ddot{r}_0 + 2\dot{x}\dot{\theta} + x\ddot{\theta} - \dot{\theta}^2(z - r_0) + \frac{g_e r_e^2(z - r_0)}{[x^2 + y^2 + (z - r_0)^2]^{3/2}} = 0$$

We are now ready to make some logical simplifying assumptions. Our assumptions will involve:

(1) The nature of the orbit in which the origin is assumed to be moving, and

(2) The magnitude of the motion ($\bar{\rho}$) considered.

In order to be able to use the equations as they stand, the quantities

$$\left.\begin{array}{c} r_0 \\ \dot{r}_0 \\ \ddot{r}_0 \\ \dot{\theta} \\ \ddot{\theta} \end{array}\right\} \text{ must be } \underline{\text{specified}}.$$

These quantities relate to the motion of the coordinate system itself and are usually associated with a target vehicle (the LVLH coordinates are centered on the target vehicle, and we try to go to the origin).

85

Before looking at the motion of the target vehicle, however, let us look at the gravitational terms in the three equations. Each gravitational term contains the factor

$$D = [x^2 + y^2 + (z - r_0)^2]^{3/2}$$

Let us rewrite D as

$$D = \left[r_0^2\left\{\left(\frac{x}{r_0}\right)^2 + \left(\frac{y}{r_0}\right)^2 + \left[\frac{z - r_0}{r_0}\right]^2\right\}\right]^{3/2}$$

$$D = r_0^3\left[\left(\frac{x}{r_0}\right)^2 + \left(\frac{y}{r_0}\right)^2 + \left(\frac{z}{r_0}\right)^2 - \frac{2z}{r_0} + 1\right]^{3/2}$$

This term can be substituted into the equations of motion where appropriate. However, we can also go one step farther with our simplification. Recall that,

$$(1 + v)^n = 1 + nv + \frac{n(n-1)v^2}{2!} + \frac{n(n-1)(n-2)}{3!}v^3 + \ldots$$

Our equations contain $(1 + v)^{-3/2}$ where

$$v = \frac{2z}{r_0} + \left(\frac{x}{r_0}\right)^2 + \left(\frac{y}{r_0}\right)^2 + \left(\frac{z}{r_0}\right)^2$$

Making the appropriate substitutions, we get

$$(1 + v)^{-3/2} = 1 - \frac{3}{2}\left[-\frac{2z}{r_0} + \left(\frac{x}{r_0}\right)^2 + \left(\frac{y}{r_0}\right)^2 + \left(\frac{z}{r_0}\right)^2\right]$$

$$+ \left(-\frac{3}{2}\right)\left(-\frac{5}{2}\right)\left(\frac{1}{2!}\right)\left[-\frac{2z}{r_0} + \left(\frac{x}{r_0}\right)^2 + \left(\frac{y}{r_0}\right)^2 + \left(\frac{z}{r_0}\right)^2\right]^2$$

$$+ \ldots$$

$$(1 + v)^{-3/2} = 1 + \frac{3z}{r_0} - \frac{3}{2}\left(\frac{x}{r_0}\right)^2 - \frac{3}{2}\left(\frac{y}{r_0}\right)^2 - \frac{3}{2}\left(\frac{z}{r_0}\right)^2$$

$$+ \frac{15}{2}\left(\frac{z^2}{r_0^2}\right) + \{\text{terms with } r_0^3 \text{ and higher in the denominator}\}$$

86
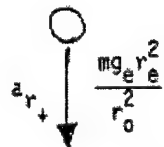
$$(1 + v)^{-3/2} = 1 + \frac{3z}{r_o} + 6\frac{z^2}{r_o} - \frac{3}{2r_o^2}(x^2 + y^2)$$

This simplification will be used in conjunction with others. Now, let us assume that the origin of the LVLH coordinates is moving in a circular orbit of radius r_o. In this case, the equations simplify greatly.

Assume

$$r_o = constant$$
$$\dot{r}_o = 0$$
$$\ddot{r}_o = 0$$
$$\dot{\theta} = \omega = constant$$
$$\ddot{\theta} = 0$$

If we draw a free-body diagram of a particle at the origin of the LVLH coordinates,

$$ma_r = mr_o\omega^2 = \frac{mg_e r_e^2}{r_o^2}$$

$$\boxed{\omega^2 = \frac{g_e r_e^2}{r_o^3}} = constant$$

Now let us rewrite our equations and make the substitutions we have developed.

87

$$\ddot{x} - 2\omega\dot{z} - x\omega^2 + \omega^2 \quad [1 + \frac{3z}{r_0} + 6(\frac{z}{r_0})^2 - \frac{3}{2r_0^2}(x^2 + y^2)] = 0$$

$$\boxed{\ddot{x} - 2\omega\dot{z} + \frac{3\omega^2 xz}{r_0} + \frac{6\omega^2 xz^2}{r_0^2} - \frac{3\omega^2 x(x^2 + y^2)}{2r_0^2} = 0}$$

$$\ddot{y} + \omega^2 y\left[1 + \frac{3z}{r_0} + 6(\frac{z}{r_0})^2 - \frac{3(x^2 + y^2)}{2r_0^2}\right] = 0$$

$$\boxed{\ddot{y} + \omega^2 y + \frac{3\omega^2 yz}{r_0} + \frac{6\omega^2 yz^2}{r_0^2} - \frac{3\omega^2 y(x^2 + y^2)}{2r_0^2} = 0}$$

$$\ddot{z} + 2\dot{x}\omega - \omega^2 z + \omega^2 r_0 + \omega(z - r_0)(1 + \frac{3z}{r_0} + \ldots) = 0$$

$$\boxed{\begin{aligned}
\ddot{z} + 2\dot{x}\omega + \omega^2 \cancel{r_0} + \frac{3\omega^2 xz}{r_0} + \frac{6\omega^2 z^3}{r_0^2} + \frac{3\omega^2 z(x^2 + y^2)}{2r_0^2} &= 0 \\
- \omega^2 \cancel{r_0} - \frac{3\omega^2 \cancel{r_0} z}{\cancel{r_0}} - \frac{6\omega^2 z^2 \cancel{r_0}}{r_0^2} - \frac{3\omega^2 \cancel{r_0}(x^2 + y^2)}{2r_0^{\cancel{2}}} &= 0
\end{aligned}}$$

If we now neglect terms of higher order than third, we get

$$\begin{cases}
\ddot{x} - 2\omega\dot{z} + 3\omega^2 xz/r_0 = 0 \\
\ddot{y} + \omega^2 y + 3\omega^2 yz/r_0 = 0 \\
\ddot{z} + 2\omega\dot{x} + 3\omega^2 xz/r_0 - 3\omega^2 z = 0
\end{cases}$$

If we neglect terms containing r_0 in the denominator, we get

$$\ddot{x} - 2\omega\dot{z} + 3\omega^2 xz/r_0 = 0$$
$$\ddot{y} + \omega^2 y + 3\omega^2 yz/r_0 = 0$$
$$\ddot{z} + 2\omega\dot{x} + 3\omega^2 xz/r_0 - 3\omega^2 z = 0$$

The next step is to solve these equations in closed form. The first equation

$$\ddot{x} - 2\omega\dot{z} + 3\omega^2 xz/r_0 = 0$$

can be integrated to yield

$$\dot{x} - 2\omega z = \text{constant}$$

$$\dot{x} - 2\omega z = \dot{x}_0 - 2\omega z_0$$

Substituting this equation into the $\ddot{z}$ equation yields

$$\ddot{z} + 2\omega(\dot{x}_0 - 2\omega z_0 + 2\omega z) - 3\omega^2 z = 0$$

$$\ddot{z} + 4\omega^2 z - 3\omega^2 z + 2\omega\dot{x}_0 - 4\omega^2 z_0) = 0$$

$$\ddot{z} + \omega^2 z = 4\omega^2 z_0 - 2\omega\dot{x}_0 = C_z$$

$$z = A\cos\omega t + B\sin\omega t + K$$

$$\ddot{z} = A\omega^2\cos\omega t - B\omega^2\sin\omega t$$

$$\ddot{z} + \omega^2 z = \omega^2 K = 4\omega^2 z_0 - 2\omega\dot{x}_0$$

$$K = 4z_0 - 2\frac{\dot{x}_0}{\omega}$$

89

$$z = A \cos \omega t + B \sin \omega t + 4z_0 - 2 \frac{\dot{x}_0}{\omega}$$

$$\dot{z} = -A\omega \sin \omega t + B\omega \cos \omega t$$

$$\text{At} \quad t = 0, \quad z = z_0, \quad \dot{z} = \dot{z}_0$$

$$\dot{z}_0 = B\omega \qquad B = \frac{\dot{z}_0}{\omega}$$

$$z_0 = A + 4z_0 - 2 \frac{\dot{x}_0}{\omega}$$

$$A = \left(\frac{2\dot{x}_0}{\omega} - 3z_0 \right)$$

Thus,

$$\boxed{\begin{aligned} z = \left(\frac{2\dot{x}_0}{\omega} - 3z_0 \right) \cos \omega t + \frac{\dot{z}_0}{\omega} \sin \omega t \\ + \left(4z_0 - \frac{2\dot{x}_0}{\omega} \right) \end{aligned}}$$

Substituting the solution for z back into the $\dot{x}$ eqn., we get

$$\dot{x} - 2\omega z = \dot{x}_0 - 2\omega z_0$$

$$\dot{x} - 2\omega \left(\frac{2\dot{x}_0}{\omega} - 3z_0 \right) \cos \omega t - 2\dot{z}_0 \sin \omega t - 2\omega \left(4z_0 - \frac{2\dot{x}_0}{\omega} \right) = \dot{x}_0 - 2\omega z_0$$

$$\dot{x} = \left[\left(\frac{4\dot{x}_0}{\omega} - 6z_0 \right) \omega \right] \cos \omega t + 2\dot{z}_0 \sin \omega t + 6\omega z_0 - 3\dot{x}_0$$

Assume

$$x = D \cos \omega t + E \sin \omega t + Ft + G$$

$$\dot{x} = -D\omega \sin \omega t + E\omega \cos \omega t + F$$

Equating like terms, we get

$$E = \left(\frac{4\dot{x}_0}{\omega} - 6z_0\right)$$

$$-D\omega = 2\dot{z}_0$$

$$D = -2\frac{\dot{z}_0}{\omega}$$

$$F = 6\omega z_0 - 3\dot{x}_0$$

And now, from the first equations,

$$x_0 = -\frac{2\dot{z}_0}{\omega}\cos(0) + \left(\frac{4\dot{x}_0}{\omega} - 6z_0\right)\sin(0) + (6\omega z_0 - 3\dot{x}_0)\sin(0)$$

$$+ (6\omega z_0 - 3\dot{x}_0)t\Big|_{t=0} + G$$

$$G = x_0 + \frac{2\dot{z}_0}{\omega}$$

$$\boxed{x = -\frac{2\dot{z}_0}{\omega}\cos\omega t + \left(\frac{4\dot{x}_0}{\omega} - 6z_0\right)\sin\omega t + \left(6z_0 - \frac{3\dot{x}_0}{\omega}\right)\omega t + x_0 + \frac{2\dot{z}_0}{\omega}}$$

Similarly,

$$y = y_0\cos\omega t + \frac{\dot{y}_0}{\omega}\sin\omega t$$

91

EQUATIONS SUMMARY

$$x = -\left(\frac{2\dot{z}_0}{\omega}\right) \cos\omega t + \left(\frac{4\dot{x}_0}{\omega} - 6z_0\right) \sin\omega t + \left(6z_0 - \frac{3\dot{x}_0}{\omega}\right)\omega t + \left(x_0 + \frac{2\dot{z}_0}{\omega}\right)$$

$$y = (y_0) \cos\omega t + \left(\frac{\dot{y}_0}{\omega}\right) \sin\omega t$$

$$z = \left(\frac{2\dot{x}_0}{\omega} - 3z_0\right) \cos\omega t + \left(\frac{\dot{z}_0}{\omega}\right) \sin\omega t + \left(4z_0 - \frac{2\dot{x}_0}{\omega}\right)$$

$$\dot{x} = \left(\frac{4\dot{x}_0}{\omega} - 6z_0\right)\omega \cos\omega t + 2\dot{z}_0 \sin\omega t + \left(6z_0 - \frac{3\dot{x}_0}{\omega}\right)\omega$$

$$\dot{y} = (-y_0\omega) \sin\omega t + (\dot{y}_0) \cos\omega t$$

$$\dot{z} = -\left(\frac{2\dot{x}_0}{\omega} - 3z_0\right)\omega \sin\omega t + (\dot{z}_0) \cos\omega t$$

$$\omega = \frac{g_e r_e^2}{r_0^3}$$

C-W TARGETING

Now let us use the equations for targeting. As written, they will give us

$$x(t) \; , \; y(t) \; , \; z(t) \; , \; \dot{x}(t) \; , \; \dot{y}(t) \; , \; \text{and} \; \dot{z}(t)$$

if we supply $x_0 \; , \; y_0 \; , \; z_0 \; , \; \dot{x}_0 \; , \; \dot{y}_0 \; , \; \dot{z}_0 \; ,$ and ω .

What we want to do is to set the clock at $t_0 = 0$, specify $x(t)$, $y(t)$, $z(t)$ given that we are "currently" at $x_0 \; , \; y_0 \; , \; z_0 \; ,$ and solve for the $(\dot{x}_0, \; \dot{y}_0 \; , \; \dot{z}_0)$ necessary to cause us to be able to fly to the required point in space.
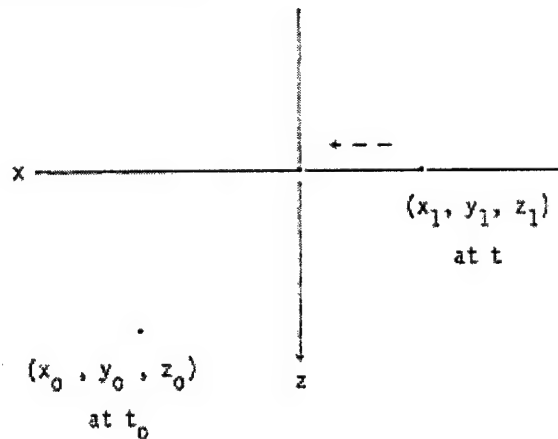
or

$$\begin{bmatrix} A & B \\ C & D \end{bmatrix} \begin{bmatrix} \dot{x}_0 \\ \dot{z}_0 \end{bmatrix} = \begin{bmatrix} E \\ F \end{bmatrix}$$

The inverse is

$$\frac{1}{(AD - BC)} \begin{bmatrix} D & -B \\ -C & A \end{bmatrix}$$

93

and

$$\dot{x}_0 = (DE - BF)/(AD - BC)$$

$$\dot{z}_0 = (FA - CE/(AD - BC)$$

$$AD = \frac{4}{\omega^2} \sin^2 \omega t_1 - \frac{3t_1}{\omega} \sin \omega t_1$$

$$BC = -\frac{4}{\omega^2} \cos^2 \omega t_1 + \frac{8}{\omega^2} \cos \omega t_1 - \frac{4}{\omega^2}$$

$$AD - BC = \frac{4}{\omega^2}(\sin^2 \omega t_1 + \cos^2 \omega t_1) - \frac{3t_1}{\omega} \sin \omega t - \frac{8}{\omega^2} \cos \omega t_1 + \frac{4}{\omega^2}$$

$$AD - BC = \frac{8}{\omega^2}(1 - \cos \omega t_1) - \frac{3t_1}{\omega} \sin \omega t_1$$

94

C-W Targeting

We can write the equation in matrix form as

$$\begin{bmatrix} \bar{\rho} \\ \dot{\bar{\rho}} \end{bmatrix} = [T] \begin{bmatrix} \bar{\rho}_0 \\ \dot{\bar{\rho}}_0 \end{bmatrix}$$

where $\bar{\rho} = \begin{bmatrix} x \\ y \\ z \end{bmatrix}$, $\dot{\bar{\rho}} = \begin{bmatrix} \dot{x} \\ \dot{y} \\ \dot{z} \end{bmatrix}$, and

$$T = \begin{bmatrix} 1 & 0 & (-6\sin\omega t + 6\omega t) & (\frac{4}{\omega}\sin\omega t - 3t) & 0 & (-\frac{2}{\omega}\cos\omega t + \frac{2}{\omega}) \\ 0 & \cos\omega t & 0 & 0 & \frac{\sin\omega t}{\omega} & 0 \\ 0 & 0 & (-3\cos\omega t + 4) & (\frac{2}{\omega}\cos\omega t - \frac{2}{\omega}) & 0 & \frac{\sin\omega t}{\omega} \\ 0 & 0 & (-6\omega\cos\omega t + 6\omega) & (4\cos\omega t - 3) & 0 & 2\sin\omega t \\ 0 & -\omega\sin\omega t & 0 & 0 & \cos\omega t & 0 \\ 0 & 0 & 3\omega\sin\omega t & -2\sin\omega t & 0 & \cos\omega t \end{bmatrix}$$

In this form we can solve several problems.

Example 1: Given the initial state $(\vec{\rho}_0, \dot{\vec{\rho}}_0)$ and ω we can describe the position and velocity as a function of time.

Given some information at each end point , the remaining information at the endpoints may be determined.

Example 2: Assume $\vec{\rho}_0$, $\vec{\rho}$, t_0 , and t are specified and the velocity at t_0 is to be found that will complete the transfer. Rewriting the matrix form of the equation as

$$\begin{bmatrix} \vec{\rho} \\ \dot{\vec{\rho}} \end{bmatrix} = \begin{bmatrix} A & B \\ C & D \end{bmatrix} \begin{bmatrix} \vec{\rho}_o \\ \dot{\vec{\rho}}_o \end{bmatrix}$$

then $\quad \vec{\rho}(t) = A(t)\vec{\rho}_0 + B(t)\dot{\vec{\rho}}_0$

Rearranging terms, we find

$$\dot{\vec{\rho}}_o = B^{-1}(t)\left[\,\vec{\rho}(t) - A(t)\vec{\rho}_o\right]$$

The submatrices A, B, C, and D are 3×3 matrices and the inverses are straight forward.

If we assume, $y = \dot{y} = y_0 = \dot{y}_0 = 0$ then the problem is reduced from three to two dimensions. The matrix B can be written as

$$B = \begin{bmatrix} b_{11} & b_{12} \\ b_{21} & b_{22} \end{bmatrix} \quad \text{and} \quad B^{-1} = \frac{1}{b_{11}b_{12} - b_{12}b_{21}} \begin{bmatrix} b_{22} & -b_{12} \\ -b_{21} & b_{11} \end{bmatrix}$$

Example 3: After some time t , the velocity $\dot{\rho}$ is to be zero. Given that the particle is initially at $\vec{\rho}_0$, the initial velocity required for the particle to have zero velocity at time t is found from

$$\dot{\vec{\rho}} = C\vec{\rho}_o + D\dot{\vec{\rho}}_o = 0$$
$$\dot{\vec{\rho}}_o = -D^{-1}C\vec{\rho}_o$$

Note: For $\omega t = 2\pi$, then $C = [0]$ and $D = I$.

96

APPENDIX C

Model Diagrams for Geometric Representation [30]

International Space Station
(Isometric Explosion)

LIST OF ITEMS:

1. AIRLOCK
2. LIFE SUPPORT MODULE
3. MINI PRESSURIZED LOGISTICS MODULE, COLUMBUS ORBITAL FACILITY
4. DOCKING COMPARTMENT
5. CUPOLA
6. FGB
7. JEM
8. JEM ELM
9. U.S. HAB, LAB & CENTRIFUGE MODULES
10. PMA
11. SERVICE MODULE
12. RESEARCH, DOCKING/ STOWAGE
13. PROGRESS-M
14. SOYUZ-TM
15. NODE
16. SPP CORE (DEPLOYED)

17. SPP PV ARRAYS
18. SPP ACTIVATOR
19. Z-1 TRUSS
20. PVA-US
21. RADIATOR (ELECTRICAL POWER SYSTEM)
22. RADIATOR (THERMAL CONTROL SYSTEM)
23. JEM EXPOSED FACILITY
24. SPP RADIATOR
25. MOBILE TRANSPORTER W/TRANSPORTER
26. UDM (FGB)
27. JEM ROBOT ARM
28. SSRMS ROBOT ARM
29. S5/6, P5/6 TRUSS
30. S0 TRUSS
31. S3/4-P3/4 TRUSS
32. S1-P1 TRUSS

REVISIONS

REV | DESCRIPTION | DATE | APPROVED

TITLE: International Space Station (Isometric Explosion)

DRAWN BY: Cake Engineer Gary Keeley

SIZE: B   ITEM NO.   DRAWING NO. 12   REV
SCALE: N/A   SHEET 12 OF 12

98

ITEM #2 (2 REQUIRED)
LIFE SUPPORT MODULE

ITEM #5
CUPOLA

ITEM #1
AIRLOCK

LOCATIONS FOR UP TO ELEVEN (11) REPLACEABLE
GAS CANNISTERS EQUALLY SPACED ABOUT 360°:
TYPICALLY FOUR (4) INSTALLED AT ONE TIME.

ITEM #3 (2 REQUIRED)
MINI PRESSURIZED LOGISTICS MODULE,
COLUMBUS ORBITAL FACILITY

ITEM #4
DOCKING COMPARTMENT

REV	DESCRIPTION	DATE	APPROVED
	REVISIONS		

TITLE: AIRLOCK, LIFE SUPPORT MODULE, ESA, DOCKING COMPARTMENT, CUPOLA

SIZE B	ITEM # 1, 2, 3, 4, 5	DRAWING NO. 1		REV
SCALE: 1:100	DRAWN BY: PAUL W. KACZMARSKI	SHEET 1	OF 12	

99

SECTION A-A

SEE NOTE 1.

NOTES:
1. AT FULL SCALE SOLAR PANELS & RADIATORS
ARE ONLY ABOUT ONE INCH THICK. IT IS IMPRACTICAL
TO MAINTAIN TRUE SCALE. USE ANY THIN SHEET
MATERIAL AVAILABLE.

TITLE		FGB		
DRAWING NO.	2			
SIZE B	ITEM NO. 6	DRAWN BY: PAUL R. HAZOUROPER	SHEET 1	OF 12
SCALE: 1:100			2	REV

ITEM #6
FGB

ITEM #8
JEM ELM

ITEM #10 (3 REQUIRED)
PMA

ITEM #7
JEM

ITEM #9 (2 REQUIRED)
U.S. HAB & LAB MODULE

TITLE
JEM, JEM ELM,
U.S. HAB & LAB MODULE, PMA

SIZE	ITEM NO.	DRAWING NO.	REV
B	7, 8, 9, 10	3	

DRAWN BY: PMA H. MCENROMEN
SHEET 3 OF 12
SCALE: 1:100

101

ITEM #25
MOBILE TRANSPORTER W/BASE

ITEM #23
JEM EXPOSED FACILITY

ITEM #24
SPP RADIATOR

SEE NOTE 1.

NOTES:
1. AT FULL SCALE SOLAR PANELS &
RADIATORS ARE ONLY ABOUT ONE
INCH THICK. IT IS IMPRACTICAL TO
MAINTAIN TRUE SCALE. USE ANY
THIN SHEET MATERIAL AVAILABLE.

REVISIONS			
REV	DESCRIPTION	DATE	APPROVED

TITLE
JEM EXPOSED FACILITY, SPP RADIATOR,
MOBILE TRANSPORTER W/BASE.

SIZE	ITEM NO.	DRAWING NO.		REV
B	23, 24, 25	9		

DRAWN BY: PAUL R. KACZMOREK

SCALE: 1:100   SHEET 9 OF 12

107

REVISIONS

REV	DESCRIPTION	DATE	APPROVED

ITEM #27
JEM ROBOT ARM

ITEM #28
SSRMS ROBOT ARM

ITEM #26
UDM (FGB)

SECTION A-A

ITEM #29 (2 REQUIRED)
S-5/6 — P-5/6 TRUSS

TITLE	UDM (FGB), JEM ROBOT ARM, SSRMS ROBOT ARM, S-6/P-6 TRUSS.			REV
SIZE	ITEM NO.	DRAWING NO.	10	
B	24, 25, 26	DRAWN BY: PAUL N. KACZMARSKI	SHEET 10 OF 12	
SCALE: 1:100				

APPENDIX D

TK Solver Program

To use the TK Solver Program to determine initial and final velocities and to generate trajectories:

•On the Variables Sheet, type the values for the following variables into the Input column:
-Ro (Earth radius plus altitude of circular orbit)
-xo, yo, and zo (Initial coordinates for trajectory with respect to the LVLH origin)
-x, y, and z (Coordinates of the target site with respect to the LVLH origin)
-t (Desired time of flight to reach the target)
-tf (Final time to which you want the values defining the trajectory to be calculated; set to the same time as for "t" if you just want the trajectory to the target site, set to a greater value to examine extended path past the target)
-steps (The number of points along the trajectory for which you want position and velocity values to be calculated and output into the data list)

•Set the variable "Switch" to any number other than 1 in the Input Column.

•Select the Solve option under the Command Column

•Set the variable "Switch" to the number 1 in the Input Column

•Select the Solve option under the Command Column

•The values for the velocities at the initial coordinates and at the target are found in the Output Column of the Variable Sheet.

•The values for position and velocity at each time step along the trajectory are listed in the Table called States (Click on the arrow next to the Tables: window in the Object Bar and drag it down to select States)

•Plots for in- and out-of-plane motion can be viewed by clicking on the arrow next to the Plots: window in the Object Bar and drag it down to select the desired plot

111

RULES

Rule
;" Basic Hill's Equations (CW Form) - RELATIVE MOTION TRAJECTORIES
x =   -2*S2*cos(w*t) +   2*S1*sin(w*t) + 3*S3*w*t + (xo+2*S2)
y =   yo*cos(w*t) + (vyo/w)*sin(w*t)
z =   S1*cos(w*t) +   S2*sin(w*t) +   2*S3
vx = 2*S1*w*cos(w*t) +   2*vzo*sin(w*t) + 3*S3*w
vy =   vyo*cos(w*t) -   yo*w*sin(w*t)
vz =   vzo*cos(w*t) -   S1*w*sin(w*t)
S1 = 2*vxo/w-3*zo
S2 = vzo/w
S3 = 2*zo-vxo/w
w = sqrt(Ge*Re^2/ro^3)
mu = Ge*Re^2
;>>>"The distance of the second body from the origin of the LVLH system
;>>>"is given by:
dist = sqrt(x^2 + y^2 + z^2)
;>>>"The following equations set up new output variables which make the
;>>>" interpretation of plotted output easier (zout is up).
zout = -z
vzout = -vz
If Switch = 1 then call LisaGen(xo,yo,zo,vxo,vyo,vzo,tf,steps)

LISAGEN

Comment:
Parameter Variables: Ge,Re,ro
Input Variables: xo,yo,zo,vxo,vyo,vzo,tf,steps
Output Variables:

Statement
call blank ('xG1)
call blank ('yG1)
call blank ('zG1)
call blank ('vxG1)
call blank ('vyG1)
call blank ('vzG1)
call blank ('tOut)
"Set initial conditions for the period
mu = Ge*Re^2
Period = 2*pi()*sqrt(ro^3/mu)
Dt = tf/steps
t = 0
sp1 = steps+1
for i = 1 to sp1 step 1
" Find state at the given time
call Propag(xo,yo,zo,vxo,vyo,vzo,t;x,y,z,zout,vx,vy,vz,vzout)
'xG1[i] = x
'yG1[i] = y
'zG1[i] = zout
'vxG1[i] = vx
'vyG1[i] = vy
'vzG1[i] = vzout
'tOut[i] = t
t = t + Dt
next i
return

PROPAG

Comment:
Parameter Variables: Ge,Re,ro
Argument Variables: xo,yo,zo,vxo,vyo,vzo,t
Result Variables: x,y,z,vx,vy,vz,vzout

Rule
" Basic Hill's Equations (CW Form) - Propagation
S1 = 2*vxo/w-3*zo
S2 = vzo/w
S3 = 2*zo-vxo/w
w = sqrt(Ge*Re^2/ro^3)
mu = Ge*Re^2
x =   -2*S2*cos(w*t) +   2*S1*sin(w*t) + 3*S3*w*t + (xo+2*S2)
y =   yo*cos(w*t) + (vyo/w)*sin(w*t)
z =   S1*cos(w*t) +   S2*sin(w*t) +   2*S3
vx = 2*S1*w*cos(w*t) +   2*vzo*sin(w*t) + 3*S3*w
vy =   vyo*cos(w*t) -   yo*w*sin(w*t)
vz =   vzo*cos(w*t) -   S1*w*sin(w*t)
dist = sqrt(x^2 + y^2 + z^2)
zout = -z
vzout = -vz
Period = 2*pi()*sqrt(ro^3/mu)

VARIABLES

Sta	Input	Name	Output	Unit	Comment
	6378	Re		km	Radius of the Earth
	9.81	Ge		m/s^2	Earth's Surface Gravitational Accel.
	6778	ro		km	Base Orbit Radius (LVLH Origin)
	-23.834	xo		ft	
	25.458	yo		ft	
	3.646	zo		ft	
	-146.999	x		ft	
	0	y		ft	
	1.313	z		ft	
	26	t		min	
	1	Switch			
		vxo	-.02623616	ft/s	
		vyo	.005698362	ft/s	
		vzo	-.08162583	ft/s	
	26	tf		min	
	65	steps			
		vx	-.03151832	ft/s	
		vy	-.02937775	ft/s	
		vz	.079455823	ft/s	
		vzout	-.07945582	ft/s	
		mu	1.40927E16		
		dist	147.004864		
		zout	-1.313		
		w	.001132053		
		S1	-57.289477		
		S2	-72.104261		
		S3	30.4677385		

tOut	xG1	zG1	yG1	vxG1	vzG1	vyG1
0.000	-23.834	-3.646	25.458	-0.026	0.082	0.006
24.000	-24.517	-1.708	25.585	-0.031	0.080	0.005
48.000	-25.303	0.186	25.694	-0.035	0.078	0.004
72.000	-26.191	2.034	25.783	-0.039	0.076	0.003
96.000	-27.179	3.837	25.854	-0.043	0.074	0.003
120.000	-28.263	5.591	25.905	-0.047	0.072	0.002
144.000	-29.441	7.297	25.937	-0.051	0.070	0.001
168.000	-30.711	8.952	25.951	-0.055	0.068	0.000
192.000	-32.069	10.555	25.945	-0.058	0.066	-0.001
216.000	-33.512	12.106	25.919	-0.062	0.063	-0.001
240.000	-35.039	13.603	25.875	-0.065	0.061	-0.002
264.000	-36.645	15.044	25.812	-0.069	0.059	-0.003
288.000	-38.328	16.430	25.729	-0.072	0.057	-0.004
312.000	-40.085	17.759	25.628	-0.075	0.054	-0.005
336.000	-41.913	19.029	25.507	-0.078	0.052	-0.005
360.000	-43.808	20.241	25.368	-0.080	0.049	-0.006
384.000	-45.767	21.392	25.210	-0.083	0.047	-0.007
408.000	-47.787	22.483	25.034	-0.085	0.044	-0.008
432.000	-49.865	23.512	24.839	-0.088	0.042	-0.009
456.000	-51.997	24.479	24.625	-0.090	0.039	-0.009
480.000	-54.180	25.383	24.394	-0.092	0.036	-0.010
504.000	-56.410	26.223	24.144	-0.094	0.034	-0.011
528.000	-58.684	26.999	23.877	-0.096	0.031	-0.012
552.000	-60.998	27.710	23.592	-0.097	0.028	-0.012
576.000	-63.350	28.355	23.289	-0.099	0.026	-0.013
600.000	-65.734	28.934	22.970	-0.100	0.023	-0.014
624.000	-68.149	29.448	22.633	-0.101	0.020	-0.014
648.000	-70.589	29.894	22.280	-0.102	0.017	-0.015
672.000	-73.052	30.274	21.910	-0.103	0.014	-0.016
696.000	-75.533	30.586	21.525	-0.104	0.012	-0.016
720.000	-78.030	30.830	21.123	-0.104	0.009	-0.017
744.000	-80.538	31.007	20.705	-0.105	0.006	-0.018
768.000	-83.054	31.116	20.273	-0.105	0.003	-0.018
792.000	-85.574	31.157	19.825	-0.105	0.000	-0.019
816.000	-88.095	31.130	19.363	-0.105	-0.003	-0.020
840.000	-90.612	31.035	18.886	-0.105	-0.005	-0.020
864.000	-93.122	30.872	18.396	-0.104	-0.008	-0.021
888.000	-95.621	30.642	17.892	-0.104	-0.011	-0.021
912.000	-98.106	30.344	17.375	-0.103	-0.014	-0.022
936.000	-100.570	29.978	16.845	-0.102	-0.017	-0.022
960.000	-103.020	29.546	16.302	-0.101	-0.019	-0.023
984.000	-105.440	29.046	15.748	-0.100	-0.022	-0.023

116

tOut	xG1	zG1	yG1	vxG1	vzG1	vyG1
1,008.000	-107.830	28.480	15.182	-0.099	-0.025	-0.024
1,032.000	-110.190	27.848	14.604	-0.098	-0.028	-0.024
1,056.000	-112.510	27.151	14.016	-0.096	-0.030	-0.025
1,080.000	-114.790	26.389	13.418	-0.094	-0.033	-0.025
1,104.000	-117.030	25.562	12.809	-0.092	-0.036	-0.026
1,128.000	-119.230	24.671	12.191	-0.090	-0.038	-0.026
1,152.000	-121.370	23.717	11.564	-0.088	-0.041	-0.026
1,176.000	-123.460	22.701	10.929	-0.086	-0.044	-0.027
1,200.000	-125.490	21.623	10.286	-0.083	-0.046	-0.027
1,224.000	-127.460	20.484	9.635	-0.081	-0.049	-0.027
1,248.000	-129.370	19.285	8.977	-0.078	-0.051	-0.028
1,272.000	-131.210	18.026	8.312	-0.075	-0.054	-0.028
1,296.000	-132.980	16.710	7.641	-0.072	-0.056	-0.028
1,320.000	-134.680	15.336	6.964	-0.069	-0.058	-0.028
1,344.000	-136.300	13.905	6.283	-0.066	-0.061	-0.029
1,368.000	-137.850	12.420	5.596	-0.063	-0.063	-0.029
1,392.000	-139.310	10.880	4.906	-0.059	-0.065	-0.029
1,416.000	-140.690	9.288	4.212	-0.056	-0.067	-0.029
1,440.000	-141.970	7.643	3.515	-0.052	-0.070	-0.029
1,464.000	-143.170	5.948	2.815	-0.048	-0.072	-0.029
1,488.000	-144.270	4.204	2.113	-0.044	-0.074	-0.029
1,512.000	-145.280	2.411	1.409	-0.040	-0.076	-0.029
1,536.000	-146.190	0.572	0.705	-0.036	-0.078	-0.029
1,560.000	-147.000	-1.313	0.000	-0.032	-0.079	-0.029

117

APPENDIX E

In-Plane and Out-of-Plane Motion Plots for Trajectories to All Targets

118

X Z Plane Positions

outofplane

Joint Airlock to Target #1   Time of Flight - 26 minutes

119

X Z Plane Positions

outofplane
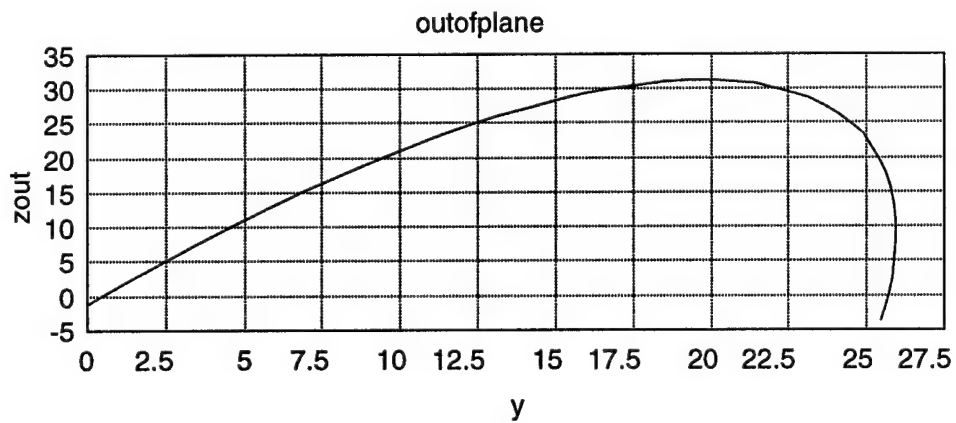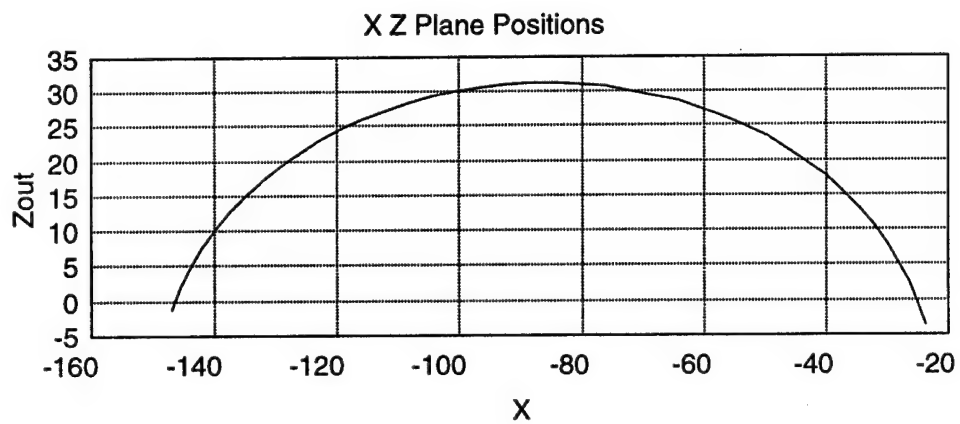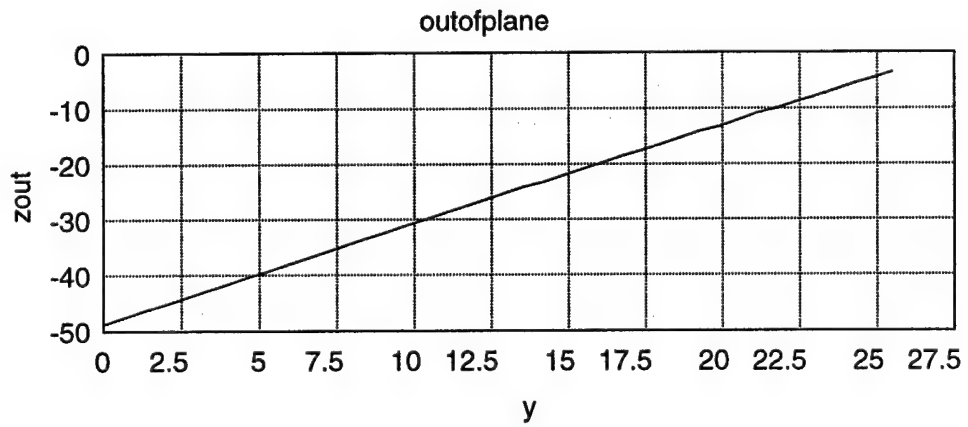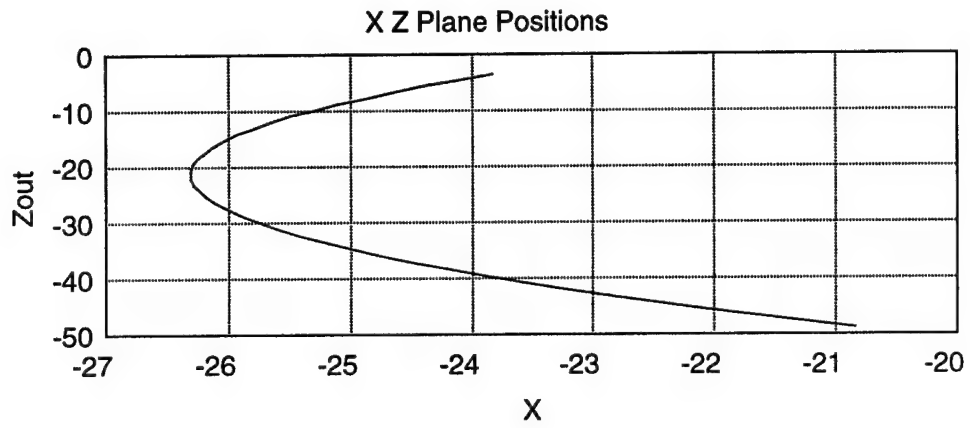
Joint Airlock to Target #2   Time of Flight -5 minutes

X Z Plane Positions

outofplane
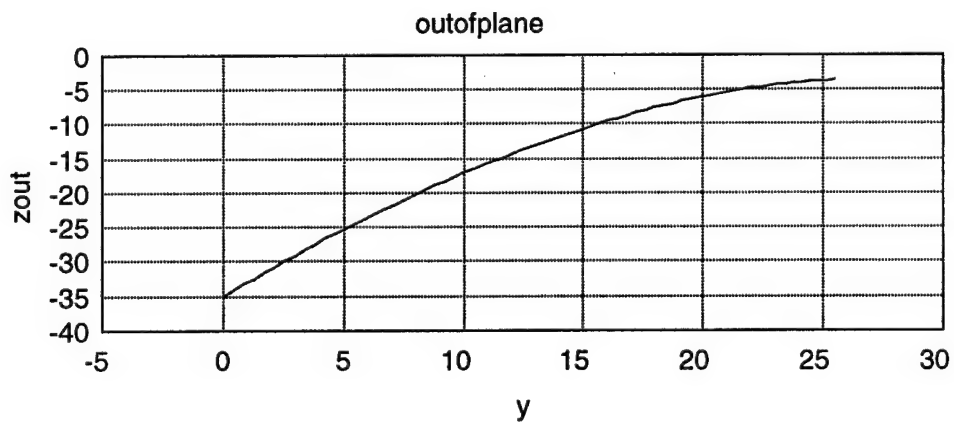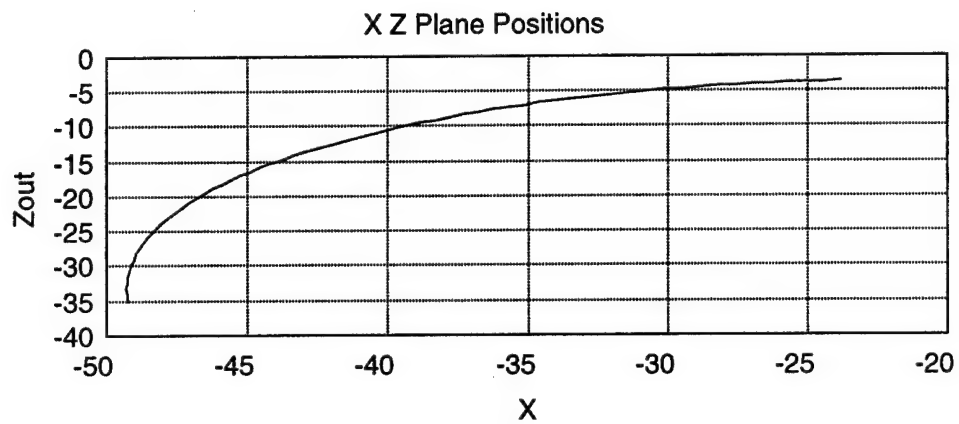
Joint Airlock to Target #3   Time of Flight - 10 minutes

X Z Plane Positions

outofplane
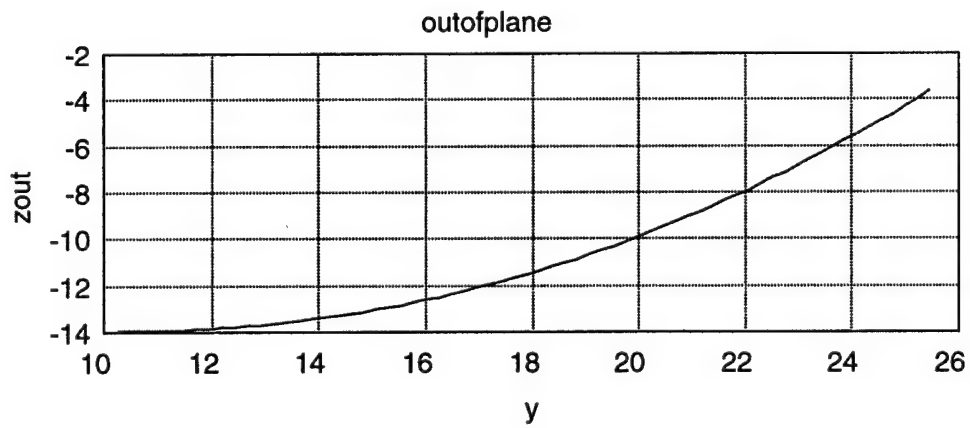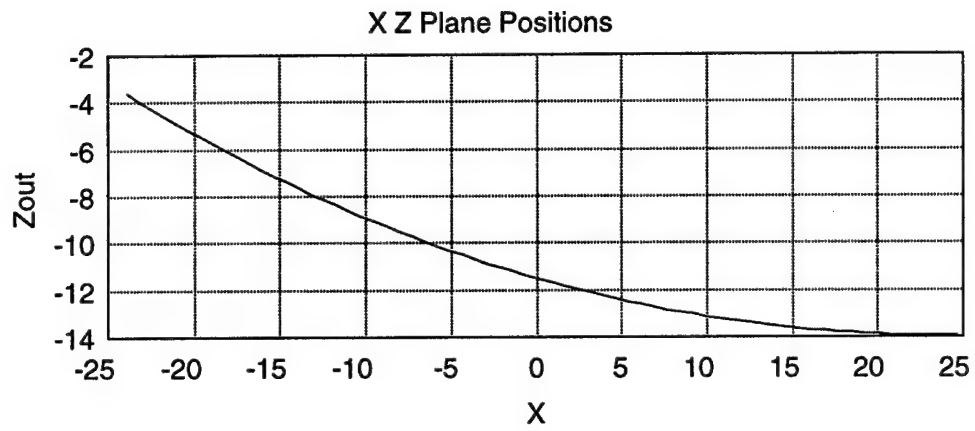
Joint Airlock to Target #4   Time of Flight - 3.5 minutes

122

X Z Plane Positions

outofplane
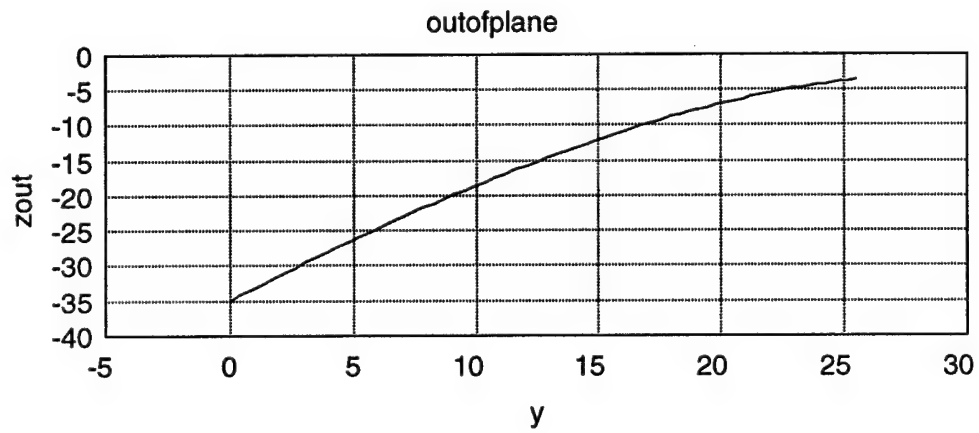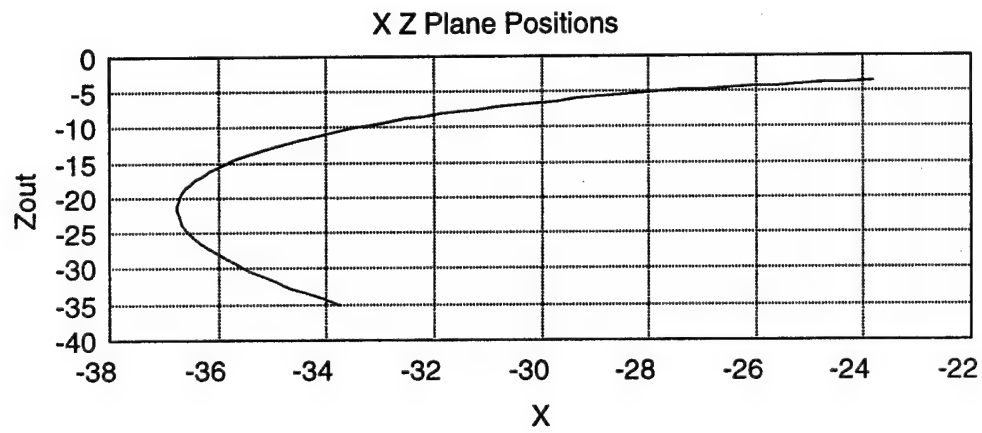
Joint Airlock to Target #5   Time of Flight - 12 minutes

123

X Z Plane Positions

outofplane

Joint Airlock to Target #6   Time of Flight -65 minutes

X Z Plane Positions

outofplane
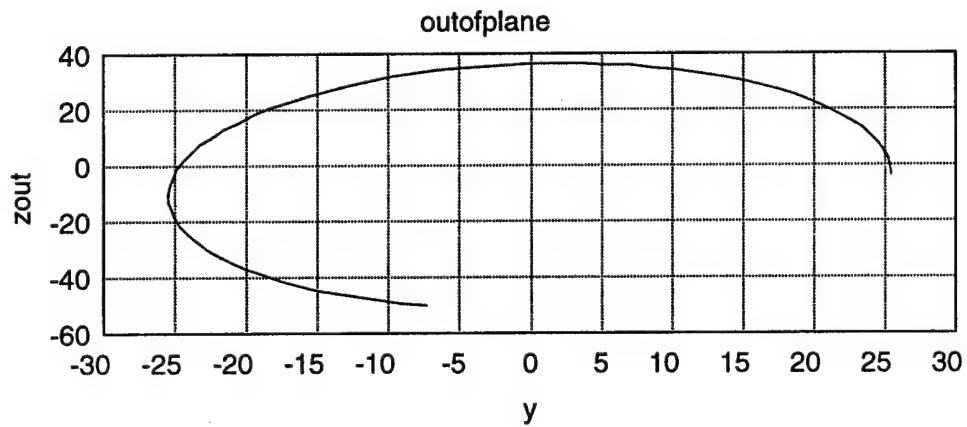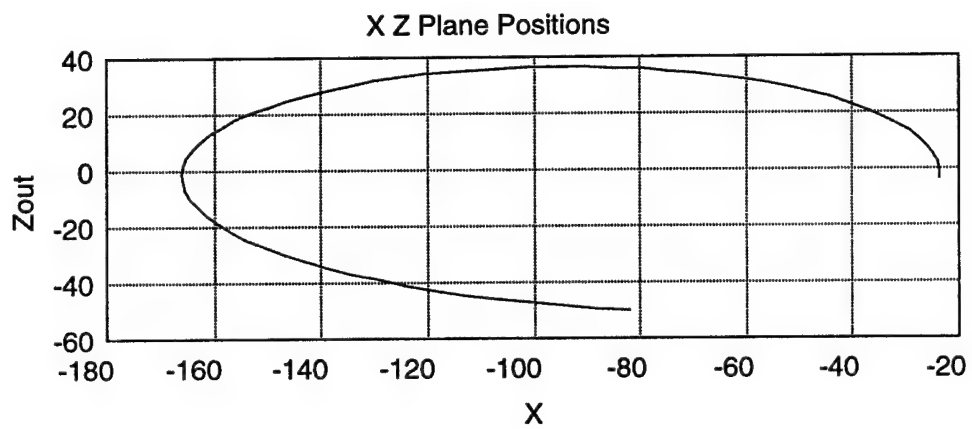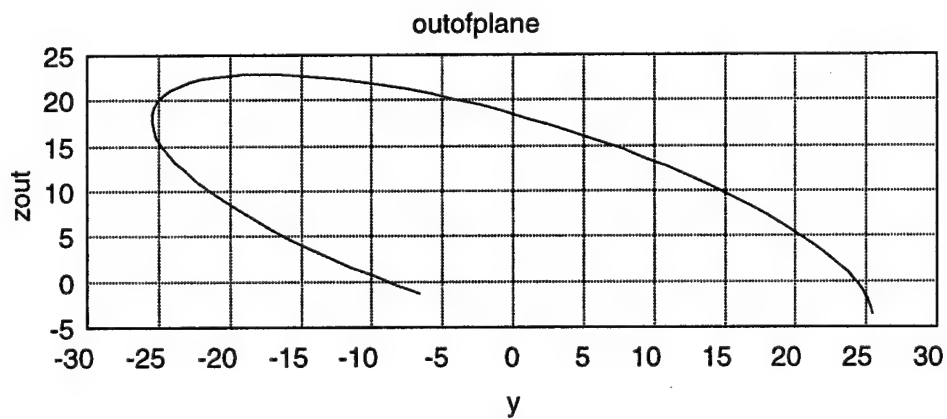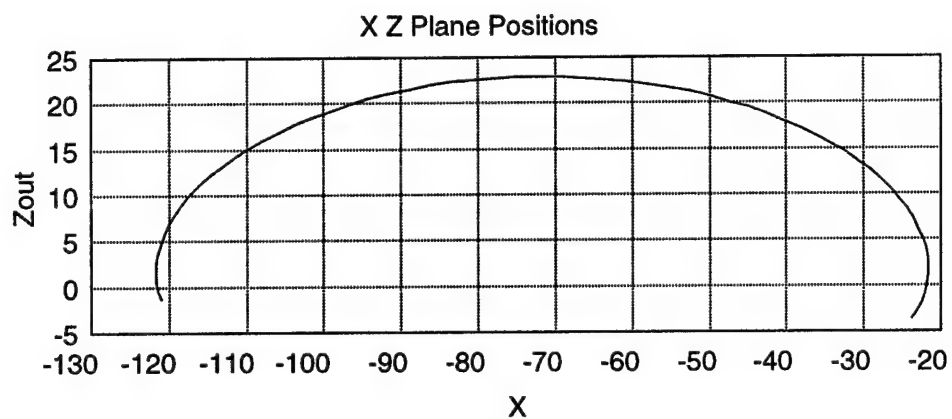
Joint Airlock to Target #8   Time of Flight - 65 minutes

125

X Z Plane Positions

outofplane
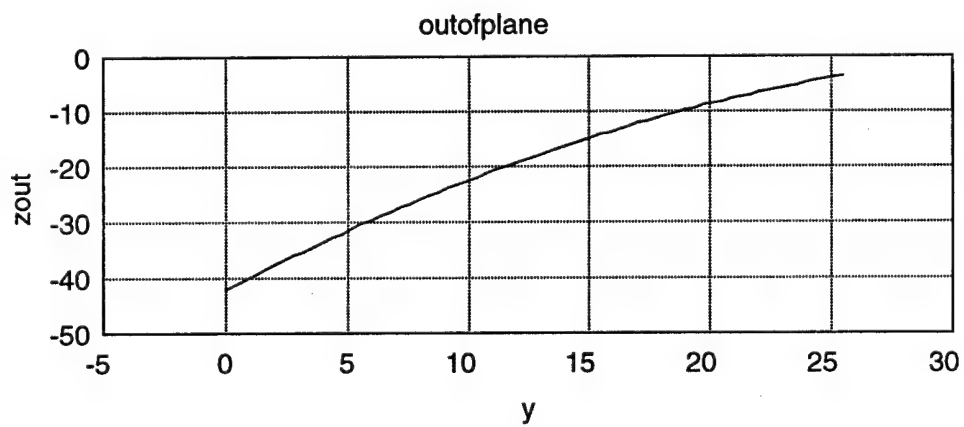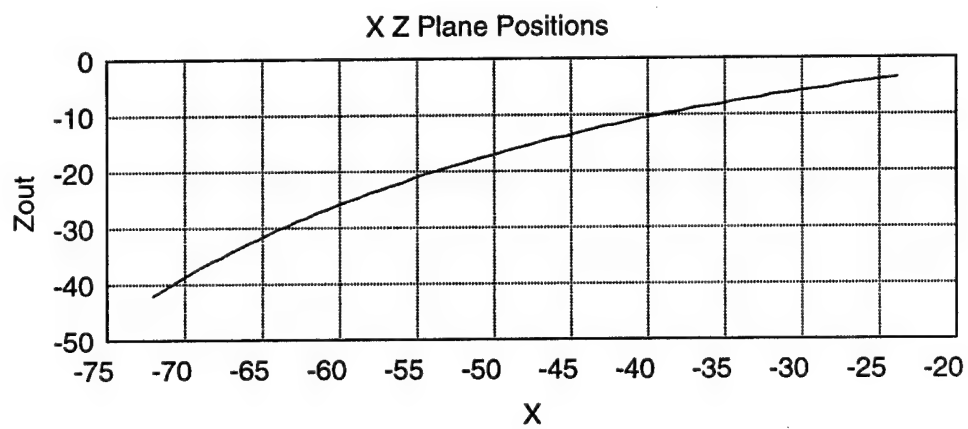
Joint Airlock to Target #9   Time of Flight - 5 minutes

126

X Z Plane Positions

outofplane
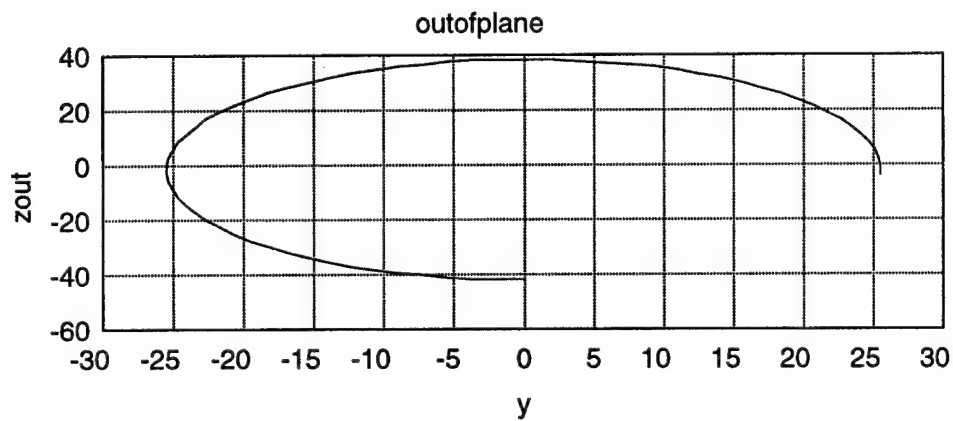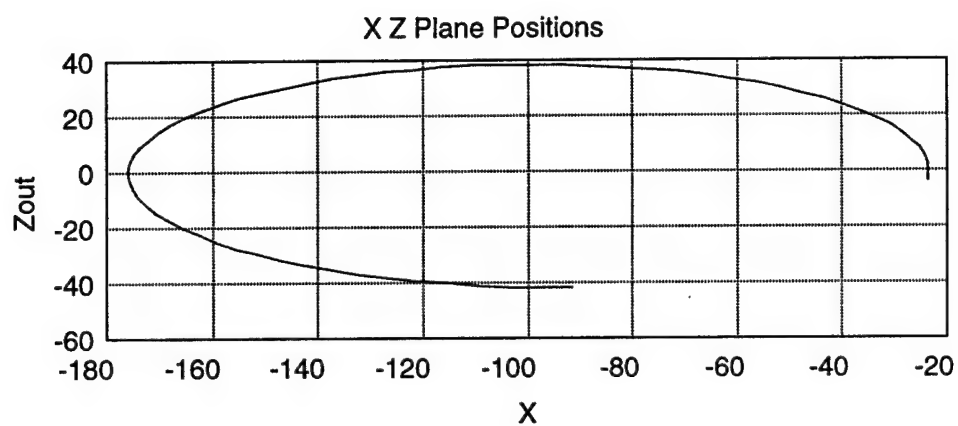
Joint Airlock to Target #11   Time of Flight - 70 minutes

127

X Z Plane Positions

outofplane
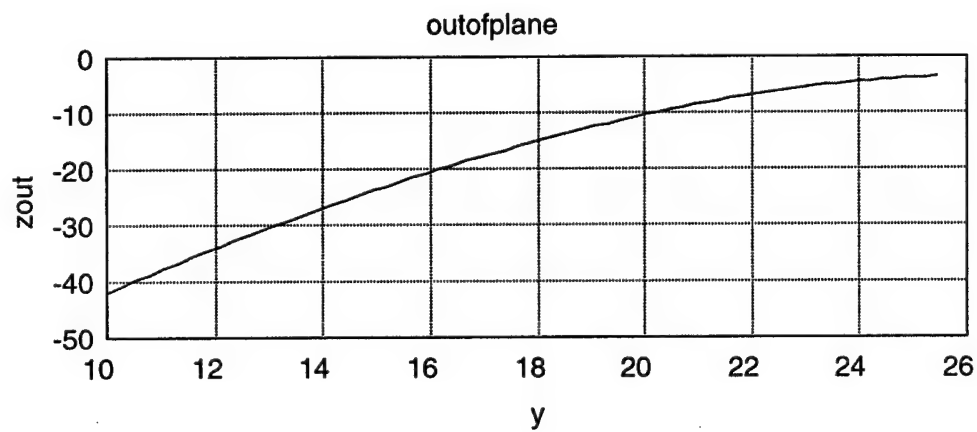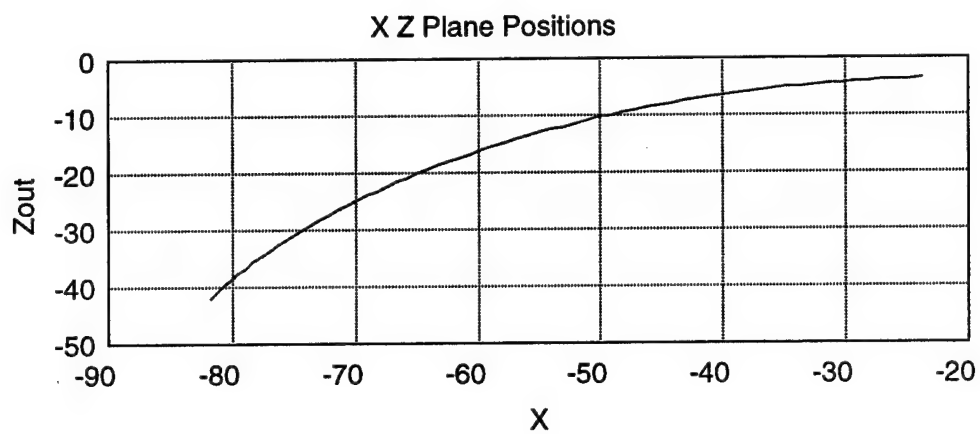
Joint Airlock to Target #12   Time of Flight - 7 minutes

128

X Z Plane Positions

outofplane

Joint Airlock to Target #13   Time of Flight - 65 minutes

129

X Z Plane Positions

outofplane
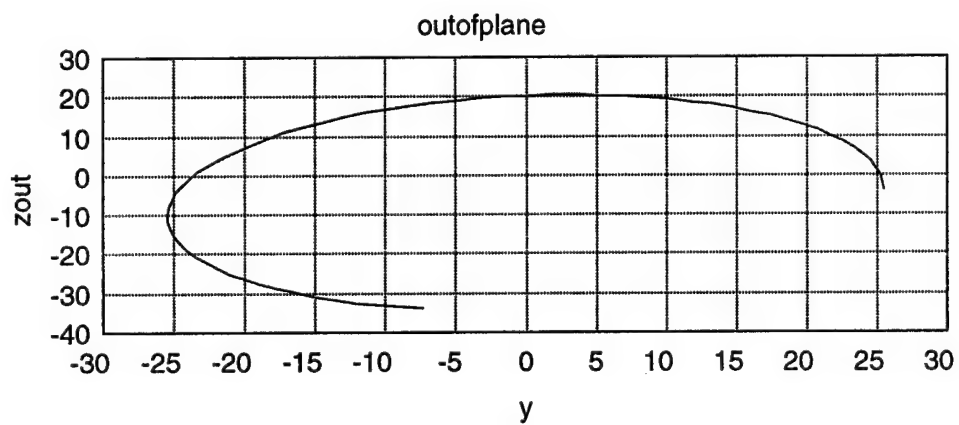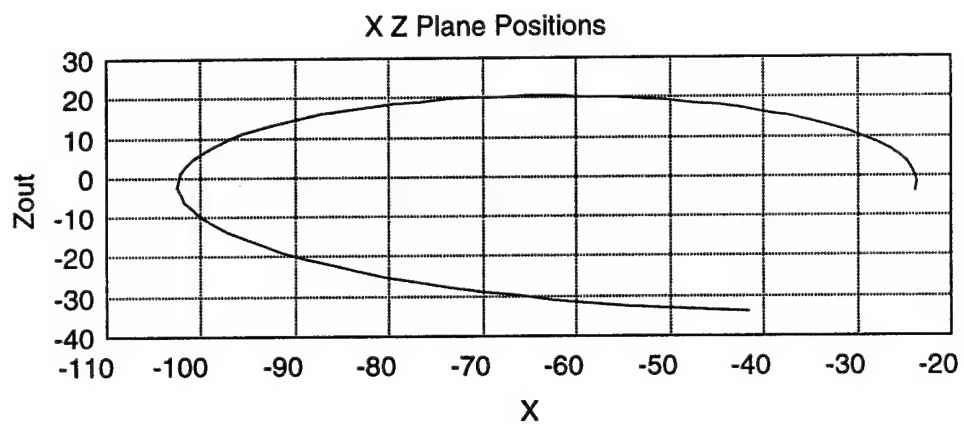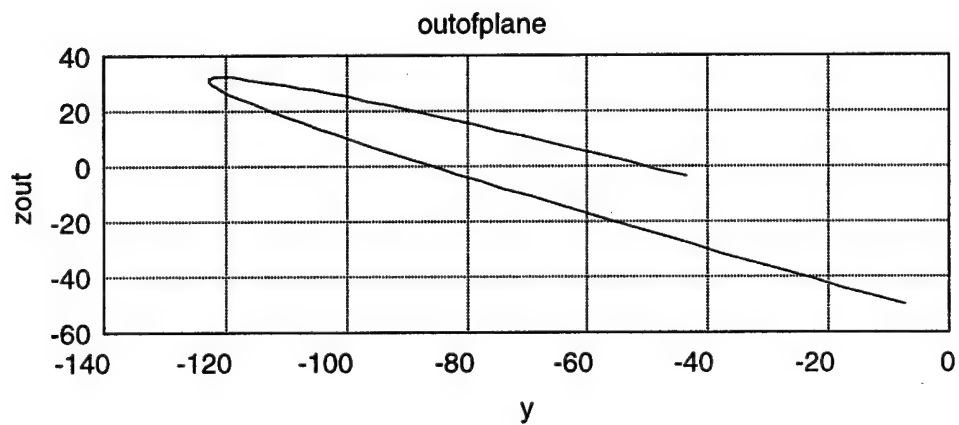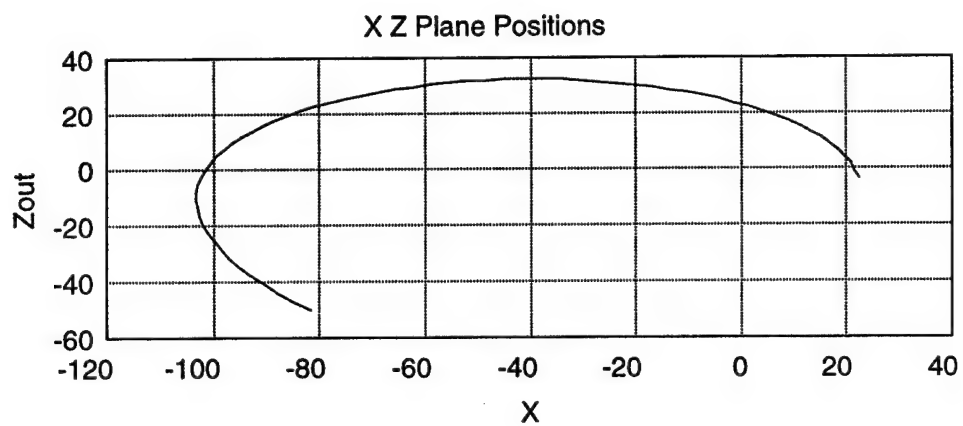
JEM Airlock to Target #6   Time of Flight - 40 minutes

130

X Z Plane Positions

outofplane

JEM Airlock to Target #10   Time of Flight - 10 minutes

X Z Plane Positions

outofplane
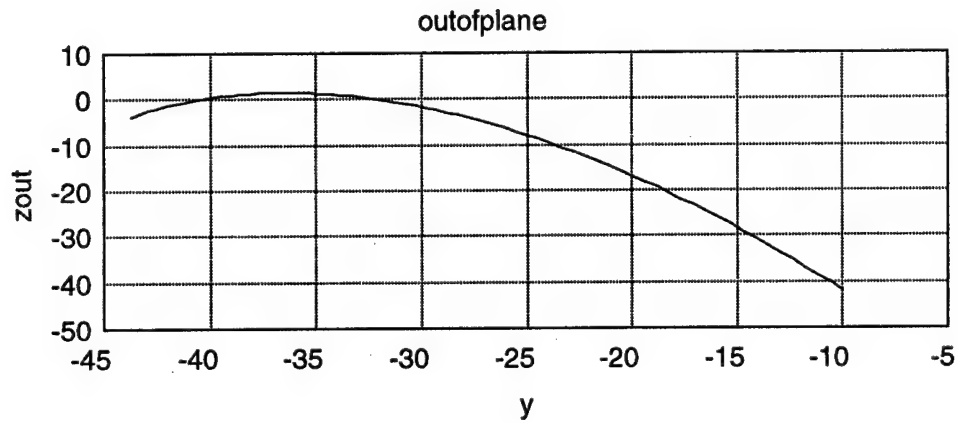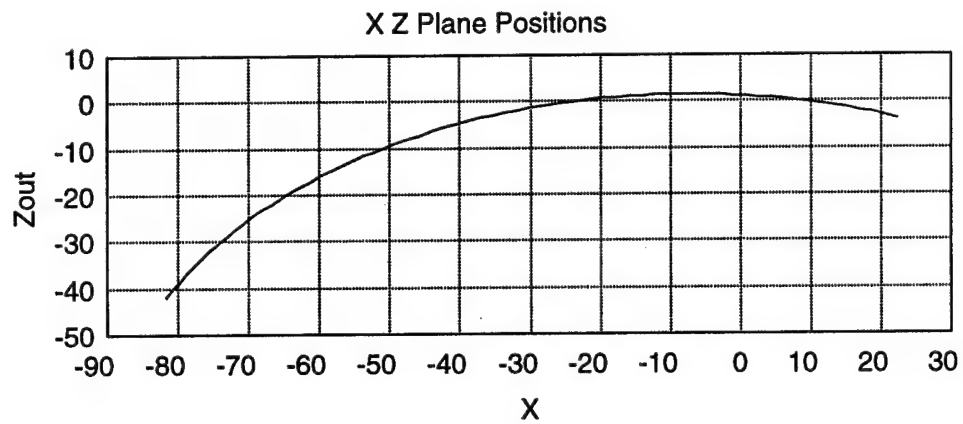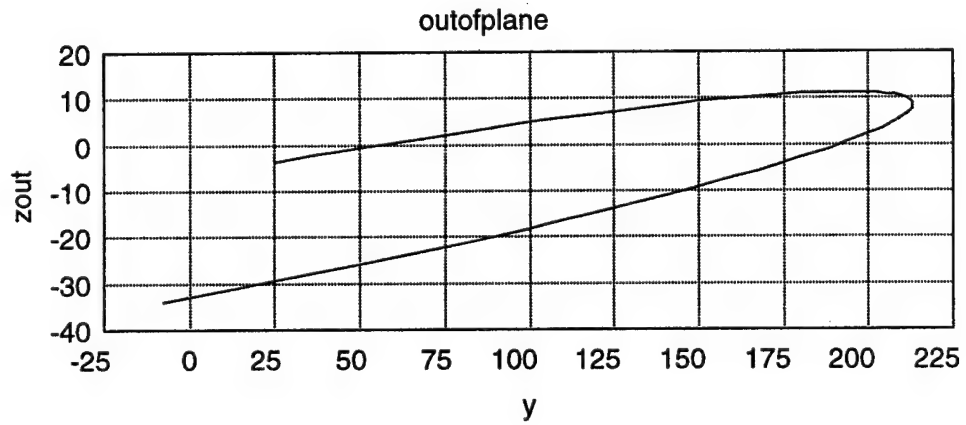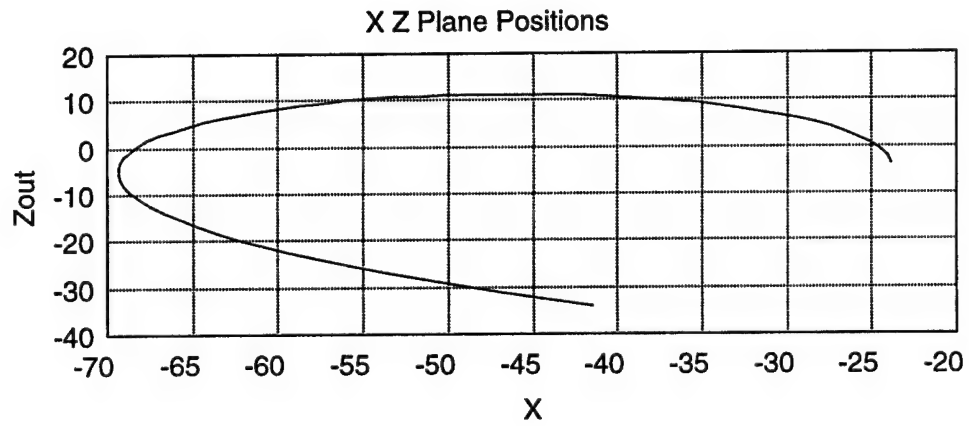
JEM Airlock to Target #13   Time of Flight - 45 minutes

132

APPENDIX F

Excel Coordinates and Acceleration Data

133

x (ft)	z (ft)	Xacc (ft/s^2)	Zacc*10^5 (ft/s^2)
115.908	-4.685	0.000	-1.925
110.908	-4.685	0.000	-1.925
105.908	-4.685	0.000	-1.925
100.908	-4.685	0.000	-1.925
95.908	-4.685	0.000	-1.925
90.908	-4.685	0.000	-1.925
85.908	-4.685	0.000	-1.925
80.908	-4.685	0.000	-1.925
75.908	-4.685	0.000	-1.925
70.908	-4.685	0.000	-1.925
65.908	-4.685	0.000	-1.925
60.908	-4.685	0.000	-1.925
55.908	-4.685	0.000	-1.925
50.908	-4.685	0.000	-1.925
45.908	-4.685	0.000	-1.925
41.833	-4.685	0.000	-1.925
41.833	1.685	0.000	0.692
41.833	6.685	0.000	2.747
41.833	9.685	0.000	3.980
41.833	11.604	0.000	4.769
37.875	11.604	0.000	4.769
34.875	11.604	0.000	4.769
34.875	16.604	0.000	6.824
34.875	21.604	0.000	8.878
34.875	26.604	0.000	10.933
34.875	31.604	0.000	12.988
34.875	34.270	0.000	14.084
29.875	34.270	0.000	14.084
24.875	34.270	0.000	14.084
19.875	34.270	0.000	14.084
14.292	34.270	0.000	14.084
14.292	29.270	0.000	12.029
14.292	24.270	0.000	9.974
14.292	19.270	0.000	7.919
14.292	13.937	0.000	5.728
9.292	13.937	0.000	5.728
4.292	13.937	0.000	5.728
-0.551	13.937	0.000	5.728
-0.551	18.937	0.000	7.782
-0.551	23.937	0.000	9.837
-0.551	28.937	0.000	11.892

-0.551	33.937	0.000	13.947
-0.551	38.937	0.000	16.002
-0.551	42.313	0.000	17.389
-5.551	42.313	0.000	17.389
-10.551	42.313	0.000	17.389
-13.751	42.771	0.000	17.577
-15.209	45.771	0.000	18.810
-15.209	48.854	0.000	20.077
-20.834	48.854	0.000	20.077
-26.273	48.854	0.000	20.077
-26.273	52.730	0.000	21.670
-30.273	52.730	0.000	21.670
-34.084	52.730	0.000	21.670
-34.084	55.730	0.000	22.903
-39.084	55.730	0.000	22.903
-44.084	55.730	0.000	22.903
-48.917	55.730	0.000	22.903
-48.917	52.730	0.000	21.670
-53.917	52.730	0.000	21.670
-56.727	52.730	0.000	21.670
-56.727	49.896	0.000	20.505
-61.727	49.896	0.000	20.505
-66.727	49.896	0.000	20.505
-71.727	49.896	0.000	20.505
-75.125	49.896	0.000	20.505
-75.125	54.896	0.000	22.560
-75.125	57.229	0.000	23.519
-70.125	57.229	0.000	23.519
-66.523	57.229	0.000	23.519
-66.523	62.229	0.000	25.574
-66.523	67.896	0.000	27.903
-71.523	67.896	0.000	27.903
-74.334	67.896	0.000	27.903
-74.334	70.896	0.000	29.135
-79.334	70.896	0.000	29.135
-84.334	70.896	0.000	29.135
-89.167	70.896	0.000	29.135
-89.167	67.896	0.000	27.903
-92.167	67.896	0.000	27.903
-96.977	67.896	0.000	27.903
-96.977	62.896	0.000	25.848
-96.977	57.229	0.000	23.519
-91.977	57.229	0.000	23.519

-88.375	57.229	0.000	23.519
-88.375	52.229	0.000	21.464
-88.375	49.896	0.000	20.505
-93.375	49.896	0.000	20.505
-98.375	49.896	0.000	20.505
-103.375	49.896	0.000	20.505
-108.375	49.896	0.000	20.505
-112.445	49.896	0.000	20.505
-112.445	44.896	0.000	18.451
-112.445	39.896	0.000	16.396
-112.445	34.396	0.000	14.135
-107.445	34.396	0.000	14.135
-102.445	34.396	0.000	14.135
-97.445	34.396	0.000	14.135
-91.459	34.396	0.000	14.135
-91.459	29.396	0.000	12.081
-91.459	24.396	0.000	10.026
-91.459	19.396	0.000	7.971
-91.459	14.396	0.000	5.916
-91.968	9.063	0.000	3.725
-96.833	9.063	0.000	3.725
-99.833	11.021	0.000	4.529
-104.833	11.021	0.000	4.529
-109.833	11.021	0.000	4.529
-114.833	11.021	0.000	4.529
-119.833	11.021	0.000	4.529
-124.166	11.021	0.000	4.529
-124.166	7.896	0.000	3.245
-129.166	7.896	0.000	3.245
-134.166	7.896	0.000	3.245
-138.499	7.896	0.000	3.245
-141.499	8.854	0.000	3.639
-146.999	8.854	0.000	3.639
-146.999	3.854	0.000	1.584
-146.999	-2.854	0.000	-1.173
-146.999	-6.229	0.000	-2.560
-141.499	-6.229	0.000	-2.560
-138.499	-5.271	0.000	-2.166
-133.499	-5.271	0.000	-2.166
-130.177	-5.271	0.000	-2.166
-130.177	-10.271	0.000	-4.221
-130.177	-14.296	0.000	-5.875
-136.163	-14.296	0.000	-5.875

136

-136.163	-19.296	0.000	-7.930
-136.163	-24.296	0.000	-9.985
-136.163	-29.296	0.000	-12.040
-136.163	-32.629	0.000	-13.409
-131.163	-32.629	0.000	-13.409
-126.163	-32.629	0.000	-13.409
-121.163	-32.629	0.000	-13.409
-116.163	-32.629	0.000	-13.409
-111.163	-32.629	0.000	-13.409
-106.163	-32.629	0.000	-13.409
-101.163	-32.629	0.000	-13.409
-96.163	-32.629	0.000	-13.409
-91.163	-32.629	0.000	-13.409
-88.887	-32.629	0.000	-13.409
-88.887	-37.629	0.000	-15.464
-88.887	-42.629	0.000	-17.519
-88.887	-47.629	0.000	-19.574
-88.887	-52.629	0.000	-21.628
-88.887	-57.629	0.000	-23.683
-88.887	-62.629	0.000	-25.738
-88.887	-68.521	0.000	-28.159
-93.887	-68.521	0.000	-28.159
-98.887	-68.521	0.000	-28.159
-103.887	-68.521	0.000	-28.159
-108.887	-68.521	0.000	-28.159
-110.209	-68.521	0.000	-28.159
-110.209	-76.101	0.000	-31.275
-105.209	-76.101	0.000	-31.275
-101.958	-76.101	0.000	-31.275
-98.958	-81.101	0.000	-33.329
-93.958	-81.101	0.000	-33.329
-88.958	-81.101	0.000	-33.329
-83.958	-81.101	0.000	-33.329
-78.958	-81.101	0.000	-33.329
-73.958	-81.101	0.000	-33.329
-68.958	-81.101	0.000	-33.329
-64.541	-81.101	0.000	-33.329
-61.541	-76.101	0.000	-31.275
-56.541	-76.101	0.000	-31.275
-53.292	-76.101	0.000	-31.275
-53.292	-68.521	0.000	-28.159
-58.292	-68.521	0.000	-28.159
-63.292	-68.521	0.000	-28.159

137

-68.292	-68.521	0.000	-28.159
-74.613	-68.521	0.000	-28.159
-74.613	-63.521	0.000	-26.105
-74.613	-58.521	0.000	-24.050
-74.613	-53.521	0.000	-21.995
-74.613	-48.521	0.000	-19.940
-74.613	-43.521	0.000	-17.885
-74.613	-38.521	0.000	-15.831
-74.613	-32.604	0.000	-13.399
-69.613	-32.604	0.000	-13.399
-64.613	-32.604	0.000	-13.399
-59.613	-32.604	0.000	-13.399
-54.613	-32.604	0.000	-13.399
-49.613	-32.604	0.000	-13.399
-44.613	-32.604	0.000	-13.399
-39.613	-31.728	0.000	-13.039
-34.613	-31.728	0.000	-13.039
-29.613	-31.728	0.000	-13.039
-24.613	-31.728	0.000	-13.039
-19.613	-31.728	0.000	-13.039
-14.613	-31.728	0.000	-13.039
-9.613	-31.728	0.000	-13.039
-6.885	-31.728	0.000	-13.039
-6.885	-26.728	0.000	-10.984
-6.885	-20.729	0.000	-8.519
-1.885	-20.729	0.000	-8.519
0.949	-20.729	0.000	-8.519
0.949	-22.520	0.000	-9.255
6.034	-22.520	0.000	-9.255
6.034	-27.520	0.000	-11.310
6.034	-32.520	0.000	-13.364
6.034	-37.520	0.000	-15.419
6.034	-42.520	0.000	-17.474
6.034	-47.520	0.000	-19.529
6.034	-52.520	0.000	-21.584
6.034	-57.520	0.000	-23.638
6.034	-63.354	0.000	-26.036
9.699	-63.354	0.000	-26.036
13.364	-63.354	0.000	-26.036
13.364	-58.354	0.000	-23.981
13.364	-53.354	0.000	-21.926
13.364	-48.354	0.000	-19.872
13.364	-43.354	0.000	-17.817

13.364	-38.354	0.000	-15.762
13.364	-33.354	0.000	-13.707
13.364	-28.354	0.000	-11.652
13.364	-23.354	0.000	-9.598
13.364	-18.354	0.000	-7.543
13.364	-13.939	0.000	-5.728
14.292	-13.939	0.000	-5.728
14.292	-18.939	0.000	-7.783
14.292	-23.939	0.000	-9.838
14.292	-28.939	0.000	-11.893
14.292	-33.939	0.000	-13.948
14.292	-35.063	0.000	-14.410
19.292	-35.063	0.000	-14.410
24.292	-35.063	0.000	-14.410
29.292	-35.063	0.000	-14.410
34.875	-35.063	0.000	-14.410
34.875	-30.063	0.000	-12.355
34.875	-25.063	0.000	-10.300
34.875	-20.063	0.000	-8.245
34.875	-13.939	0.000	-5.728
39.875	-13.939	0.000	-5.728
44.875	-13.939	0.000	-5.728
49.875	-13.939	0.000	-5.728
54.875	-13.939	0.000	-5.728
59.875	-13.939	0.000	-5.728
64.875	-13.939	0.000	-5.728
69.875	-13.939	0.000	-5.728
74.875	-13.939	0.000	-5.728
79.875	-13.939	0.000	-5.728
84.875	-13.939	0.000	-5.728
89.875	-13.939	0.000	-5.728
94.875	-13.939	0.000	-5.728
99.875	-13.939	0.000	-5.728
104.875	-13.939	0.000	-5.728
109.875	-13.939	0.000	-5.728
114.875	-13.939	0.000	-5.728
118.908	-13.939	0.000	-5.728
121.908	-13.939	0.000	-5.728
121.908	-8.939	0.000	-3.674
121.908	-4.685	0.000	-1.925
-10.543	13.937	0.000	5.728
-10.543	18.937	0.000	7.782
-10.543	23.937	0.000	9.837

-10.543	28.937	0.000	11.892
-10.543	33.937	0.000	13.947
-10.543	38.854	0.000	15.967
-31.126	13.937	0.000	5.728
-31.126	18.937	0.000	7.782
-31.126	23.937	0.000	9.837
-31.126	28.937	0.000	11.892
-31.126	33.937	0.000	13.947
-31.126	38.937	0.000	16.002
-31.126	42.063	0.000	17.286
-34.875	42.063	0.000	17.286
-34.875	37.063	0.000	15.231
-34.875	33.646	0.000	13.827
-33.750	30.646	0.000	12.594
-33.750	25.646	0.000	10.540
-33.750	20.646	0.000	8.485
-33.750	15.646	0.000	6.430
-33.750	13.937	0.000	5.728
-49.250	11.230	0.000	4.615
-49.250	16.230	0.000	6.670
-49.250	21.230	0.000	8.725
-49.250	26.230	0.000	10.780
-49.250	31.230	0.000	12.834
-49.250	36.230	0.000	14.889
-49.250	42.063	0.000	17.286
-58.008	42.063	0.000	17.286
-58.008	37.063	0.000	15.231
-58.008	34.396	0.000	14.135
-63.008	34.396	0.000	14.135
-68.008	34.396	0.000	14.135
-72.042	34.396	0.000	14.135
-72.042	29.396	0.000	12.081
-72.042	24.396	0.000	10.026
-72.042	19.396	0.000	7.971
-72.042	14.396	0.000	5.916
-72.042	11.230	0.000	4.615
-67.042	11.230	0.000	4.615
-62.042	11.230	0.000	4.615
-57.042	11.230	0.000	4.615
-52.042	11.230	0.000	4.615

x (ft)	y (ft)	Xacc (ft/s^2)	Yacc*10^5 (ft/s^2)
7.657	-187.249	0.000	-2.565
17.657	-187.249	0.000	-2.565
27.657	-187.249	0.000	-2.565
37.657	-187.249	0.000	-2.565
47.657	-187.249	0.000	-2.565
57.657	-187.249	0.000	-2.565
67.657	-187.249	0.000	-2.565
77.657	-187.249	0.000	-2.565
87.657	-187.249	0.000	-2.565
97.657	-187.249	0.000	-2.565
107.657	-187.249	0.000	-2.565
117.657	-187.249	0.000	-2.565
121.908	-187.249	0.000	-2.565
121.908	-177.249	0.000	-2.428
121.908	-167.249	0.000	-2.291
121.908	-157.249	0.000	-2.154
121.908	-147.249	0.000	-2.017
121.908	-137.249	0.000	-1.880
121.908	-127.249	0.000	-1.743
121.908	-117.249	0.000	-1.606
121.908	-107.249	0.000	-1.469
121.908	-100.164	0.000	-1.372
111.908	-100.164	0.000	-1.372
101.908	-100.164	0.000	-1.372
91.908	-100.164	0.000	-1.372
81.908	-100.164	0.000	-1.372
71.908	-100.164	0.000	-1.372
61.908	-100.164	0.000	-1.372
51.908	-100.164	0.000	-1.372
41.908	-100.164	0.000	-1.372
31.908	-100.164	0.000	-1.372
21.908	-100.164	0.000	-1.372
11.908	-100.164	0.000	-1.372
3.491	-100.164	0.000	-1.372
3.491	-88.998	0.000	-1.219
5.907	-85.998	0.000	-1.178
5.907	-75.998	0.000	-1.041
5.907	-66.665	0.000	-0.913
2.260	-63.665	0.000	-0.872
2.260	-53.665	0.000	-0.735
2.260	-43.665	0.000	-0.598

141

2.260	-33.665	0.000	-0.461
2.260	-24.665	0.000	-0.338
4.366	-21.665	0.000	-0.297
4.366	-11.333	0.000	-0.155
10.616	-10.292	0.000	-0.141
14.291	-10.292	0.000	-0.141
14.291	-20.292	0.000	-0.278
14.291	-30.292	0.000	-0.415
14.291	-40.292	0.000	-0.552
18.874	-44.209	0.000	-0.606
18.874	-55.042	0.000	-0.754
9.541	-55.042	0.000	-0.754
9.541	-65.042	0.000	-0.891
9.541	-72.126	0.000	-0.988
19.541	-72.126	0.000	-0.988
29.541	-72.126	0.000	-0.988
32.624	-72.126	0.000	-0.988
32.624	-61.042	0.000	-0.836
34.874	-58.042	0.000	-0.795
34.874	-48.042	0.000	-0.658
34.874	-38.042	0.000	-0.521
34.874	-28.042	0.000	-0.384
34.874	-18.042	0.000	-0.247
34.874	-7.083	0.000	-0.097
41.833	-7.083	0.000	-0.097
41.833	-2.083	0.000	-0.029
41.833	3.083	0.000	0.042
41.833	7.083	0.000	0.097
34.874	7.083	0.000	0.097
34.874	17.083	0.000	0.234
34.874	27.083	0.000	0.371
29.874	30.625	0.000	0.420
19.874	30.625	0.000	0.420
14.291	30.625	0.000	0.420
14.291	20.625	0.000	0.283
14.291	10.292	0.000	0.141
10.616	10.292	0.000	0.141
4.366	11.333	0.000	0.155
4.366	21.665	0.000	0.297
2.260	24.665	0.000	0.338
2.260	34.665	0.000	0.475
2.260	44.665	0.000	0.612
2.260	54.665	0.000	0.749

2.260	64.665	0.000	0.886
5.907	66.665	0.000	0.913
5.907	76.665	0.000	1.050
5.907	85.998	0.000	1.178
3.491	88.998	0.000	1.219
3.491	100.164	0.000	1.372
11.908	100.164	0.000	1.372
21.908	100.164	0.000	1.372
31.908	100.164	0.000	1.372
41.908	100.164	0.000	1.372
51.908	100.164	0.000	1.372
61.908	100.164	0.000	1.372
71.908	100.164	0.000	1.372
81.908	100.164	0.000	1.372
91.908	100.164	0.000	1.372
101.908	100.164	0.000	1.372
111.908	100.164	0.000	1.372
121.908	100.164	0.000	1.372
121.908	110.164	0.000	1.509
121.908	120.164	0.000	1.646
121.908	130.164	0.000	1.783
121.908	140.164	0.000	1.920
121.908	150.164	0.000	2.057
121.908	160.164	0.000	2.194
121.908	170.164	0.000	2.331
121.908	180.164	0.000	2.468
121.908	187.249	0.000	2.565
117.657	187.249	0.000	2.565
107.657	187.249	0.000	2.565
97.657	187.249	0.000	2.565
87.657	187.249	0.000	2.565
77.657	187.249	0.000	2.565
67.657	187.249	0.000	2.565
57.657	187.249	0.000	2.565
47.657	187.249	0.000	2.565
37.657	187.249	0.000	2.565
27.657	187.249	0.000	2.565
17.657	187.249	0.000	2.565
7.657	187.249	0.000	2.565
4.657	182.249	0.000	2.497
4.657	170.165	0.000	2.331
-6.657	170.165	0.000	2.331
-12.926	175.165	0.000	2.400

143

-12.926	187.249	0.000	2.565
-22.926	187.249	0.000	2.565
-32.926	187.249	0.000	2.565
-42.926	187.249	0.000	2.565
-52.926	187.249	0.000	2.565
-62.926	187.249	0.000	2.565
-72.926	187.249	0.000	2.565
-82.926	187.249	0.000	2.565
-92.926	187.249	0.000	2.565
-102.926	187.249	0.000	2.565
-112.926	187.249	0.000	2.565
-122.926	187.249	0.000	2.565
-130.177	187.249	0.000	2.565
-130.177	177.249	0.000	2.428
-130.177	167.249	0.000	2.291
-130.177	157.249	0.000	2.154
-130.177	147.249	0.000	2.017
-130.177	137.249	0.000	1.880
-130.177	127.249	0.000	1.743
-130.177	117.249	0.000	1.606
-130.177	107.249	0.000	1.469
-130.177	100.164	0.000	1.372
-120.177	100.164	0.000	1.372
-110.177	100.164	0.000	1.372
-100.177	100.164	0.000	1.372
-90.177	100.164	0.000	1.372
-80.177	100.164	0.000	1.372
-70.177	100.164	0.000	1.372
-60.177	100.164	0.000	1.372
-50.177	100.164	0.000	1.372
-40.177	100.164	0.000	1.372
-30.177	100.164	0.000	1.372
-20.177	100.164	0.000	1.372
-11.760	100.164	0.000	1.372
-11.760	90.164	0.000	1.235
-14.176	85.998	0.000	1.178
-14.176	75.998	0.000	1.041
-14.176	66.665	0.000	0.913
-10.010	58.290	0.000	0.798
-13.510	55.290	0.000	0.757
-23.510	52.248	0.000	0.716
-33.510	52.248	0.000	0.716
-43.510	52.248	0.000	0.716

144

-53.292	52.248	0.000	0.716
-53.292	62.498	0.000	0.856
-53.292	74.333	0.000	1.018
-63.292	74.333	0.000	1.018
-73.292	74.333	0.000	1.018
-83.292	74.333	0.000	1.018
-93.292	74.333	0.000	1.018
-103.292	74.333	0.000	1.018
-110.209	69.333	0.000	0.950
-110.209	59.333	0.000	0.813
-110.209	49.333	0.000	0.676
-110.209	39.333	0.000	0.539
-110.209	29.333	0.000	0.402
-110.209	19.333	0.000	0.265
-110.209	9.709	0.000	0.133
-119.500	9.709	0.000	0.133
-122.500	6.584	0.000	0.090
-133.415	6.584	0.000	0.090
-133.415	16.584	0.000	0.227
-138.415	20.208	0.000	0.277
-144.082	20.208	0.000	0.277
-144.082	10.208	0.000	0.140
-144.082	7.542	0.000	0.103
-146.999	4.542	0.000	0.062
-146.999	-4.542	0.000	-0.062
-144.082	-7.542	0.000	-0.103
-144.082	-10.208	0.000	-0.140
-144.082	-20.208	0.000	-0.277
-138.415	-20.208	0.000	-0.277
-133.415	-16.584	0.000	-0.227
-133.415	-6.584	0.000	-0.090
-122.500	-6.584	0.000	-0.090
-119.500	-9.709	0.000	-0.133
-110.209	-9.709	0.000	-0.133
-115.804	-14.709	0.000	-0.201
-115.804	-24.336	0.000	-0.333
-120.804	-29.336	0.000	-0.402
-125.804	-34.336	0.000	-0.470
-130.804	-39.336	0.000	-0.539
-135.804	-44.336	0.000	-0.607
-135.804	-54.336	0.000	-0.744
-135.804	-60.772	0.000	-0.832
-131.086	-56.054	0.000	-0.768

-126.086	-51.054	0.000	-0.699
-121.086	-46.054	0.000	-0.631
-116.086	-41.054	0.000	-0.562
-110.209	-39.054	0.000	-0.535
-110.209	-49.054	0.000	-0.672
-110.209	-59.054	0.000	-0.809
-110.209	-69.054	0.000	-0.946
-103.209	-74.333	0.000	-1.018
-93.209	-74.333	0.000	-1.018
-83.209	-74.333	0.000	-1.018
-73.209	-74.333	0.000	-1.018
-63.209	-74.333	0.000	-1.018
-53.292	-74.333	0.000	-1.018
-53.292	-66.333	0.000	-0.909
-53.292	-52.248	0.000	-0.716
-43.292	-52.248	0.000	-0.716
-33.292	-52.248	0.000	-0.716
-23.292	-52.248	0.000	-0.716
-13.510	-55.290	0.000	-0.757
-10.010	-58.290	0.000	-0.798
-14.176	-66.665	0.000	-0.913
-14.176	-75.665	0.000	-1.037
-14.176	-85.665	0.000	-1.173
-11.760	-90.998	0.000	-1.247
-11.760	-100.164	0.000	-1.372
-22.760	-100.164	0.000	-1.372
-32.760	-100.164	0.000	-1.372
-42.760	-100.164	0.000	-1.372
-52.760	-100.164	0.000	-1.372
-62.760	-100.164	0.000	-1.372
-72.760	-100.164	0.000	-1.372
-82.760	-100.164	0.000	-1.372
-92.760	-100.164	0.000	-1.372
-102.760	-100.164	0.000	-1.372
-112.760	-100.164	0.000	-1.372
-122.760	-100.164	0.000	-1.372
-130.177	-100.164	0.000	-1.372
-130.177	-107.164	0.000	-1.468
-130.177	-117.164	0.000	-1.605
-130.177	-127.164	0.000	-1.742
-130.177	-137.164	0.000	-1.879
-130.177	-147.164	0.000	-2.016
-130.177	-157.164	0.000	-2.153

-130.177	-167.164	0.000	-2.290
-130.177	-177.164	0.000	-2.427
-130.177	-187.249	0.000	-2.565
-123.177	-187.249	0.000	-2.565
-113.177	-187.249	0.000	-2.565
-103.177	-187.249	0.000	-2.565
-93.177	-187.249	0.000	-2.565
-83.177	-187.249	0.000	-2.565
-73.177	-187.249	0.000	-2.565
-63.177	-187.249	0.000	-2.565
-53.177	-187.249	0.000	-2.565
-43.177	-187.249	0.000	-2.565
-33.177	-187.249	0.000	-2.565
-23.177	-187.249	0.000	-2.565
-15.926	-187.249	0.000	-2.565
-12.926	-175.249	0.000	-2.401
-6.926	-170.165	0.000	-2.331
4.657	-170.165	0.000	-2.331
4.657	-182.165	0.000	-2.495
4.657	-187.249	0.000	-2.565
-53.292	45.082	0.000	0.618
-53.292	37.082	0.000	0.508
-53.292	27.082	0.000	0.371
-53.292	22.250	0.000	0.305
-46.083	22.250	0.000	0.305
-46.083	12.250	0.000	0.168
-41.083	6.209	0.000	0.085
-34.000	6.209	0.000	0.085
-34.000	15.875	0.000	0.217
-26.834	18.875	0.000	0.259
-26.834	27.458	0.000	0.376
-16.834	27.458	0.000	0.376
-13.834	18.875	0.000	0.259
-10.010	24.665	0.000	0.338
-10.010	34.665	0.000	0.475
-13.510	42.040	0.000	0.576
-18.510	45.082	0.000	0.618
-28.510	45.082	0.000	0.618
-38.510	45.082	0.000	0.618
-48.510	45.082	0.000	0.618
-53.292	-45.082	0.000	-0.618
-53.292	-37.082	0.000	-0.508
-53.292	-27.082	0.000	-0.371

147

-46.083	-22.250	0.000	-0.305
-46.083	-12.250	0.000	-0.168
-41.083	-6.709	0.000	-0.092
-37.833	-15.227	0.000	-0.209
-27.833	-15.227	0.000	-0.209
-17.833	-15.227	0.000	-0.209
-12.635	-21.665	0.000	-0.297
-10.010	-23.665	0.000	-0.324
-10.010	-33.665	0.000	-0.461
-13.510	-42.040	0.000	-0.576
-18.510	-45.082	0.000	-0.618
-28.510	-45.082	0.000	-0.618
-38.510	-45.082	0.000	-0.618
-48.510	-45.082	0.000	-0.618

y (ft)	z (ft)	Yacc*10^5 (ft/s^2)	Zacc*10^5 (ft/s^2)	Magnitude
187.249	-16.022	2.565	-0.658	2.648
187.249	-8.522	2.565	-0.350	2.589
187.249	-2.602	2.565	-0.107	2.567
177.249	-2.602	2.428	-0.107	2.430
167.249	-2.602	2.291	-0.107	2.294
154.665	-2.602	2.119	-0.107	2.121
154.665	7.398	2.119	0.304	2.140
154.665	17.398	2.119	0.715	2.236
154.665	27.398	2.119	1.126	2.399
154.665	37.398	2.119	1.537	2.617
154.665	42.313	2.119	1.739	2.741
144.665	42.313	1.982	1.739	2.636
137.498	42.313	1.884	1.739	2.563
137.498	37.313	1.884	1.533	2.429
137.498	27.313	1.884	1.122	2.193
137.498	17.313	1.884	0.711	2.013
137.498	7.313	1.884	0.301	1.907
137.498	-2.602	1.884	-0.107	1.887
127.498	-2.602	1.747	-0.107	1.750
117.498	-2.602	1.610	-0.107	1.613
111.211	-2.687	1.523	-0.110	1.527
111.211	7.313	1.523	0.301	1.553
111.211	17.313	1.523	0.711	1.681
111.211	27.313	1.523	1.122	1.892
111.211	37.313	1.523	1.533	2.162
111.211	42.230	1.523	1.735	2.309
103.500	42.230	1.418	1.735	2.241
94.044	42.230	1.288	1.735	2.161
94.044	32.230	1.288	1.325	1.848
94.044	22.230	1.288	0.914	1.579
94.044	12.230	1.288	0.503	1.383
94.044	2.230	1.288	0.092	1.292
89.044	-2.687	1.220	-0.110	1.225
80.988	-2.187	1.109	-0.090	1.113
69.665	-2.187	0.954	-0.090	0.959
58.290	-0.645	0.798	-0.027	0.799
58.290	10.355	0.798	0.426	0.905
48.290	10.355	0.662	0.426	0.787
39.040	10.355	0.535	0.426	0.683
39.040	-0.645	0.535	-0.027	0.535
30.625	4.355	0.420	0.179	0.456

149

30.625	13.937	0.420	0.573	0.710
20.625	13.937	0.283	0.573	0.639
10.292	13.937	0.141	0.573	0.590
10.292	23.937	0.141	0.984	0.994
10.292	34.396	0.141	1.414	1.421
20.292	34.396	0.278	1.414	1.441
27.101	34.396	0.371	1.414	1.461
27.101	44.396	0.371	1.825	1.862
27.101	49.896	0.371	2.051	2.084
15.227	49.896	0.209	2.051	2.061
10.227	52.730	0.140	2.167	2.172
3.625	57.229	0.050	2.352	2.352
15.227	57.229	0.209	2.352	2.361
15.227	67.896	0.209	2.790	2.798
7.417	67.896	0.102	2.790	2.792
4.417	70.896	0.061	2.914	2.914
-4.417	70.896	-0.061	2.914	2.914
-7.417	67.896	-0.102	2.790	2.792
-15.227	67.896	-0.209	2.790	2.798
-15.227	57.229	-0.209	2.352	2.361
-3.625	57.229	-0.050	2.352	2.352
-10.227	52.730	-0.140	2.167	2.172
-15.227	49.896	-0.209	2.051	2.061
-25.227	49.896	-0.346	2.051	2.079
-34.054	49.896	-0.466	2.051	2.103
-34.054	39.896	-0.466	1.640	1.705
-29.054	34.396	-0.398	1.414	1.469
-19.054	34.396	-0.261	1.414	1.437
-10.292	34.396	-0.141	1.414	1.421
-10.292	24.396	-0.141	1.003	1.012
-10.292	13.937	-0.141	0.573	0.590
-20.292	13.937	-0.278	0.573	0.637
-30.292	13.937	-0.415	0.573	0.707
-38.209	13.937	-0.523	0.573	0.776
-47.000	14.812	-0.644	0.609	0.886
-58.000	14.812	-0.795	0.609	1.001
-66.042	12.312	-0.905	0.506	1.037
-72.042	12.312	-0.987	0.506	1.109
-72.042	1.562	-0.987	0.064	0.989
-62.042	1.562	-0.850	0.064	0.852
-66.665	-0.645	-0.913	-0.027	0.914
-69.665	-2.187	-0.954	-0.090	0.959
-79.665	-2.187	-1.091	-0.090	1.095

-88.998	-2.687	-1.219	-0.110	1.224
-94.044	2.313	-1.288	0.095	1.292
-94.044	12.313	-1.288	0.506	1.384
-94.044	22.313	-1.288	0.917	1.581
-94.044	32.313	-1.288	1.328	1.850
-94.044	42.230	-1.288	1.735	2.161
-104.044	42.230	-1.425	1.735	2.246
-111.044	42.230	-1.521	1.735	2.308
-111.044	32.230	-1.521	1.325	2.017
-111.044	22.230	-1.521	0.914	1.774
-111.044	12.230	-1.521	0.503	1.602
-111.044	2.230	-1.521	0.092	1.524
-116.082	-2.602	-1.590	-0.107	1.594
-126.082	-2.602	-1.727	-0.107	1.730
-137.498	-2.602	-1.884	-0.107	1.887
-137.498	7.398	-1.884	0.304	1.908
-137.498	17.398	-1.884	0.715	2.015
-137.498	27.398	-1.884	1.126	2.194
-137.498	37.398	-1.884	1.537	2.431
-137.498	42.313	-1.884	1.739	2.563
-147.498	42.313	-2.021	1.739	2.666
-154.665	42.313	-2.119	1.739	2.741
-154.665	37.313	-2.119	1.533	2.615
-154.665	27.313	-2.119	1.122	2.398
-154.665	17.313	-2.119	0.711	2.235
-154.665	7.313	-2.119	0.301	2.140
-154.665	-2.602	-2.119	-0.107	2.121
-164.665	-2.602	-2.256	-0.107	2.258
-174.665	-2.602	-2.393	-0.107	2.395
-187.249	-2.602	-2.565	-0.107	2.567
-187.249	-7.602	-2.565	-0.312	2.584
-187.249	-16.022	-2.565	-0.658	2.648
-177.249	-16.022	-2.428	-0.658	2.516
-167.249	-16.022	-2.291	-0.658	2.384
-157.249	-16.022	-2.154	-0.658	2.252
-147.249	-16.022	-2.017	-0.658	2.122
-137.249	-16.022	-1.880	-0.658	1.992
-127.249	-16.022	-1.743	-0.658	1.863
-117.249	-16.022	-1.606	-0.658	1.736
-108.082	-15.937	-1.481	-0.655	1.619
-98.082	-15.937	-1.344	-0.655	1.495
-88.998	-15.937	-1.219	-0.655	1.384
-85.998	-19.187	-1.178	-0.789	1.418

-75.998	-19.187	-1.041	-0.789	1.306
-65.665	-20.729	-0.900	-0.852	1.239
-58.290	-20.729	-0.798	-0.852	1.168
-58.290	-32.629	-0.798	-1.341	1.561
-48.290	-32.629	-0.662	-1.341	1.495
-38.290	-32.629	-0.525	-1.341	1.440
-28.290	-32.629	-0.388	-1.341	1.396
-18.290	-32.629	-0.251	-1.341	1.364
-10.292	-32.629	-0.141	-1.341	1.348
-7.275	-40.063	-0.100	-1.646	1.649
-7.275	-50.063	-0.100	-2.057	2.060
-7.275	-60.063	-0.100	-2.468	2.470
-12.275	-70.101	-0.168	-2.881	2.886
-22.275	-70.101	-0.305	-2.881	2.897
-32.275	-70.101	-0.442	-2.881	2.915
-42.275	-70.101	-0.579	-2.881	2.939
-52.275	-70.101	-0.716	-2.881	2.969
-62.275	-70.101	-0.853	-2.881	3.005
-74.333	-70.101	-1.018	-2.881	3.056
-74.333	-76.101	-1.018	-3.127	3.289
-64.333	-76.101	-0.881	-3.127	3.249
-54.333	-76.101	-0.744	-3.127	3.215
-44.333	-76.101	-0.607	-3.127	3.186
-34.333	-76.101	-0.470	-3.127	3.163
-24.333	-76.101	-0.333	-3.127	3.145
-14.333	-76.101	-0.196	-3.127	3.134
-3.750	-78.687	-0.051	-3.234	3.234
0.000	-78.687	0.000	-3.234	3.234
5.750	-78.687	0.079	-3.234	3.235
15.750	-76.101	0.216	-3.127	3.135
25.750	-76.101	0.353	-3.127	3.147
35.750	-76.101	0.490	-3.127	3.166
45.750	-76.101	0.627	-3.127	3.190
55.750	-76.101	0.764	-3.127	3.219
65.750	-76.101	0.901	-3.127	3.255
74.333	-76.101	1.018	-3.127	3.289
74.333	-70.101	1.018	-2.881	3.056
64.333	-70.101	0.881	-2.881	3.013
54.333	-70.101	0.744	-2.881	2.975
44.333	-70.101	0.607	-2.881	2.944
34.333	-70.101	0.470	-2.881	2.919
24.333	-70.101	0.333	-2.881	2.900
14.333	-70.101	0.196	-2.881	2.888

7.138	-63.521	0.098	-2.610	2.612
7.138	-53.521	0.098	-2.200	2.202
7.138	-43.521	0.098	-1.789	1.791
7.138	-35.063	0.098	-1.441	1.444
10.292	-25.063	0.141	-1.030	1.040
20.292	-20.729	0.278	-0.852	0.896
30.292	-20.729	0.415	-0.852	0.948
39.040	-20.729	0.535	-0.852	1.006
39.040	-31.729	0.535	-1.304	1.409
49.040	-31.729	0.672	-1.304	1.467
58.290	-31.729	0.798	-1.304	1.529
58.290	-20.729	0.798	-0.852	1.168
66.665	-20.729	0.913	-0.852	1.249
74.665	-19.187	1.023	-0.789	1.291
85.998	-19.187	1.178	-0.789	1.418
93.998	-15.937	1.288	-0.655	1.445
103.998	-15.937	1.425	-0.655	1.568
113.082	-15.937	1.549	-0.655	1.682
116.082	-16.022	1.590	-0.658	1.721
126.082	-16.022	1.727	-0.658	1.848
136.082	-16.022	1.864	-0.658	1.977
146.082	-16.022	2.001	-0.658	2.107
156.082	-16.022	2.138	-0.658	2.237
166.082	-16.022	2.275	-0.658	2.368
176.082	-16.022	2.412	-0.658	2.500
181.082	-16.022	2.481	-0.658	2.566

References

[1]Bosman, R.A. and J.F.T. Bos. "Control of the Joint Runaway Hazard for the European Robotic Arm." Http://www.fokkerspace.nl/products/era/esrel98.pdf.

[2]Boumans, R., et al. "ERA: Baseline Capabilities and Future Perspectives." Http://www.fokkerspace.nl/products/era/paper.pdf.

[3]Http://eegle1.simplenet.com/stationweb/html/aercam.html.

[4]Http://jem.tksc.nasda.go.jp/iss_jem/doc04_e.html.

[5]Http://spaceflight.nasa.gov/history/shuttle-mir/mir23/status/week20/culbertson.html.

[6]Http://spaceflight.nasa.gov/history/shuttle-mir/specrpts/june/collision.html.

[7]Http://spaceflight.nasa.gov/shuttle/archives/sts-76/orbit/payloads/science/meteor.html.

[8]Http://spaceflight.nasa.gov/spacenews/factsheets/pdfs/factbook/issfactbook.pdf "ISS Fact Book."

[9]Http://spaceflight.nasa.gov/spacenews/factsheets/pdfs/issovw.pdf. "The International Space Station: An Overview."

[10]Http://spaceflight.nasa.gov/spacenews/factsheets/pdfs/servmod.pdf "The Service Module: A Cornerstone of Russian International Space Station Modules."

[11]Http://spaceflight.nasa.gov/spacenews/factsheets/pdfs/td9702.pdf. "ISS Familiarization Manual."

[12]Http://tommy.jsc.nasa.gov/ARSD/report_FY96/hess_fy963.html.

[13]Http://tommy.jsc.nasa.gov/projects/Sprint/aercam-sprint-overview.html.

[14]Http://utopia.tno.nl/instit/fel/div2/pointer.html.

[15]Http://www.boeing.com/defense-space/space/spacestation/node1.html.

[16]Http://www.boeing.com/defense-space/space/spacestation/overview/world_wide_team.html.

[17]Http://www.boeing.com/defense-space/space/spacestation/overview/background_goals_html.

[18]Http://www.cnn.com/TECH/9707/mir/spacewalk/external.html.

[19]Http://www.estec.esa.nl./spaceflight/issdescr.html.

[20]Http://www.fokkerspace.nl/products/era/era.html.

[21]Http://www.shuttlepresskit.com/ISS_OVR/orbit_assembly.html.

[22]Http://www.space.gc.ca/eng/about/space%5Fsystems/station3.html.

[23]Http://www.space.gc.ca/eng/news%5Freleases/990312.html.

[24]Http://www.space.gc.ca/eng/publications/poster/cssp%5Fp4%5Fe.html.

[25]Http://www.space.gc.ca/eng/whats%5Fnew/990414e.html.

[26]Http://www.spaceflight.nasa.gov/realdata/tracking/index.html.

[27]Http://www.spaceflight.nasa.gov/station/assembly/elements.

[28]Http://www.spaceflight.nasa.gov/station/assembly/index.html.

[29]Http://www.spaceflight.nasa.gov/station/assembly/plaid

[30]Http://www.spaceflight.nasa.gov/station/assembly/models/index.html.

[31]Http://www.spaceflight.nasa.gov/station/assembly/sprint/index.html.

[32]Http://www.spaceflight.nasa.gov/station/eva.

[33]Http://www.spaceflight.nasa.gov/station/eva/outside.html.

[34]Http://www.spaceflight.nasa.gov/station/eva/robotics.html.

[35]Http://www.spaceflight.nasa.gov/station/eva/spacesuit.html.

[36]Http://www.spar.ca/space/mms.html.

[37]Http://yyy.tksc.nasda.go.jp/Home/This/This-e/contribution_e.html.

[38]Lockhart, Paul. "Unassisted Rendezvous Techniques for the Manned Maneuvering
Unit." Master's Thesis. University of Texas at Austin, August 1981.

[39]Vallado, David A. Fundamentals of Astrodynamics and Applications. McGraw-Hill:
New York, 1997. p. 343-351.

<u>Vita</u>

Lisa Kaplan was born in Chicago, Illinois on 28 November 1973, the daughter of Barbara Knight Warren and Leonard A. Kaplan. She grew up in Charleston, West Virginia where she graduated from George Washington High School in 1992. From 1992-1994 she attended Virginia Polytechnic Institute and State University in Blacksburg, Virginia, working as a Chemical Engineering CO-OP student with Union Carbide. In the summer of 1994 she entered the United States Air Force Academy (USAFA) in Colorado Springs, Colorado. She received a Bachelor of Science degree in Astronautical Engineering and an officer commission in the U.S. Air Force on 27 May, 1998. A National Science Foundation fellowship made it possible for her to enter the Graduate School of Engineering at the University of Texas at Austin in September, 1998.

Permanent Address: 1620 Woodvale Dr.
                    Charleston, WV 25314

This thesis was typed by the author.